Low-Complexity Iterative Detection Algorithms for Multi-Antenna Systems

This thesis is submitted in partial fulfilment of the requirements for

Doctor of Philosophy (Ph.D.)

Peng Li

Communications Research Group

Department of Electronics

University of York

December 2011

Abstract

Multiple input multiple output (MIMO) techniques have been widely employed by different wireless systems with many advantages. By using multiple antennas, the system is able to transmit multiple data streams simultaneously and within the same frequency band. The methods known as spatial multiplexing (SM) and spatial diversity (SD) improves the high spectral efficiency and link reliability of wireless communication systems without requiring additional transmitting power. By introducing channel coding in the transmission procedure, the information redundancy is introduced to further improve the reliability of SM links and the quality of service for the next generation communication systems.

However, the throughput performance of these systems is limited by interference. A number of different interference suppression techniques have been reported in the literature. Theses techniques can be generally categorised into two aspects: the preprocessing techniques at the transmitter side and the decoding techniques at the receiver side.

Generally speaking, in the ideal case, the preprocessing techniques orthogonalize the interfering channels, and therefore, the receiver experiences interference free transmission. However, a feedback channel is required to provide the channel information. On the other hand, in this thesis we are interested in the decoding part which uses various techniques to improve the signal-to-interference-and-noise ratio (SINR) of the desired symbols. To achieve this goal, a number of low-complexity iterative detection algorithms have been investigated. In the context of the thesis, the mainly focus is on the interference cancellation techniques.

Firstly, we investigate the traditional successive interference cancellation (SIC) algo-

rithm. SIC has the ability to separate the spatially multiplexed signals on a MIMO channel. However, the low detection diversity order as well as the error propagation effect restrict the bit error performance of such detectors. We propose a multiple feedback SIC (MF-SIC) method to enhance the performance of conventional SIC detection by introducing feedback candidates and reliability checking. This algorithm is able to provide significant performance gains with little additional complexity without the protection from channel codes. The MF-SIC algorithm is then incorporated into an iterative detection and decoding (IDD) scheme to process soft information.

Secondly, in the case that the MIMO channel is time-varying, the conventional detection algorithms generally bring about expensive complexity in the time domain. In order to address this problem, a decision feedback algorithm is introduced and adaptive algorithms are derived to update the forward and backward filters to perform the detection in each time instant. A constellation based estimation refinement scheme is also introduced in the system and the performance is significantly improved. The proposed decision feedback algorithm is incorporated into an IDD scheme that performs iterative (turbo) interference cancellation.

At last, the inter-cell interference is considered in a multi-cell, high frequency reuse scenario. The distributed iterative detection (DID) algorithms are investigated. A large amount of information need to be transmitted via a wired backhaul network where optimal distributed detection exchange all the soft estimates among adjacent base stations (BSs). To address this problem we consider a reduced message passing (RMP) technique in which each BS generates a detection list with the probabilities for the desired symbol that are sorted according to the calculated probability density. RMP introduces low backhaul overhead compared with the hard bit exchange and outperforms the previously reported hard/soft information exchange algorithms.

Contents

List of Figures

List of Tables

Acknowledgements

I would like to extend my sincere gratitude to my supervisor, Dr. Rodrigo C. de Lamare, for his support and encouragement during the course of my Ph.D. study.

I would also like to thank all my dear colleagues in the Communications Research Group.

This thesis is dedicated to my parents and my love Jiao.

Declaration

Some of the research presented in this thesis has resulted in some publications. These publications are listed at the end of Chapter 1.

All work presented in this thesis as original is so, to the best knowledge of the author. References and acknowledgements to other researchers have been given as appropriate.

Chapter 1

Introduction

Contents

1.1 Overview

After Marconi pioneered radio transmission 110 years ago, wireless communications has become present in every aspect of modern life. Apart from the traditional text and voice services, the applications also include video streaming, web browsing and on-line gaming. It seems difficult to imagine our lives without wireless communications. From analogue to digital communications, from point-to-point transmission to cellular networks, more and more information can be transferred with the evolution of communications engineering. Nowadays, with the gradually increasing use of 3rd and 4th generation cellular systems

[1] and wireless LANs [2], the demands of high data rate transmission in wireless devices with high quality of service (QoS) have never been greater.

The need for high data rates motivated researchers to develop new technologies and standards. The demands on the bandwidth and spectral efficiency are endless. Many powerful and efficient transmitter and receiver schemes are under development while the network-wide design is also taken into account. For instance, cellular systems with cooperative capability have drawn great attention with the realization of base station cooperation or signal relaying strategies. In the near future, these new designs may be investigated with the launch of the new generations high-speed cellular network standards such as 4th Generation, WiMAX [3] and Long Term Evolution Advanced [4]. The growing demand for data throughput and the shortage of available bandwidth require sophisticated theoretic analysis, advanced signal processing algorithms and smart cellular deploying plans.

1.2 Motivation

The increase of system throughput often comes with the price of consumption of resources, such as energy, bandwidth or equipments. It is believed that the increase of data throughput can be realized without sacrificing the bandwidth and spectral efficiency by deploying multiple antennas. A fundamental work in obtaining the multiple-input multiple-output (MIMO) capacity in fading channels has been described by Telatar [5]. He concluded that the use of multiple antennas can greatly increase the achievable rates in fading channels. One year later, his colleague in Bell Labs, Foschini proposed a so-called diagonal-Bell Lab space time (D-BLAST) [6] processing algorithm. This high computational complexity algorithm was simplified two yeas later as vertical-BLAST [7] processing. The field demonstration of the V-BLAST algorithm showed a very promising result that a multiple antennas system has the ability to achieve more than 20 bit/s/Hz spectral efficiency, which is very hard to achieve for a traditional single antenna system. In the same year, space-time trellis code (STTC) [8] and their simplified version namely space-time block codes (STBC) [9] were introduced by Tarokh and Alamouti, respectively. These algorithms sacrifice the transmit rate to obtain a diversity gain. Therefore, a tradeoff between space diversity and multiplexing has been established and a fundamen-

tal work with analysis has been done by Zheng and Tse [10]. The diversity gains can be achieved by passing the signals through multiple propagation paths, each of which fades independently. In this case, reliable communications is possible. If we separate multiple transmit or receive antenna by a sufficient space, the diversity can be obtained [11]. In highly dynamic wireless and mobile environments, the diversity techniques provide the possibility of reliable communications among the highly mobilized users.

The array gain, diversity, and spatial multiplexing provided by point-to-point MIMO system [7, 9] naturally leads to the research on MIMO applications to multiuser systems. By using multiple antennas and appropriate signal processing tools, the point-to-point MIMO systems can be easily extended to multiuser MIMO systems. For example, the concept of multiuser detection which was first introduced in the context of code division multiple access (CDMA) systems [12], can then be widely used in the detection of multiuser MIMO systems. Significant efforts have been made to improve the performance of multiuser MIMO detection algorithms in an isolated cell [19]. On the other hand, in cellular systems, by placing antennas in space, forming a virtual MIMO system, significant gains can be attained and the antenna cooperation is very desirable. The future multicell networks require aggressive frequency reuse in order to obtain substantial gains in spectrum usage and facilitate the planning of cells [13]. The full frequency reuse also makes it possible to have seamless communications, implying switching or roaming between cells without notice by the mobile users located on the cell edges [14].

In 1993, the invention of turbo codes [17] triggered intensive research on near-capacity transmission. The pioneering near-capacity MIMO iterative detection and decoding (IDD) structure with affordable computational complexity has been reported in 2003 [18]. The multiple user IDD schemes were introduced to approach interference free performance [19]. In 2006, the application of IDD in the multiple cell environment was introduced by Mayer et al. [22], and a number of base station cooperation (BSC) schemes were developed for the sake of average cell throughput and backhaul traffic [23]- [25]. All the previously mentioned contributions motivated the development of next generation's wireless engineering, as well as this work.

1.3 Problems in MIMO Systems

The research on MIMO communication systems has flourished after the discoveries mentioned in the previous section. However, a number of problems remain and challenge researchers and designers in the following aspects:

- In highly dynamic wireless and mobile environments involving a varying number of users and time-varying transmission conditions, the characteristics of channels for each user change all the time. Parameter estimation techniques and applications such as MIMO channel estimation under these conditions require highly sophisticated signal processing techniques.

- The use of multiple antennas at both the transmitter and receiver enables significant improvement in terms of link performance. In order to exploit the space diversity, more and more transmit and receive antennas are used. However, in general, exploiting these diversity gains comes at the price of significantly increased complexity, especially at the receiver side [27]. As the research of large systems such as multiuser MIMO and cellular MIMO systems grows, it is of great interest to develop algorithms that have the ability to process a high number of data streams with good performance and affordable computational complexity.

- The performance of MIMO systems is generally limited by different types of interference, namely, inter-symbol interference (ISI), inter-antenna interference, (IAI), multiuser interference (MUI) and inter-cell interference (ICI). ISI is usually caused by multi-path effects. IAI and MUI are major interference sources arising due to the fact that the users' antennas communicate through the same channel with non-orthogonal signals [28]. ICI leads to significant losses in cell throughput mainly due to the aggressive frequency reuse, which severely limits the data throughput of users located on the cell edge. In order to address these problems, many methods have been published such as precoding [31], power control [29] and antenna beamforming [30] as well as receiver-based multi-user detection and distributed antennas systems (DAS) [32].

- Error control coding is used in wireless communications to provide protection for the transmitted bits. Linear block codes and convolutional codes [34] have low com-

plexity and decoding delay, however, there are performance losses compared with concatenated codes such as turbo codes [35] and low-density-parity-check (LDPC) codes [36]. Concatenated codes with an iterative decoder generally provide good bit-error- rate (BER) performance, however, the encoding/decoding complexity and decoding delay are increased. In terms of combination with MIMO systems, soft information is required by the channel decoder. Soft-input soft-output (SISO) detectors generally outperform hard-output detectors. In order to generate the soft-output, the maximum a posterior (MAP) detector is used which has an exponential growth of complexity with the increase of the number of data streams and symbol modulation level [18]. In recent years, a number of suboptimal detectors have been reported by using either a subset of possible vector space [18] or MMSE based soft interference cancellation [19], however, the performance loss is inevitable.

- Synchronization is required for real-world MIMO systems. The precision of synchronization algorithms has a major impact on the overall system performance [33], which degrades seriously when the estimates of the frequency offset or the symbol timing are not sufficiently accurate. Additionally, the synchronization of MIMO systems requires a much higher complexity compared with the traditional single-antenna systems.

In this thesis, the focus is on the signal processing techniques used in detecting MIMO signals and interference suppression strategies. In order to achieve the interference mitigation without consuming extra bandwidth, two aspects are considered in this context, (i) the advanced receiver processing such as multi-user detection and iterative processing with the aid of channel codes. (ii) Base station cooperation strategies in a multi-user multi-cell scenario.

1.4 Summary of Contributions

The contributions of this thesis are summarized as follows:

- The conventional V-BLAST has a performance loss compared with optimal de-

tectors. In order to address this problem, a novel low-complexity multi-feedback successive interference cancellation (MF-SIC) detection is developed for the uplink of MIMO systems. By introducing a shadow-area decision device, the unreliable estimates are replaced by the symbols which are selected from a set of candidate lists while reliable ones are quantized directly for interference cancellation. The proposed detection algorithm provides significant improvement and approaches the optimal performance at the price of little extra complexity requirements.

- The signal detection in time-varying channels requires excessive computational load in the time domain. The previously reported adaptive decision feedback detection algorithms have performances far from optimal. In this thesis, a scheme called constellation constraints (CC) is proposed and combined with the recursive least squares (RLS) based adaptive algorithm for detecting the signal transmitted in the time-varying MIMO channel. In this algorithm, an enhanced symbol estimation is achieved and the error propagation is effectively mitigated. The performance of the maximum likelihood detection is approached in various channel fading conditions. A complexity reduction strategy is also considered to avoid processing with reliable decisions to save computational resources.

- The implementation of the above described algorithms are both compared with a number of existing detection strategies for a different number of users or antenna elements. In order to achieve a higher detection diversity order, a multiple branch (MB) structure is also incorporated in the proposed schemes to achieve a near-optimal performance.

- In order to combine the detection schemes with error control codes, soft-output is required to facilitate the iterative signal processing and iterative detection and decoding (IDD) schemes. The soft-output detectors are developed based on both the proposed MF-SIC and CC aided detection algorithms. For MF-SIC, followed by multi-feedback processing, the soft interference cancellation is performed to compute the bit probability. This so-called soft cancellation aided MF-SIC (MF-SIC-SC) reduces the decoding delay and allows a near interference free performance. Similarly to list sphere decoders (LSD) [18], the proposed CC aided decision feedback detector uses the tentative decisions to form a "list" to calculate the likelihood of each transmitted bit. By concatenating the soft-output detector with the channel decoder, the probability of decision errors is significantly reduced.

- In terms of multi-cell cooperative processing, a distributed iterative detection structure with reduced message passing is proposed. By sorting the probability of transmit symbol with a decreased order, a list is generated at each cooperating base station. A selection unit (SU) is proposed to collect the index information and select the best from each list. The transmission of quantized soft information can be avoided which significantly reduces the backhaul traffic.

1.5 Thesis Outline

The rest of the thesis is organized as follows:

- In Chapter 2, a literature review is presented. The capacities of traditional and cellular MIMO systems are analysed and followed by the description of a number of existing optimal and sub-optimal MIMO detection techniques. The interference suppression, detection diversity, multi-user detection algorithms and adaptive signal processing techniques are also considered in the context.

- In Chapter 3, a novel low-complexity MF-SIC detection is introduced, the performance and complexity analysis are given. The simulations illustrate that the performance of the proposed algorithm significantly outperforms the traditional SIC scheme with negligible additional complexity.

- In Chapter 4, by using the RLS algorithm, a decision feedback detector is introduced for detecting signals transmitted in time-varying MIMO channels. A decision refinement scheme is introduced and the proposed detector can also approach the optimal performance at the price of a low additional cost.

- In Chapter 5, we propose a parallel multi-feedback scheme which is used in a multi-cell system with base station cooperation (BSC), the simulation results indicate that the backhaul traffic is significantly reduced and the isolated cell performance is obtained with low complexity distributed detection.

- In Chapter 6, conclusions are made and a discussion on the possibility of future work is presented.

1.6 Notation

In this thesis, we use capital and small bold fonts to denote matrices and vectors, i.e., $\mathbf{A}$ and $\mathbf{a}$, respectively. Elements of the matrix and vector are denoted as $A_{m,n} = [\mathbf{A}]_{m,n}$ and $a_m = [\mathbf{a}]_m$. The symbol j is an imaginary unit $j = \sqrt{-1}$. We denote $\Re\{\cdot\}$ and $\Im\{\cdot\}$ as the real and imaginary components of a complex number, respectively; $(\cdot)^*$ denotes complex conjugate; $\mathbf{I}_Q$ denotes an $Q \times Q$ identity matrix; $(\cdot)^T$ and $(\cdot)^H$ denote matrix transpose and Hermitian transpose, respectively. $E\{\cdot\}$ denotes the statistical expectation operator and $tr\{\cdot\}$ denotes the trace operator.

1.7 Publication List

Journal Papers [108, 109]

1. P. Li and R. C. de Lamare, "Multiple Parallel Feedback Detection Through Base Station Cooperation, *IEEE Transactions on Communications*, under preparation, 2011.

2. P. Li and R. C. de Lamare, "Multiuser Decision Feedback with Constrains Processing for MIMO Systems, *IET Communications*, under preparation, 2011.

3. P. Li and R. C. de Lamare, "Adaptive Decision Feedback Detection with Constellation Constraints for MIMO Systems," *IEEE Transactions on Vehicular Technology,* vol. PP, no. 99, pp. 1, 0.

4. P. Li, R. C. de Lamare and R. Fa, "Multiple Feedback Successive Interference Cancellation Detection for Multiuser MIMO Systems," *IEEE Transactions on Wireless Communications*, vol. 10, no. 8, pp. 2434 - 2439, August 2011.

Conference Papers [110–119]

1. P. Li, R. C. de Lamare, "Adaptive Iterative Decision Multi-feedback Detection for

Multi-user MIMO System", *IEEE International Conference on Acoustics, Speech and Signal Processing ICASSP*, accpted 2012.

2. P. Li, R. C. de Lamare, "Parallel Multiple Candidate Interference Cancellation with Distributed Iterative Multi-cell Detection and Base Station Cooperation", *International ITG/IEEE Workshop on Smart Antennas WSA 2012*, accepted 2012.

3. P. Li, R. C. de Lamare "Adaptive Iterative Decision Feedback with Constellation Constraints and Soft-Output Detection for MIMO Systems," *IEEE International Symposium on Wireless Communications Systems*, pp. 670-674, November. 2011.

4. Y. Wang, P. Li, L. Li, A. G. Burr and R. C. de Lamare, "Irregular Code-Aided Low-Complexity Three-stage Turbo Space Time Processing", *IEEE International Symposium on Wireless Communications Systems*, pp. 604 - 608, Nov. 2011.

5. J. Liu, P. Li, L. Li, R. C. de Lamare and A. G. Burr, "Iterative QR Decomposition-Based Detection Algorithms with Multiple Feedback and Dynamic Tree Search for LDPC-Coded MIMO Systems", *Sensor Signal Processing for Defence (SSPD)*, accepted 2011.

6. P. Li, R. C. de Lamare, "Adaptive Decision Feedback Detection with Constellation Constraints for Multi-Antenna Systems", *Sensor Signal Processing for Defence (SSPD)*, accepted 2011.

7. P. Li, R. C. de Lamare and R. Fa, "Multi-Feedback Successive Interference Cancellation with Multi-Branch Processing for MIMO Systems", *Vehicular Technology Conference (VTC Spring), 2011 IEEE 73rd,* pp.1-5, May 2011.

8. P. Li, R. C. de Lamare and R. Fa, "Iterative Successive Interference Cancellation Based on Multiple Feedback For Multiuser MIMO Systems," *European Wireless Conference*, Vienna, Austria, April 2011.

9. P. Li, R. C. de Lamare and R. Fa, "Multiple Feedback Successive Interference Cancellation with Iterative Decoding for Point-to-Point MIMO Systems", *International ITG/IEEE Workshop on Smart Antennas WSA 2011*, Aachen, Germany, February 2011.

10. P. Li, R. C. de Lamare and R. Fa, “Multiple Feedback Successive Interference Cancellation with Shadow Area Constraints for MIMO systems”, *IEEE International Symposium on Wireless Communications Systems*, York, UK, September 2010.

Chapter 2

Fundamental Techniques

Contents

2.1 Overview

In this chapter, fundamental techniques used throughout this thesis are introduced. These include capacity of MIMO channels, channel parameter estimation, MIMO detection algorithms and error control coding, amongst the important techniques used in the design of MIMO communication systems.

2.2 Channel Capacity and Parameter Estimation

In this section, we review the capacity of deterministic and random MIMO channels as well as channel parameter estimation techniques.

2.2.1 MIMO Channel Capacity

Compared with the conventional single-antenna systems, MIMO systems have the ability to increase the channel capacity by the factor of $\min(N_T, N_R)$ where N_T is the number of transmit antennas and N_R is the number of receive antennas. Instead of time and frequency, the other dimension - space, is used to separate the co-channel data streams and provide the multiplexing gains. By deploying multiple antennas, the increase of data throughput can be realized without sacrificing the power, bandwidth and spectral efficiency. Because of these advantages, MIMO systems have been actively investigated [3] and deployed in broadband wireless access networks such as Mobile WiMAX and LTE-Advanced [4].

It has been proven that the MIMO wireless channel has the ability to obtain high channel capacity [5], which has stimulated research on the techniques to achieve high speed data transmission or high link reliability. Therefore, the studies on MIMO systems generally fall into different categories: spatial-multiplexing [6] and diversity techniques [9], and their relation is studied in [10] and [11]. On the one hand, the spatial-multiplexing configuration is used in the systems with the aim of achieving the maximum data transmission rate supported by the MIMO channel. On the other hand, when diversity techniques are used, the aim of the system is to increase the reliability and to obtain lower bit error rate [37] [39].

In order to obtain the maximum achievable transmission rate provided by the spatial multiplexing MIMO systems, in this section, we discuss the capacity provided by the wireless MIMO channel. In the following, the capacity of deterministic and random channels are derived.

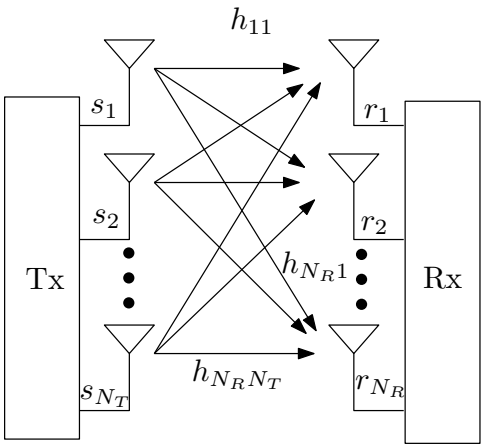

Figure 2.1: $N_R \times N_T$ MIMO system.

MIMO system model

In this thesis, we will focus on narrowband MIMO communication systems with frequency flat fading channels, the problems presented here can be generalized to the multipath fading channel by introducing orthogonal frequency-division multiplexing (OFDM) or equalization techniques.

Fig. 2.1 shows a narrowband wireless MIMO channel presented by a $N_R \times N_T$ deterministic matrix $\boldsymbol{H} \in \mathbb{C}^{N_R \times N_T}$. Let the symbol vector $\boldsymbol{s} \in \mathbb{C}^{N_T \times 1}$ denote the transmitted symbols and $\boldsymbol{s} = [s_1, s_2, \ldots, s_{N_T}]^T$ and $E\{\boldsymbol{s}^H \boldsymbol{s}\} = \sigma_s^2 \boldsymbol{I}_{N_T}$, where σ_s^2 represents the variance of the transmit symbol. Each independent transmitted signal s_k radiated from the transmit antenna is received by N_R receive antennas to form a received signal vector $\boldsymbol{r} \in \mathbb{C}^{N_R \times 1}$, given by

$$\boldsymbol{r} = \boldsymbol{H}\boldsymbol{s} + \boldsymbol{v}, \tag{2.1}$$

where the noise vector $\boldsymbol{v} = [n_1, n_2, \ldots, n_{N_R}] \in \mathbb{C}^{N_R \times 1}$ is assumed as zero-mean circular symmetric complex Gaussian. By zero-mean circular symmetric complex Gaussian, it means that $\boldsymbol{v}$ affects equally the in-phase and quadrature components from a statistical point of view. The autocorrelation of the noise vector and the transmit symbol vector are given by

$$\begin{aligned} \boldsymbol{Z}_{nn} &= E\{\boldsymbol{v}\boldsymbol{v}^H\}, \\ &= \sigma_v^2 \boldsymbol{I}_{N_R}, \end{aligned} \tag{2.2}$$

$$\begin{aligned} \boldsymbol{R}_{ss} &= E\{\boldsymbol{s}\boldsymbol{s}^H\}. \\ &= \sigma_s^2 \boldsymbol{I}_{N_T}. \end{aligned} \tag{2.3}$$

where σ_v^2 denotes the noise variance. The autocorrelation of the received vector $\boldsymbol{r}$ is obtained by

$$\begin{aligned} \boldsymbol{R}_{rr} &= E\{\boldsymbol{r}\boldsymbol{r}^H\} \\ &= E\big\{(\boldsymbol{H}\boldsymbol{s}+\boldsymbol{v})(\boldsymbol{H}\boldsymbol{s}+\boldsymbol{v})^H\big\} \\ &= E\big\{(\boldsymbol{H}\boldsymbol{s}+\boldsymbol{v})(\boldsymbol{s}^H\boldsymbol{H}^H+\boldsymbol{v}^H)\big\} \\ &= E\big\{\boldsymbol{H}\boldsymbol{s}\boldsymbol{s}^H\boldsymbol{H}^H+\boldsymbol{v}\boldsymbol{v}^H\big\} \\ &= \boldsymbol{H}\boldsymbol{R}_{ss}\boldsymbol{H}^H+\boldsymbol{Z}_{nn}. \end{aligned} \tag{2.4}$$

The capacity of a deterministic channel is defined as the maximum mutual information, that can be achieved by varying the probability density function (PDF) of the transmit signal vector $f(\boldsymbol{s})$, which is given by [5]

$$C = \max_{f(\boldsymbol{s})} I(\boldsymbol{s};\boldsymbol{r}), \tag{2.5}$$

where $f(\boldsymbol{s})$ is the PDF of the transmit vector $\boldsymbol{s}$. The mutual information between the random vectors $\boldsymbol{s}$ and $\boldsymbol{r}$ is calculated as $I(\boldsymbol{s};\boldsymbol{r}) = H(\boldsymbol{r}) - H(\boldsymbol{r}|\boldsymbol{s})$ where $H(\boldsymbol{r})$ is the differential entropy of $\boldsymbol{r}$. Since $\boldsymbol{v}$ is independent from $\boldsymbol{s}$, the equation can be rewritten as

$$I(\boldsymbol{s};\boldsymbol{r}) = H(\boldsymbol{r}) - H(\boldsymbol{v}). \tag{2.6}$$

The mutual information of $\boldsymbol{r}$ and $\boldsymbol{v}$ are

$$H(\boldsymbol{r}) = \log_2\Big\{\det(\pi e \boldsymbol{R}_{rr})\Big\}, \tag{2.7}$$

$$H(\boldsymbol{v}) = \log_2\Big\{\det(\pi e \boldsymbol{Z}_{nn})\Big\}, \tag{2.8}$$

By using the above equations, the mutual information is obtained as

$$I(\boldsymbol{s};\boldsymbol{r}) = \log_2 \det\Big(\boldsymbol{I}_{N_R} + \frac{1}{\sigma_v^2}\boldsymbol{H}\boldsymbol{R}_{\boldsymbol{ss}}\boldsymbol{H}^H\Big). \tag{2.9}$$

Therefore, the deterministic MIMO channel has a capacity given by

$$C = \max_{tr(\boldsymbol{R}_{ss})=N_T} \log_2 \det \left(\boldsymbol{I}_{N_R} + \frac{1}{\sigma_v^2} \boldsymbol{H} \boldsymbol{R}_{\boldsymbol{ss}} \boldsymbol{H}^H \right). \tag{2.10}$$

MIMO Capacity when Channel is Known to the Transmitter

By setting up feedback links in the communication system, the channel state information (CSI) is available at the transmitter side, the transmitted signal is precoded before transmitted through the channels.

In this scenario, the transmitted signal $\boldsymbol{s}$ is pre-processed by the precoder $\boldsymbol{U}$ at the transmitter side and the received signal is then post-processed with $\boldsymbol{V}^H$ at the receiver side. By using singular value decomposition (SVD), the $N_R \times N_T$ MIMO channel can be separated into N_T parallel independent virtual single-input single-output (SISO) channels [11], and the channel capacity can be obtained by summing up the capacities across all the virtual SISO channels.

This capacity analysis is only related to the systems with feedback channels, and precoding is used at the transmitter side. A detailed discussion of the capacity when the channel is known to the transmitter can be found in references such as [11] and [38].

MIMO Capacity when Channel is Unknown to the Transmitter

Since the CSI is not known at the transmitter, the transmitted signals have an equal power across N_T transmit antennas. Then, the autocorrelation function of $\boldsymbol{s}$ can be rewritten as $\boldsymbol{R}_{ss} = \sigma_s^2 \boldsymbol{I}_{N_T}$, and the channel capacity can be re-calculated as

$$\begin{aligned} C &= \log_2 \det \left(\boldsymbol{I}_{N_R} + \frac{\sigma_s^2}{\sigma_v^2} \boldsymbol{H} \boldsymbol{H}^H \right) \\ &= \log_2 \det \left(\boldsymbol{I}_{N_R} + \frac{\sigma_s^2}{\sigma_v^2} \boldsymbol{Q} \boldsymbol{\Lambda} \boldsymbol{Q}^H \right) \\ &= \log_2 \det \left(\boldsymbol{I}_{N_R} + \frac{\sigma_s^2}{\sigma_v^2} \boldsymbol{\Lambda} \right) \\ &= \sum_{k=1}^{\min(N_R,N_T)} \log_2 \left(1 + \frac{\sigma_s^2}{\sigma_v^2} \lambda_k \right), \end{aligned} \tag{2.11}$$

where the eigen-decomposition $\boldsymbol{H}\boldsymbol{H}^H = \boldsymbol{Q}\boldsymbol{\Lambda}\boldsymbol{Q}^H$ is applied and $\boldsymbol{Q}$ is the square matrix whose column is the eigenvector of $\boldsymbol{H}$, the value $\boldsymbol{\Lambda}$ is the diagonal matrix whose diagonal elements are the corresponding eigenvalues. We can see from the results that the MIMO channel is converted into $\min(N_R, N_T)$ SISO channels with the same transmit power for each transmitted signal.

Capacity of Random MIMO Channels

In reality, the channels are not deterministic, and the channels change randomly due to the mobility. The channel capacity also changes according to the random fading of the channel coefficients. Therefore, the random MIMO channel capacity can be obtained by taking the average capacity across time.

Assuming the randomness of the channel is an ergodic process, the ergodic capacity can be obtained by the following function

$$C_{\text{ergodic}} = E\Big\{ \max_{tr(\boldsymbol{R}_{ss})=N_T} \log_2 \det \Big(\boldsymbol{I}_{N_R} + \frac{1}{\sigma_v^2} \boldsymbol{H}\boldsymbol{R}_{\boldsymbol{ss}}\boldsymbol{H}^H \Big) \Big\}. \tag{2.12}$$

The ergodic MIMO channel capacity is shown in Fig. 2.2. CSI is not available to the transmitter, we can see from the figure that the ergodic capacity grows linearly as more antenna pairs are included.

2.2.2 MIMO Channel Estimation

In wireless transmission, the transmitted signal is usually distorted by the channel characteristics. To recover the transmitted bits, the channel characteristics must be measured and compensated at the receiver side [40] [41]. For instance, the CSI is not only required to perform channel equalization, but it is also required for detecting MIMO signals. By using pilot symbols or preamble which are known to both the transmitter and receiver, the channel estimation can be performed.

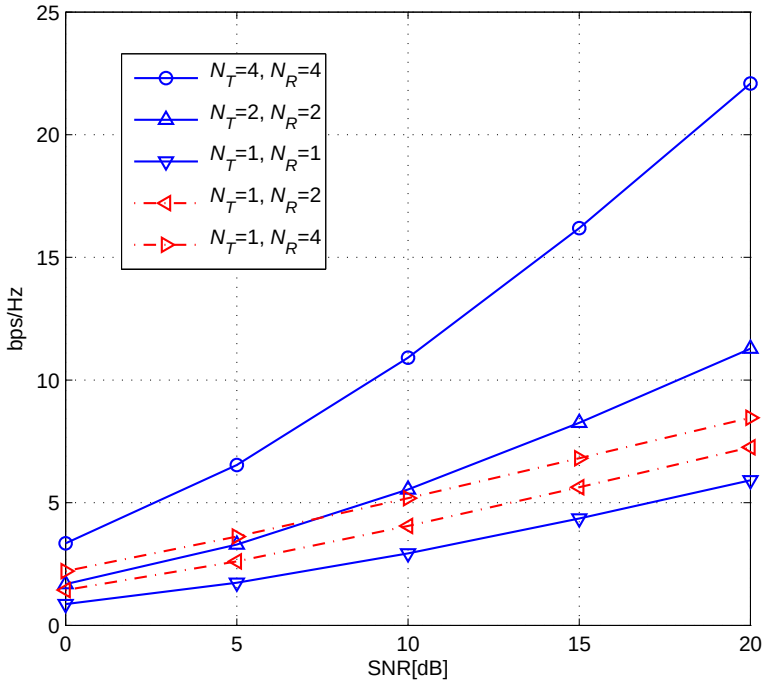

Figure 2.2: Ergodic channel capacity with various antenna configurations. CSI is not known by the transmitter.

Data-aided Channel Estimation

Compared with blind channel estimation techniques [42], data-aided channel estimation algorithms generally have better performance [43] at the cost of transmission efficiency due to the introduction of pilot symbols. One of the most widely used data-aided methods is the least-squares (LS) algorithm.

Least-squares Channel Estimation

Assuming multiple antennas are used, the channel $\boldsymbol{H}[i]$ has $N_R N_T$ tap weights and $[i]$ denotes the time index, let $\hat{\boldsymbol{H}}$ denotes the estimate of the channel. The transmitted pilot symbols $\boldsymbol{s}[i] \in \mathbb{C}^{N_T \times 1}$ are distorted by the channel $\boldsymbol{H}$ and collected as a received signal vector $\boldsymbol{r}[i] \in \mathbb{C}^{N_R \times 1}$.

The LS channel estimation algorithm computes the estimate of $\hat{\boldsymbol{H}}$ by minimizing the

following Euclidean cost function:

$$\begin{aligned}\mathcal{J}(\hat{\boldsymbol{H}}) &= \sum_{\tau=1}^{i} \lambda^{i-\tau} \left\| \boldsymbol{r}[\tau] - \hat{\boldsymbol{H}}[i]\boldsymbol{s}[\tau] \right\|^2 \\ &= \sum_{\tau=1}^{i} \lambda^{i-\tau} (\boldsymbol{r}[\tau] - \hat{\boldsymbol{H}}[i]\boldsymbol{s}[\tau])^H (\boldsymbol{r}[\tau] - \hat{\boldsymbol{H}}[i]\boldsymbol{s}[\tau]) \\ &= \sum_{\tau=1}^{i} \lambda^{i-\tau} (\boldsymbol{r}[\tau]^H - \boldsymbol{s}[\tau]^H \hat{\boldsymbol{H}}[i]^H)(\boldsymbol{r}[\tau] - \hat{\boldsymbol{H}}[i]\boldsymbol{s}[\tau]).\end{aligned} \tag{2.13}$$

where $1 < \lambda \ll 0$ is the forgetting factor. To minimize the cost function, the gradient of the cost function with regard to the channel estimate $\hat{\boldsymbol{H}}$ needs to be set to the zero matrix as

$$\begin{aligned}&\nabla_{\hat{\boldsymbol{H}}} \mathcal{J}(\hat{\boldsymbol{H}}) = \boldsymbol{0}, \\ &\sum_{\tau=1}^{i} \lambda^{i-\tau} \Big[\big(\boldsymbol{r}[\tau] - \hat{\boldsymbol{H}}[i]\boldsymbol{s}[\tau] \big) \boldsymbol{s}[\tau]^H \Big] = \boldsymbol{0}.\end{aligned} \tag{2.14}$$

The solution is given by

$$\hat{\boldsymbol{H}} = \boldsymbol{Y}\boldsymbol{X}^{-1}. \tag{2.15}$$

where $\boldsymbol{Y} = \sum_{\tau=1}^{i} \lambda^{i-\tau} \boldsymbol{r}[\tau]\boldsymbol{s}[\tau]^H$ and $\boldsymbol{X} = \sum_{\tau=1}^{i} \lambda^{i-\tau} \boldsymbol{s}[\tau]\boldsymbol{s}[\tau]^H$.

The mean-square error (MSE) of the LS channel estimation is obtained by

$$\text{MSE}_{LS} = E\big\{ (\boldsymbol{H} - \hat{\boldsymbol{H}})^H (\boldsymbol{H} - \hat{\boldsymbol{H}}) \big\}. \tag{2.16}$$

2.3 MIMO Detection Algorithms

The application of multiple antennas may be classified into the following two categories:

- By using diversity techniques, such as STBC [45] STTC etc [44] [46]. MIMO systems exploiting the resources such as space, time, frequency to compensate the deep fading effect which convert an unstable wireless fading channel into a stable AWGN-like channel.
- Without sacrificing the bandwidth, spatially multiplexed MIMO systems provide higher transmission rates as compared with the MIMO systems using the diversity

techniques mentioned above. The spatial multiplexing is generally realized by using signal detection algorithms at the receiver side to separate the co-channel data streams.

In this Chapter, we focus on the development of the detection techniques for spatially multiplexed MIMO systems.

Detecting Spatially Multiplexed MIMO

We adopt the MIMO system model described in the previous section, where $\boldsymbol{H} \in \mathbb{C}^{N_R \times N_T}$ is the complex channel matrix, each entry h_{n_r,n_t} denotes the channel gain between the n_t-th transmit antenna and the n_r-th receive antenna. The $N_R \times N_T$ MIMO system is given as

$$\begin{aligned} \boldsymbol{r}[i] &= \boldsymbol{H}\boldsymbol{s}[i] + \boldsymbol{v}[i] \\ &= \sum_{k=1}^{N_T} \boldsymbol{h}_k s_k[i] + \boldsymbol{v}[i], \end{aligned} \tag{2.17}$$

where $\boldsymbol{s}[i] \in \mathbb{C}^{N_T \times 1}$ is the transmitted data, $\boldsymbol{r}[i] \in \mathbb{C}^{N_R \times 1}$ is the received vector. The quantity $\boldsymbol{h}_k \in \mathbb{C}^{N_R \times 1}$ represents the k-th column vector of the channel matrix $\boldsymbol{H}$ and $\boldsymbol{v} \in \mathbb{C}^{N_R \times 1}$ is a zero-mean circular symmetric Gaussian noise.

2.3.1 Optimal Signal Detection

Maximum A Posteriori Probability Detection

Let us define a complex-valued noise vector $\boldsymbol{v}$ with the covariance matrix $E\{\boldsymbol{v}^H\boldsymbol{v}\} = \sigma_v^2\boldsymbol{I}$. The joint probability density function of $\boldsymbol{r}$, which is a multi-variate complex Gaussian with i.i.d. circularly symmetric component, given $\boldsymbol{s}$ and $\boldsymbol{H}$ is

$$P(\boldsymbol{r}|\boldsymbol{s},\boldsymbol{H}) = \frac{1}{(\pi\sigma_v^2)^{N_R}} \exp\Big(- \frac{\|\boldsymbol{y} - \boldsymbol{H}\boldsymbol{s}\|^2}{\sigma_v^2}\Big). \tag{2.18}$$

The maximum *a posteriori* probability (MAP) detection determines the estimate of the symbol vector by finding the possible transmitted signal vector with the highest *a*

posteriori probability,

$$\begin{aligned}\hat{\boldsymbol{s}}^{\text{MAP}} &= \arg \max_{\hat{\boldsymbol{s}} \in \mathcal{A}^{N_T}} P(\hat{\boldsymbol{s}}|\boldsymbol{r}, \boldsymbol{H}) \\ &= \arg \max_{\hat{\boldsymbol{s}} \in \mathcal{A}^{N_T}} P(\boldsymbol{r}|\hat{\boldsymbol{s}}, \boldsymbol{H}) P(\hat{\boldsymbol{s}}),\end{aligned} \tag{2.19}$$

where $\mathcal{A}$ denotes the set of complex constellations. The MAP detection achieves an optimal performance, however, the computational complexity of this algorithm increases exponentially as the number of dimensions increases, such as modulation order and the number of transmit antennas. The MAP algorithm requires the *a priori* information $P(\hat{\boldsymbol{s}})$ to compute the metric in (2.19). If it is the case that all the transmitted vectors are equally likely, then the MAP detection is equivalent to maximum likelihood (ML) detection.

Maximum Likelihood Detection

The optimal ML detection algorithm tries all the possible transmitted signal vectors with the given channel $\boldsymbol{H}$, the detector computes the Euclidean distance by $\mathcal{J}(s)_{\text{Euclidean}} = \|\boldsymbol{r} - \boldsymbol{H}\hat{\boldsymbol{s}}\|^2$, the signal vector with the minimum Euclidean distance is determined as the estimate of the transmitted signal.

$$\begin{aligned}\hat{\boldsymbol{s}}_{ML} &= \arg \max_{\boldsymbol{s} \in \mathcal{A}^{N_T}} P(\boldsymbol{r}|\boldsymbol{s}) \\ &= \arg \max_{\boldsymbol{s} \in \mathcal{A}^{N_T}} \frac{1}{(\pi\sigma_v^2)^{N_T}} \exp(-\frac{\|\boldsymbol{r} - \boldsymbol{H}\boldsymbol{s}\|^2}{\sigma_v^2}) \\ &= \arg \min_{\boldsymbol{s} \in \mathcal{A}^{N_T}} \mathcal{J}(s)_{\text{Euclidean}},\end{aligned} \tag{2.20}$$

Similarly to MAP detection, the algorithm requires an exhaustive search of $|\mathcal{A}|^{N_T}$ equations in (2.20) . The high complexity of the metric calculation prevents the actual application of these detectors in the real world, except for very small systems and constellations.

2.3.2 Linear Signal Detection

Linear detection methods recover the desired data stream from the multiple-antenna data streams by applying a linear transformation followed by a decision of the transmitted symbol. The interference signals from the other transmit antennas are suppressed or nullified before detecting the data streams from the desired transmit antenna. In the linear

detection algorithm, each symbol is estimated by a linear combination of the received signals and the filter matrix $\boldsymbol{\Omega} \in \mathbb{C}^{N_R \times N_T}$.

The linear transformation is often expressed as a filter matrix and can be obtained by solving the following optimisation problem under the minimum-mean-square-error (MMSE) criterion,

$$\boldsymbol{\Omega}_{\text{MMSE}} = \arg \min_{\boldsymbol{\Omega}_{\text{MMSE}}} \{\boldsymbol{s} - \boldsymbol{\Omega}_{\text{MMSE}}^H \boldsymbol{r}\}, \tag{2.21}$$

The solution is given by

$$\boldsymbol{\Omega}_{\text{MMSE}} = \big(\boldsymbol{H}^H \boldsymbol{H} + \frac{\sigma_v^2}{\sigma_s^2}\boldsymbol{I}\big)^{-1} \boldsymbol{H}^H. \tag{2.22}$$

The estimate of the transmitted vector $\boldsymbol{s}$ is obtained by processing the received vector $\boldsymbol{r}$ with the filter matrix $\boldsymbol{\Omega}_{\text{MMSE}}$, which is given by

$$\begin{aligned} \tilde{\boldsymbol{s}} &= \boldsymbol{\Omega}_{\text{MMSE}}^H \boldsymbol{r} \\ &= \big(\boldsymbol{H}^H \boldsymbol{H} + \frac{\sigma_v^2}{\sigma_s^2}\boldsymbol{I}\big)^{-1} \boldsymbol{H}^H \boldsymbol{r} \\ &= \boldsymbol{s} + \big(\boldsymbol{H}^H \boldsymbol{H} + \frac{\sigma_v^2}{\sigma_s^2}\boldsymbol{I}\big)^{-1} \boldsymbol{H}^H \boldsymbol{v} \\ &= \boldsymbol{s} + \boldsymbol{v}_{\text{MMSE}}. \end{aligned} \tag{2.23}$$

where $\boldsymbol{v}_{\text{MMSE}}$ is the MMSE effective noise. From the above equations we can conclude that the performance of linear detection is directly related to the power of the MMSE effective noise which is calculated as

$$\begin{aligned} E\big\{\|\boldsymbol{v}_{\text{MMSE}}\|^2\big\} &= E\Big\{\big\|\big(\boldsymbol{H}^H \boldsymbol{H} + \frac{\sigma_v^2}{\sigma_s^2}\boldsymbol{I}\big)^{-1} \boldsymbol{H}^H \boldsymbol{v}\big\|^2\Big\} \\ &= \sum_{k=1}^{N_T} \frac{\sigma_k^2 (\frac{\sigma_v}{\sigma_s})^2}{(\sigma_k^2 + (\frac{\sigma_v}{\sigma_s})^2)^2}, \end{aligned} \tag{2.24}$$

where $\sigma_k, k = 1, \ldots, \min\{N_T, N_R\}$ are diagonal elements and mathematical manipulations of the above equations can be found in Appendix A.

2.3.3 Successive Interference Cancellation

V-BLAST [7] is a non-linear successive interference cancellation (SIC) based detection algorithm with sorted cancellation ordering. Primarily, these non-linear methods have

better performance than linear algorithms at the cost of the complexity of hardware implementation.

Instead of detecting the N_T data streams simultaneously as the linear detectors do, the SIC detection algorithms detect the signal components in a sequential bias. The successively detected signal in each stream is then subtracted from the received signal, the remaining received signal with the reduced interference is used for performing the signal estimation for the following streams [47].

The conventional SIC algorithm computes the $N_R \times 1$ MMSE filter corresponding to each layer's data stream as

$$\boldsymbol{\omega}_k = (\bar{\boldsymbol{H}}_k \bar{\boldsymbol{H}}_k{}^H + \frac{\sigma_v^2}{\sigma_s^2}\boldsymbol{I})^{-1}\boldsymbol{h}_k. \tag{2.25}$$

where $\bar{\boldsymbol{H}}_k$ denotes the matrix obtained by taking the columns $k, k+1, \ldots K$ of $\boldsymbol{H}$. In this algorithm, the procedure uses nulling and symbol cancellation to successively detect the desired symbol for each data stream $\hat{s}_k[i], k = 1, \ldots, K$.

$$\hat{s}_k[i] = Q(\boldsymbol{\omega}_k^H \check{\boldsymbol{r}}_k[i]), \tag{2.26}$$

where $Q(\cdot)$ denotes the quantization operation and $[i]$ is the index of symbol period. These detected symbols construct decision vector $\hat{\boldsymbol{s}}[i] = [\hat{s}_1[i], \hat{s}_2[i], ..., \hat{s}_K[i]]^T$. The successively cancelled received vector in the k-th stage is

$$\begin{cases} \check{\boldsymbol{r}}_k[i] = \boldsymbol{r}[i], & k = 1, \\ \check{\boldsymbol{r}}_k[i] = \boldsymbol{r}[i] - \sum_{j=1}^{k-1} \boldsymbol{h}_j \hat{s}_j[i], & k \geq 2. \end{cases} \tag{2.27}$$

After subtracting the detected symbols from the received signal vector, the remaining signal vector is processed either by an MMSE or a ZF filter for the symbol estimation in the following streams. The SIC detector uses a simple sliced symbol as the feedback and its reliability is disregarded. In terms of the computational complexity, the SIC detector based on the MMSE criterion has $\mathcal{O}({N_R}^3)$. In the popular V-BLAST scheme, a signal-to-noise-ratio (SNR) ordered SIC (O-SIC) based on MMSE or zero forcing (ZF) estimation is employed. The detected signal is subtracted through a feedback loop that performs an interference cancellation and improves the overall bit error rate in MIMO systems. In the case $\hat{s}_k = s_k$, the strong interference s_k is successfully cancelled. However, if it is the case that $\hat{s}_k \neq s_k$, the subtraction operation with the erroneous detected symbol may

cause error bursts and overall performance degradation. This problem is named error propagation [48] [49], which limits the performance of SIC based detectors. In order to constrain the error propagation effect, it is desirable to detect reliable signals in the early stages, therefore, the detection nulling and cancellation order (NCO) has significant influence on the performance of SIC methods.

SINR Ordering

The post-detection signal-to-interference-plus-noise-ratio (SINR) is used to decide the order of detection. In this algorithm, the noise characteristic and the channel gains are used for deciding the NCO [50]. The SINR of each layer is given by

$$\text{SINR}_k = \frac{\sigma_s^2 |\boldsymbol{\omega}_{k,\text{MMSE}} \boldsymbol{h}_k|^2}{\sigma_s^2 \sum_{l \neq k} |\boldsymbol{\omega}_{k,\text{MMSE}} \boldsymbol{h}_l| + \sigma_v^2 \|\boldsymbol{\omega}_{k,\text{MMSE}}\|}, \tag{2.28}$$

where $\boldsymbol{\omega}_{k,\text{MMSE}}$ is the k-th row of the MMSE matrix (2.22) and $\boldsymbol{h}_k$ is the k-th column vector of the channel matrix $\boldsymbol{H}$. The MMSE criteria is considered and the post-detection SINR is maximized.

By choosing the layer with the highest SINR, the algorithm performs the nulling and the order of cancellation is decided. The estimated symbol with this layer is then cancelled from the receive vector and the corresponding column vector of of the channel $\boldsymbol{h}_k$ is removed from the channel matrix. The nulled channel matrix is then used to compute $\boldsymbol{\omega}_k$ in (2.28) and choose the highest SINR from the remaining undetected symbols. This process is repeated until all $s_1, \ldots, s_{N_T}$ are detected.

SNR Ordering

By ignoring the interference terms in (2.28), the SNR based equation used in deciding the ordering is obtained, the equation is simplified as

$$\text{SNR}_k = \frac{\sigma_s^2}{\sigma_v^2 \|\boldsymbol{\omega}_k\|^2}. \tag{2.29}$$

Similarly to SINR ordering, the procedure is required to repeat $N_T - 1$ times to obtain the order of nulling and cancelling.

Channel Norm Ordering

The aforementioned ordering methods have good performance, however, they incur rather high computational complexity. For systems with a large number of antennas, the involved matrix inversion bring about very high complexity, especially when the channel matrix is time-varying [51]. In order to reduce the ordering complexity, a scheme named channel norm ordering is introduced by using the column vectors in the channel matrix.

Let us assume the transmitted symbols have equal power, e.g. PSK modulation is used. We observe that the received signal strength of the transmitted s_k relies on the norm of the k-th column in the channel matrix $\boldsymbol{H}$, the received signal strength of the $k-$th transmitted signal is proportional to the norm of the k-th column in the channel matrix. Therefore, we can detect the signal in the order of the norms of the column vectors.

The order of detecting the signal can be configured corresponding to a decreasing order of $\|\boldsymbol{h}_k\|$ where $k = 1, \ldots, N_T$.

$$\|\boldsymbol{h}_1\|^2 \geq \|\boldsymbol{h}_2\|^2 \geq \ldots \geq \|\boldsymbol{h}_{N_T}\|^2, \tag{2.30}$$

where $\boldsymbol{h}_k$ is the k-th column vector of the channel matrix $\boldsymbol{H}$. Instead of $N_T - 1$ loops, the column norm ordering is required only once. The complexity of channel norm ordering is significantly lower than those of the SNR and SINR based ordering methods.

In Fig. 2.3, the curves represent the bit-error-rate (BER) performance of the MMSE based SIC detection with different NCO methods. In the simulations, 8 antenna pairs are used and 8-PSK symbols are transmitted. The SINR ordering method outperforms other two and the channel norm base ordering has the worst performance among the three.

2.3.4 Sphere Decoding

The tree search based sphere decoder (SD) [52] is an alternative scheme for finding the ML solution vector among all the possible transmitted symbol vectors. Instead of searching all the possible decision branches (optimal method), SD considers only a small set of possible transmitted signal vectors within a sphere [53] [18]. The dynamic adjustment

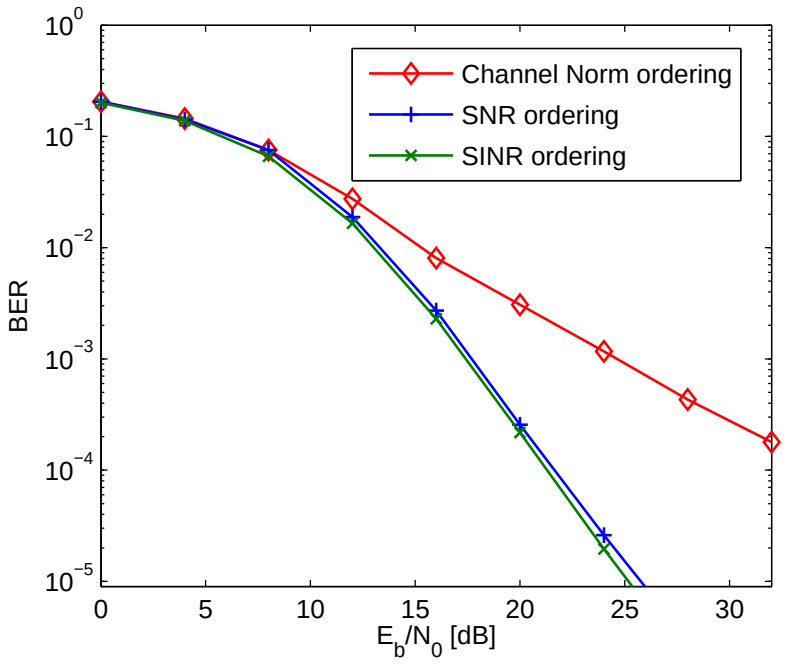

Figure 2.3: Performances of SIC detection with different detection ordering methods. CSI is perfectly known by the receiver. MMSE receiver with 8-PSK modulation on a 4×4 MIMO channel.

of the sphere radius is also introduced in order to find the single ML solution vector. Consider (2.1) expressed in an alternative form by the following equations:

$$\bar{\boldsymbol{r}} = \bar{\boldsymbol{H}}\bar{\boldsymbol{s}} + \bar{\boldsymbol{v}} \tag{2.31}$$

where

$$\bar{\boldsymbol{r}} = \begin{bmatrix} \Re\{\boldsymbol{r}\} \\ \Im\{\boldsymbol{r}\} \end{bmatrix} \qquad \bar{\boldsymbol{s}} = \begin{bmatrix} \Re\{\boldsymbol{s}\} \\ \Im\{\boldsymbol{s}\} \end{bmatrix} \qquad \bar{\boldsymbol{v}} = \begin{bmatrix} \Re\{\boldsymbol{v}\} \\ \Im\{\boldsymbol{v}\} \end{bmatrix}, \tag{2.32}$$

and

$$\bar{\boldsymbol{H}} = \begin{bmatrix} \Re\{\boldsymbol{H}\} & -\Im\{\boldsymbol{H}\} \\ -\Im\{\boldsymbol{H}\} & \Re\{\boldsymbol{H}\} \end{bmatrix} \in \mathbb{R}^{2N_R \times 2N_T}. \tag{2.33}$$

The SD exploits the following relations and the mathematical manipulations of the following equations can be found below

$$\begin{aligned} \hat{\bar{\boldsymbol{s}}} &= \arg\min_{\hat{\bar{\boldsymbol{s}}}} \|\bar{\boldsymbol{r}} - \bar{\boldsymbol{H}}\|^2 \\ &= \arg\min_{\hat{\bar{\boldsymbol{s}}}} (\bar{\boldsymbol{s}} - \hat{\bar{\boldsymbol{s}}})^T \bar{\boldsymbol{H}}^T \bar{\boldsymbol{H}} (\bar{\boldsymbol{s}} - \hat{\bar{\boldsymbol{s}}}) \\ &= \arg\min_{\hat{\bar{\boldsymbol{s}}}} (\bar{\boldsymbol{s}} - \hat{\bar{\boldsymbol{s}}})^T \bar{\boldsymbol{R}}^T \bar{\boldsymbol{Q}}^T \bar{\boldsymbol{Q}} \bar{\boldsymbol{R}} (\bar{\boldsymbol{s}} - \hat{\bar{\boldsymbol{s}}}) \\ &= \arg\min_{\hat{\bar{\boldsymbol{s}}}} \|\bar{\boldsymbol{R}}(\bar{\boldsymbol{x}} - \hat{\bar{\boldsymbol{x}}})\|^2 \end{aligned} \tag{2.34}$$

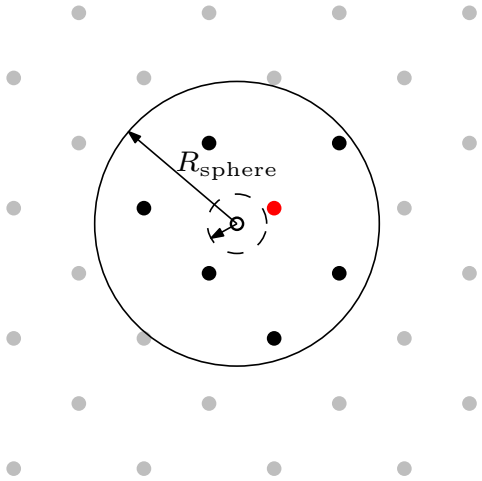

Figure 2.4: Illustration of sphere radius. The center of the circus denotes the linear ZF estimation and the red dot denotes the ML vector.

where $\bar{\boldsymbol{H}} = \bar{\boldsymbol{Q}}\bar{\boldsymbol{R}}$ is the QR decomposition of the channel matrix and the metric $\|\bar{\boldsymbol{R}}(\bar{\boldsymbol{x}} - \hat{\bar{\boldsymbol{x}}})\|^2$ is constrained within the sphere radius

$$\|\bar{\boldsymbol{R}}(\bar{\boldsymbol{x}} - \hat{\bar{\boldsymbol{x}}})\|^2 \leq R^2_{\text{sphere}}. \tag{2.35}$$

Fig.2.4 illustrates a sphere with a centre of $\hat{\bar{\boldsymbol{s}}} = (\bar{\boldsymbol{H}}^H\bar{\boldsymbol{H}})^{-1}\bar{\boldsymbol{H}}^H\hat{\bar{\boldsymbol{r}}}$. The algorithm only considers the lattice points inside the sphere, the ML solution vector is included. The ML vector is represented as the lattice point which is closest among the candidates. For the sake of detection simplicity, the sphere radius can be reduced such that we may have a single vector remaining. However, if we choose the radius too small, and zero lattice point is included in the sphere, the sphere radius R^2_{sphere} needs to be enlarged to cover at least one lattice point. The upper-triangle structure of $\bar{\boldsymbol{R}}$ provides

$$\sum_{k=1,\ldots,N_T} \left| \sum_{j=N_T,\ldots,k} \bar{r}_{k,j}(\bar{s}_j - \hat{\bar{s}}_j) \right|^2 \leq R^2_{\text{sphere}}, \tag{2.36}$$

where $\bar{s}_j$ and $\hat{\bar{s}}_j$ is the j-th element of the vector $\bar{\boldsymbol{s}}$ and $\hat{\bar{\boldsymbol{s}}}$ respectively. The quantity $\bar{r}_{k,j}$ is the element in the k-th row and j-th column of $\bar{\boldsymbol{R}}$.

The performance of the SD is the same as the optimal ML detector provided the radius is appropriately selected, whereas the computational complexity can be significantly reduced.

2.4 Iterative Processing

In this chapter, a number of iterative processing methods are reviewed. First, we introduce the encoding and decoding structure of the turbo codes. And then, as the extension of the turbo decoding, a method named iterative detection and decoding (IDD) algorithm with spatially multiplexed MIMO systems is described. Finally, an analytical tool namely *extrinsic* information transfer (EXIT) chart, is given to analyse the behaviour of the iterative processing procedure.

2.4.1 Turbo Codes

In 1993, the gap between the channel coding systems and Shannon's theoretical limit was closed by Berrou, Glavieux and Thitimajshima. The term "turbo codes" was then used to describe a class of concatenation codes that employ an iterative decoding structure to achieve a near-capacity signal transmission in wireless communications.

Parallel Concatenated Codes

The first version of the Turbo Codes is the parallel concatenation of two component codes, as illustrated in Fig. 2.5, the constituent code is known as recursive systematic convolutional (RSC) code. Two identical RSC encode two bit sequences in a parallel manner. One stream of bit sequence is the message bits, the other stream is the interleaved message bit sequence. The encoded message (parity bits) and the original message (systematic bits) are then distorted by noise and used for decoding. The decoding scheme for the parallel concatenated codes is described as follows. By using the soft-input soft-output (SISO) based MAP decoding algorithm, two codes are decoded separately. Each decoder uses the extrinsic information on the systematic bits of the other decoder as *a priori* knowledge. After a number of iterations, the decoder converges and the estimates of the *a posteriori* probability of the transmitted bits are obtained at the output of the decoder.

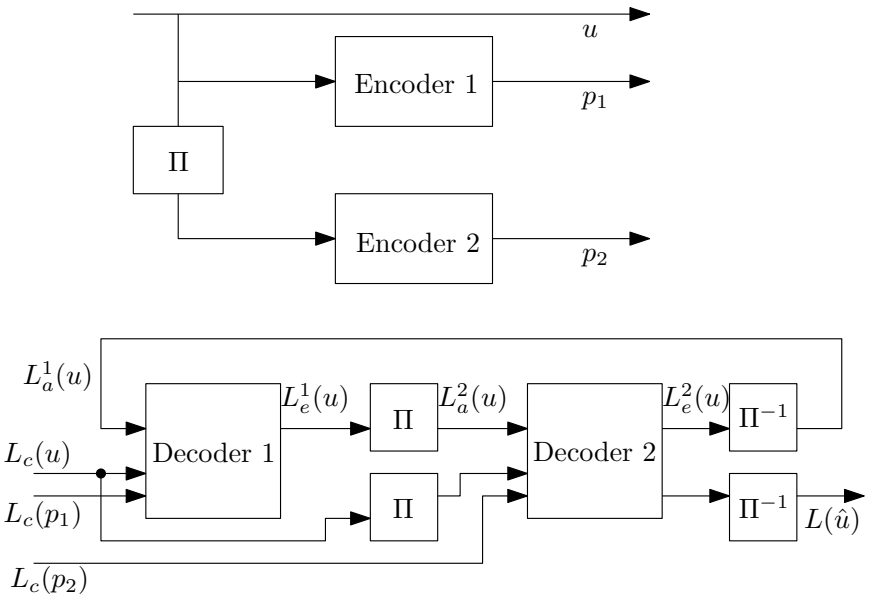

Figure 2.5: Parallel concatenated encoding and decoding structure. $L(\hat{u})$, $L_c(u)$, $L_a(u)$ and $L_e(u)$ denote the *a posteriori*, channel, *a priori* and *extrinsic* information, respectively. The upper scripts ^{1} and ^{2} denote the values are used or produced by the decoder 1 and decoder 2, respectively.

Serial Concatenated Codes

The encoding and decoding of a serially concatenated code is depicted in Fig.2.6. The coded bits of the outer encoder are interleaved before being fed to the inner encoder. The constituent outer code is non-systematic convolutional codes (NSC). In order to achieve the interleaver gain, RSC is required by the outer code. The outer code should have a large free distance and a good distance spectrum [54]. Similarly to decoding parallel concatenated codes, the two decoders in serial exchange the extrinsic information as the the decoding iterations are performed. The difference with the parallel concatenated code is that the outer decoder only receives the channel information through the inner decoder. Since no extra input is required for the outer decoder, the serial concatenation is naturally easily generalized for application in many communications scenarios.

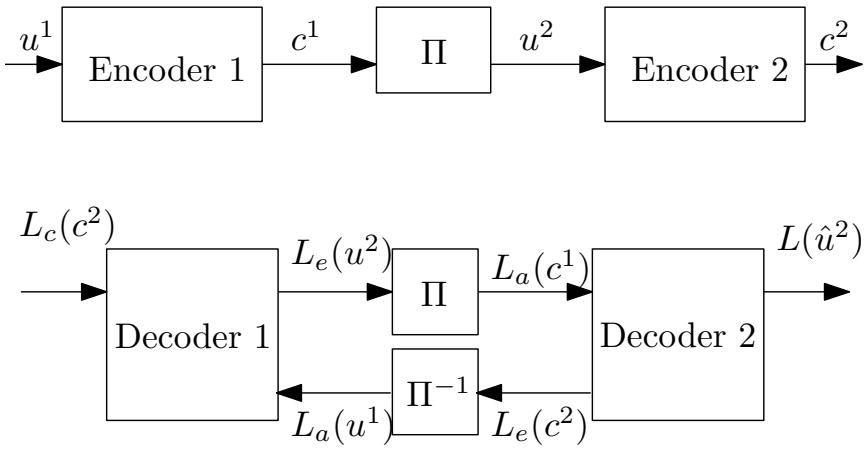

Figure 2.6: Serial concatenated encoding and decoding structure. $L(\hat{u})$, $L_c(c)$, $L_a(u)$ and $L_e(u)$ denote the *a posteriori*, channel, *a priori* and extrinsic information, respectively. The upper scripts ^{1} and ^{2} denote the values are used or produced by the decoder 1 and decoder 2, respectively.

2.4.2 Iterative Detection and Decoding

Shortly after the introduction of turbo codes, the concept of iterative decoding has been recognized as central for solving a large number of decoding and detection problems in wireless communication systems [55]. The so-called "turbo concept" has been incorporated as a general methodology for advanced system design in the following applications,

- iterative equalization [57] [19]
- iterative BICM [58] [59]
- iterative MIMO detection and decoding [18] [19]
- iterative multiuser detection [56] [19]
- iterative channel estimation [63]
- iterative detection with base station cooperation [22] [60]
- iterative interleave division multiple access [64]

In this thesis, the author is generally interested in developing iterative detection and decoding (IDD) algorithms for spatially multiplexed MIMO data streams. Fig. 2.7 illustrate

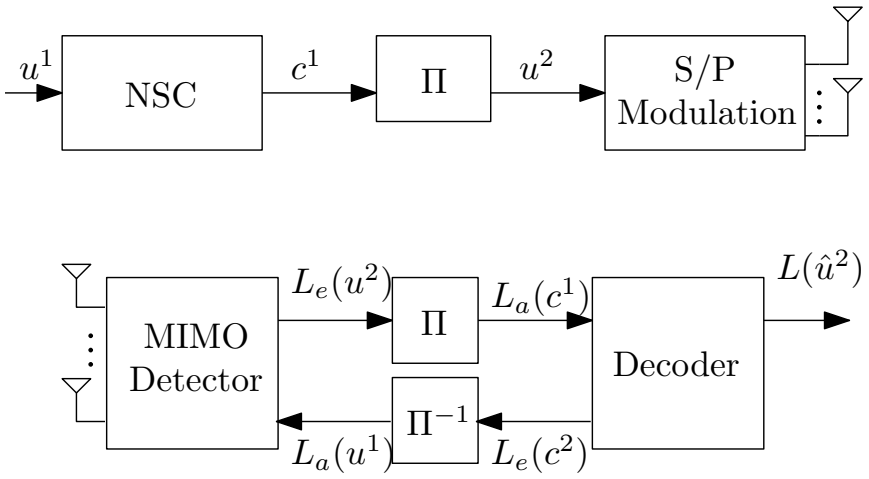

Figure 2.7: Block diagram of a iterative MIMO detection and decoding transmission system.

the structure of a MIMO IDD transmission system. The message is first encoded by a NSC, the coded bits are then interleaved and fed to the device which performs spatial multiplexing, the multiplexed bits are modulated to symbols before radiating from N_T transmitting antennas. At the receiver side, the SISO MIMO detector is applied to detect the transmitted symbols and convert the symbol probability to bit probability in the form of log-likelihood ratios (LLRs). The extrinsic information $L_e(\cdot)$ is then exchanged between the detector and the decoder with several iterations. The *a posteriori* probability of the transmitted bits are then finally obtained at the output of the decoder.

On one hand, the NSC and decoder blocks are considered as the outer code of the serially concatenated structure, when NSC is applied, BCJR [65] based MAP or log-MAP decoding algorithm can be applied as well as the lower complexity alternative named soft-output Viterbi algorithms (SOVA) [66]. Instead of using NSC as the channel code, turbo codes and LDPC codes have also been used in this structure to obtain a near-capacity performance [18] [67]. On the other hand, the S/P modulation and MIMO detection blocks are considered as the inner component of the serially concatenated structure. In general, MAP is the optimal algorithm used as the SISO detection component in the IDD receiver. The MAP detection and its simplified version such as log-MAP, max-log-MAP provide the optimal BER performance, however, the complexity is extreme even with a moderate number of antennas and modulation level. In order to solve this problem, a "list" version of SD was developed by Hochwald and Ten Brink without significant loss of performance [18]. The complexity of the MIMO detection is further brought

down by introducing soft parallel interference cancellation (SPIC) in [19], [91] at the cost of performance loss. Recently, the SPIC was successfully applied to the hardware implementation by Studer in his thesis [27].

2.4.3 EXIT Chart Analysis

The iterative processing principle provides substantial gains in each "turbo" iteration. It is difficult to analyse the behavior and the performances of its two constituent components. Many efforts have been made to investigate the convergence behavior of iterative decoding, such as the methods mentioned in [69] and [70]. Among them, the extrinsic information transfer (EXIT) chart reported in 2001 by Ten Brink is the one widely used by researchers and designers. By using this tool, mutual information is measured and used to describe the flow of extrinsic information through the SISO components.

With the restriction of binary inputs $x \in \{+1, -1\}$, the mutual information between the transmitted data X and the respective information L is obtained as [70]

$$\begin{aligned} I(L;X) &= 1 - \int_{-\infty}^{+\infty} p(L|x=+1)\log_2(1+e^{-L})dL, \\ &= 1 - E\{\log_2(1+e^{-L})\}, \\ &\approx 1 - \frac{1}{N}\sum_{j=1}^{N}\log_2(1+e^{-x_n L_n}), \end{aligned} \tag{2.37}$$

where L is in the form of log-likelihood-ratio (LLR). The expectation operation is approximated by time averages, a large number of samples x_n is required for an accurate estimation.

Fig. 2.8 illustrates the EXIT chart for outer convolutional codes with memories 2, 3, 4, 5 and rates 1/2, 1/4, respectively. All curves start at (0,0) and finish at (1,1) point, the mutual information at the output of the log-MAP decoder I_E is plotted in the horizontal axis, and at the input of the decoder, mutual information I_A is given in the vertical axis.

Let us assume a serial concatenation given by Fig. 2.7, where the modulator and the detector are considered as the inner component for the IDD receiver structure. In this configuration, we also assume a single antenna is used for both transmitter and receiver. The

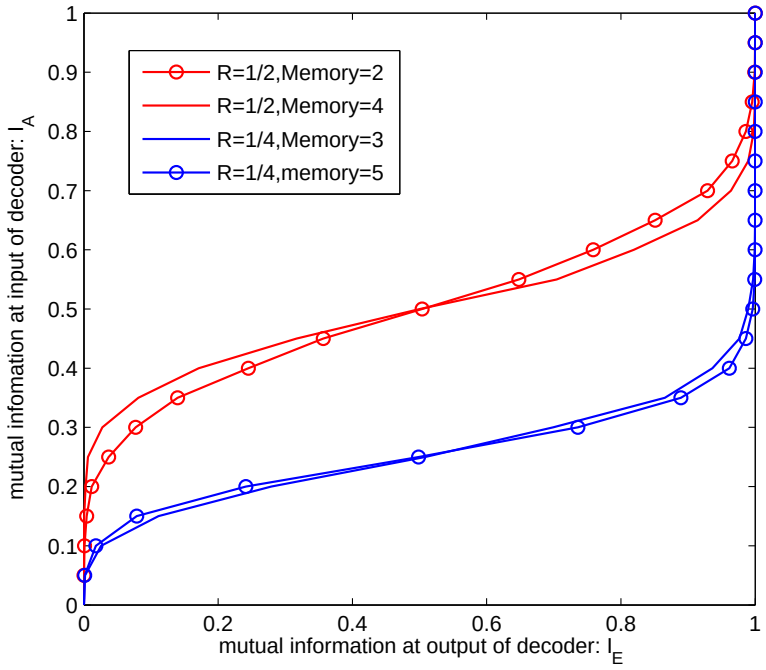

Figure 2.8: EXIT charts of a coded system with different convolutional codes as outer codes.

EXIT charts for the outer component (detector) are given in Fig. 2.9 by using different bit mappings. We can see that Gray labelling does not benefit from the *a priori* mutual information which means there is no iteration gain with the application of IDD. Other labelling methods such as anti-Gray, maximum euclidean weight (MSEW) and set partitioning (SP) [71], all benefit from the *a priori* knowledge. With the help of EXIT charts, the behaviour of the IDD structure can be analysed and the design of the concatenation components are also easier.

Fig. 2.10 illustrates a spatially multiplexed 4×4 MIMO system with IDD receiver. The exchange of extrinsic information is shown in terms of the trajectory. In this figure, the solid lines denotes the EXIT curves which are obtained by $E_b/N_0 = 7$ dB, and the dashed lines show the curves plotted with $E_b/N_0 = 5$ dB. Due to noise, the detection and decoding tunnel is closed and the trajectory is terminated at the early stage. In this situation, the *a priori* information provided by the decoder is not helping the detection and a higher SNR is needed to raise the detector curve and to create an open tunnel. There are also a number of ways to create a tunnel without increasing the SNR, such as using different mapping scheme or precoding techniques [113].

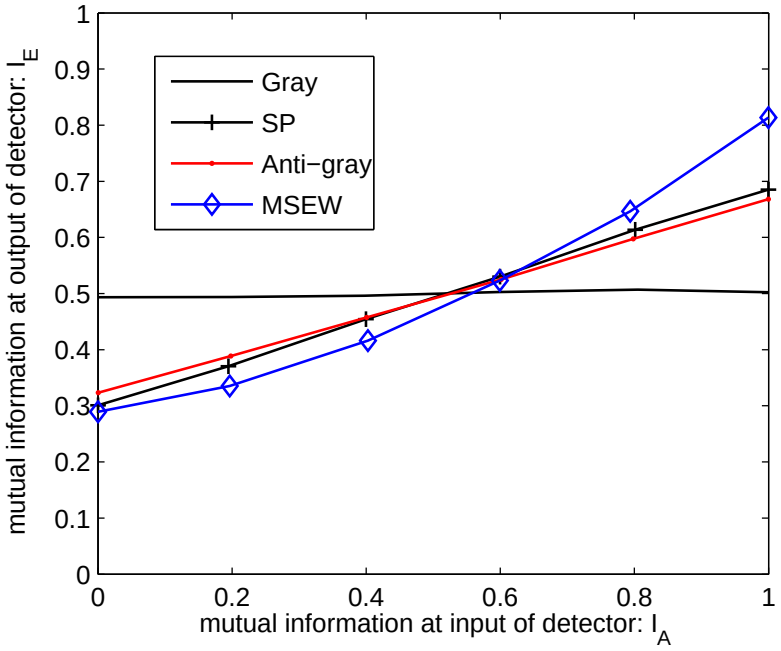

Figure 2.9: EXIT charts for 8-PSK modulation , 1×1 antenna system. The detector uses log-MAP algorithm and $E_b/N_0 = 7dB$.

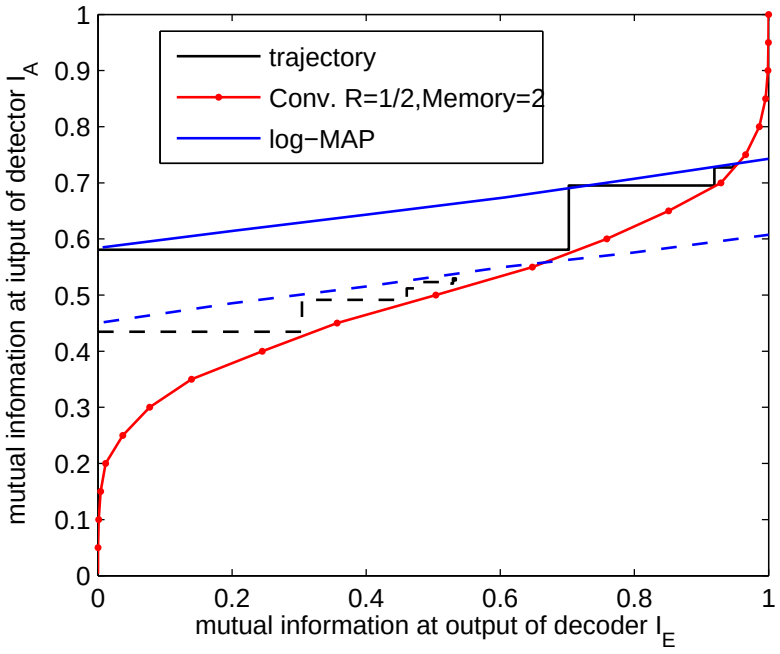

Figure 2.10: EXIT charts for a 4×4 system, with log-MAP detection and rate 1/2 convoltuional code.

2.5 Summary

In this chapter, we introduced background knowledge of MIMO systems and the corresponding receiver techniques which are used in the later chapters of this thesis. In the first part of this chapter, we described the transmission model of multiple antenna systems and the analysis of the capacity of MIMO systems was given in detail. It is evident that the multiple antenna systems have an attractive ability to increase the bandwidth efficiency with the spatial multiplexing configuration. Then, the parameter estimation methods used for channel estimation have been also included in order to facilitate the use of channel state information (CSI) in the detection and decoding operations. In the second part of the chapter, we started from reviewing the optimal MAP and ML detectors and then, a series of sub-optimal detectors have also been described in detail, namely the MMSE based linear detection, MMSE based SIC detection as well as sphere decoding algorithm. These sub-optimal detection algorithms have computational complexities significantly lower than the optimal ones. Meanwhile, the channel control coding such as convolutional codes and turbo codes are described as the components of the iterative processing structure. The SISO iterative detection and decoding algorithm was also illustrated and the EXIT chart analysis was introduced.

Chapter 3

Multiple Feedback Successive Interference Cancellation for Multi-Antenna Systems

Contents

3.1 Overview

In this chapter, a low-complexity multiple feedback successive interference cancellation (MF-SIC) strategy is proposed for point-to-point and multiuser MIMO systems. This is motivated by the fact that, for detection algorithms, optimal maximum likelihood detection (MLD) and sphere decoder (SD) require an exponential complexity as the number of

data streams and the modulation level increases. In the proposed MF-SIC algorithm with shadow area constraints (SAC) strategy, enhanced interference cancellation is achieved by introducing constellation points as the candidates to combat the error propagation in decision feedback loops. We also combine the MF-SIC with multi-branch (MB) processing, which achieves a higher detection diversity order.

For coded systems, a low-complexity soft-input soft-output (SISO) iterative (turbo) detector is proposed based on the MF and the MB-MF interference suppression techniques for detecting MIMO signals.

The computational complexity of the MF-SIC algorithm is comparable to the conventional SIC algorithm since very little additional complexity is required. Simulation results show that the proposed algorithms significantly outperform the conventional SIC scheme and approach the optimal ML detector.

3.2 Introduction

It has been recognized that deploying multiple transmit and receive antennas can significantly improve the performance of wireless links in communication systems [8]. Multiple co-located antennas provide dramatic spatial multiplexing [6] and diversity gains [9]. The multiplexing gains allow higher spectral efficiency whereas diversity gains provide more reliable transmission with lower detection error rate over wireless fading channels. In this chapter, we focus on the multiplexing gains provided by the MIMO systems as well as the detection performance.

Significant capacity gains can be achieved with MIMO systems using a spatial multiplexing configuration. The capacity grows linearly with the number of transmissions of individual data streams from the transmitter to the receiver [8]. In order to separate these streams, several detection techniques have been developed:

- The optimum maximum likelihood detection (MLD) scheme which performs an exhaustive search of the constellation map has exponential complexity with the

increasing number of data streams and constellation points. [38]. Therefore, the investigation of sub-optimal low-complexity detection schemes that can approach the optimal performance is of fundamental importance.

- The tree search-based sphere decoding (SD) can successfully separate each data stream with reduced complexity compared with the MLD [72]. However, the complexity of the SD can be polynomial or exponential depending on the size of the constellation map and the SNR values. The complexity of these algorithms is always high for low to moderate SNR values with a high number of antenna streams [76]. For the coded systems, as we know, the detector is typically operated at low to moderate SNRs.

- Linear detection (LD) [38] based on the minimum mean-square error (MMSE) or the zero-forcing (ZF) criteria is a low-complexity scheme but the error performance is unacceptable due to the co-channel interference (CCI).

- On the other hand, there are also other strategies to achieve the capacity gains of MIMO systems, non-linear detection techniques such as the successive interference cancellation (SIC) with a decision feedback (DF) structure [75], used in the vertical Bell Labs layered space-time (V-BLAST) [7] have a low-complexity, while achieving a reduced CCI as compared to their linear counterparts. However, these decision-driven detection algorithms suffer from error propagation and performance degradation.

Thus, all the mentioned detectors are either unable to provide satisfactory error rate performance or have an impractical computational complexity. Therefore, the design of alternative low-complexity detection algorithms is an important research topic for future MIMO wireless communication systems.

In this work, inspired by the error propagation mitigation in decision feedback detection [48, 49, 76, 84, 92], we introduce a novel multiple feedback SIC (MF-SIC) algorithm with shadow area constraints (SAC) strategy for detection of multiple data streams which requires low computational complexity. The MF selection algorithm searches several constellation points rather than one and chooses the most appropriate constellation symbol as the decision. In the subsequent layers, signal cancellation is performed with these

decisions. By doing so, even if a previous decision error is made, the correct cancellation may still carry on subject to the condition that the right decision is included in the feedback set. More points in the decision tree are considered and the error propagation is efficiently mitigated. The selection procedure is constrained to one selected symbol in each spatial layer to prevent the search space from growing exponentially, unlike sphere decoders which employ a search procedure for more layers that increases the computational load. Furthermore, SAC further saves computational complexity by evaluating the quality of decisions and avoiding unnecessary multiple feedback procedures for reliable estimates.

The MF-SIC is also combined with a multi-branch (MB) [76] processing framework to further improve the performance. A two stage iterative receiver structure is developed for coded systems and a low-complexity soft-input soft-output (SISO) detector is proposed based on the MF-SIC strategy. In addition, for soft-output nulling/cancelling based detection, the MF-SIC strategy is combined with the soft interference cancellation (SC) for the sake of reducing the required number of iterations to achieve the full iteration gain.

Simulation results show that the proposed schemes significantly outperform the conventional SIC schemes and have a comparable performance with the interference free bound.

The contributions of this chapter can be summarized as follows:

- A novel low-complexity MF-SIC detector is developed.
- MB processing is incorporated into the proposed MF-SIC to achieve a higher detection diversity order and to yield a close to optimal performance.
- An iterative detection and decoding (IDD) receiver is introduced to approach the interference free performance in coded systems.
- A study of the proposed MF-SIC and some existing detection schemes for MIMO systems is conducted.

3.3 System and Data Model

In this section, the mathematical models of both point-to-point and multiuser MIMO systems are given.

3.3.1 Point-to-point MIMO Systems

Let us consider a spatial multiplexing MIMO system with K transmit antennas and N_R receive antennas, where $N_R \geq K$. At each time instant $[i]$, the system transmits K symbols which are organized into a $K \times 1$ vector

$$\boldsymbol{s}[i] = \big[s_1[i],\ \ldots,\ s_k[i],\ \ldots,\ s_K[i]\big]^T, \tag{3.1}$$

from a constellation $\mathcal{A} = \{a_1,\ a_2,\ \ldots,\ a_C\}$, where $(\cdot)^T$ denotes transpose and C denotes the number of constellation points. In this work, the indices $1,\ \ldots,\ k,\ \ldots K$ are referred to layers. The symbol vector $\boldsymbol{s}[i]$ is then transmitted over flat fading channel and the signals are demodulated and sampled at the receiver equipped with N_R antennas. Let us assume the users a perfect synchronized. The received signal after demodulation, matched filtering and sampling is collected in an $N_R \times 1$ vector

$$\boldsymbol{r}[i] = \big[r_1[i],\ r_2[i],\ \ldots,\ r_{N_R}[i]\big]^T, \tag{3.2}$$

with sufficient statistics for detection

$$\begin{aligned} \boldsymbol{r}[i] &= \sum_{k=1}^{K} \boldsymbol{h}_k s_k[i] + \boldsymbol{v}[i] \\ &= \boldsymbol{H}\boldsymbol{s}[i] + \boldsymbol{v}[i], \end{aligned} \tag{3.3}$$

where the elements $h_{n_R,k}$ of the $N_R \times K$ channel matrix $\boldsymbol{H}$ are the complex channel gains from the k-th transmit antenna to the n_R-th receive antenna and $\boldsymbol{h}_k = [h_{1,k}, \ldots, h_{N_R,k}]^T$. The $N_R \times 1$ vector $\boldsymbol{v}[i]$ is a zero mean complex circular symmetric Gaussian noise with covariance matrix $E\big[\boldsymbol{v}[i]\boldsymbol{v}^H[i]\big] = \sigma_v^2\boldsymbol{I}$, where $E[\cdot]$ stands for expected value, $(\cdot)^H$ denotes the Hermitian operator, σ_v^2 is the noise variance and $\boldsymbol{I}$ is the identity matrix. The symbol vector $\boldsymbol{s}[i]$ has a covariance matrix $E\big[\boldsymbol{s}[i]\boldsymbol{s}^H[i]\big] = \sigma_s^2\boldsymbol{I}$, where σ_s^2 is the signal power.

In the coded systems, the model (3.3) is used repeatedly to describe transmit streams of data bits which are separated into blocks representing uses of channels. For a given block, the symbol vector $\boldsymbol{s}$ is obtained by mapping $\boldsymbol{x} = [x_1, ..., x_j, ..., x_{K \cdot J}]$ coded bits. The quantity J is the number of bits per constellation symbol. The rate of uncoded transmitted information is KJ bits per use of (3.3). For coded transmissions, the vector $\boldsymbol{x}$ is designated to be the output of a forward error-correction code of rate $R < 1$ that introduces redundancy. The transmission rate is then RKJ bits per (3.3) use. In the IDD processing, the detector makes decisions by using the knowledge of correlations across time instants $[i], i = 0, 1, \ldots, I$ provided by the channel decoder, and the channel decoder needs to decode the bit information by using the likelihood information on all blocks obtained from the soft output detector.

3.3.2 Multiuser MIMO Systems

A system model for the uplink of a multiuser MIMO system is similarly defined except that we consider N_R receive antennas at an access point (AP) and K users equipped with a single antenna ($N_T = 1$) at the transmitter end. This is effectively a space-division-multiple access (SDMA) approach. At each time instant, the users transmit K symbols which are organized into a $K \times 1$ vector $\boldsymbol{s}[i] = \left[s_1[i],\ s_2[i],\ \ldots,\ s_k[i],\ \ldots,\ s_K[i]\right]^T$ and each entry is also taken from a modulation constellation $\mathcal{A}$. The symbol vector $\boldsymbol{s}[i]$ is then passed through the flat fading channels and corrupted by the AWGN noise. The AP collects the received signal in an $N_R \times 1$ vector $\boldsymbol{r}[i]$ which is given by

$$\begin{aligned} \boldsymbol{r}[i] &= \sum_{k=1}^{K} \boldsymbol{h}_k s_k[i] + \boldsymbol{v}[i] \\ &= \boldsymbol{H}\boldsymbol{s}[i] + \boldsymbol{v}[i], \end{aligned} \tag{3.4}$$

where $s_k[i]$ is the transmitted symbol for user k, the term $\boldsymbol{h}_k$ represents the $N_R \times 1$ vector of channel coefficients of user k, and $\boldsymbol{H}$ is the matrix of the channel vectors for all users. In this system we assume all K users are perfectly synchronized and transmit symbols simultaneously. The symbols have a variance of σ_s^2 as the signal power. The model is also used repeatedly to transmit a stream of data bits which are separated into blocks representing uses of channels.

In the coded system, the message of each user is encoded separately by the channel

codes with $R < 1$. For a given block, the symbol transmitted by user s_k is obtained by mapping it into the vector $\boldsymbol{x}_k = [x_{k,1}, ..., x_{k,j}, ..., x_{k,J}]$ with the coded bits, where $2^J = C$. Let us assume all users have same power received at the AP.

3.4 Proposed Multi-Feedback Receiver Design

This section is devoted to the description of the proposed MF concept and its application in the SIC and QR decomposition based MIMO signal detection. A multi-branch processing framework is also developed to improve the performance of the proposed detection algorithms. In the following subsections, we only introduce the detection procedure with a multiuser MIMO model, the application of a point-to-point MIMO system is straightforward.

3.4.1 The MF-SIC Detection

The structure of the MF-SIC scheme is depicted in Fig.3.1. The structure considers the feedback diversity by using a number of selected constellation points as the candidates when a previous decision is determined unreliable. In order to find the optimal feedback, a selection algorithm is introduced. This selection scheme prevents the search space from growing exponentially. The reliability of the previous detected symbol is determined by the SAC, which saves the computational complexity by avoiding redundant processing with reliable decisions.

In the following, we only describe the procedure for detecting $\hat{s}_k[i]$ for user k. The detection of other user streams $\hat{s}_1[i]$, $\hat{s}_2[i]$,...,$\hat{s}_K[i]$ can be obtained accordingly. The soft estimation of the k-th user is obtained by

$$u_k[i] = \boldsymbol{\omega}_k^H \check{\boldsymbol{r}}_k[i], \tag{3.5}$$

where the $N_r \times 1$ MMSE filter vector is given by

$$\boldsymbol{\omega}_k = (\bar{\boldsymbol{H}}_k \bar{\boldsymbol{H}}_k{}^H + \frac{\sigma_v^2}{\sigma_s^2}\boldsymbol{I})^{-1}\boldsymbol{h}_k, \tag{3.6}$$

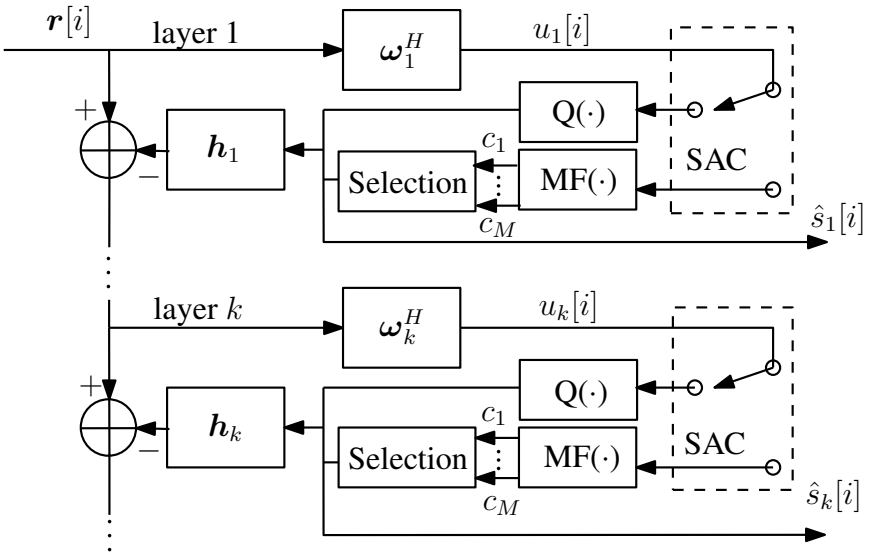

Figure 3.1: Block diagram of the MF-SIC detection. A reliable interference cancellation is performed. The SAC determines the reliability of the filter output, function MF$(\cdot)$ generates $\mathcal{L} = [c_1, \ldots, c_M]$.

and $\bar{\boldsymbol{H}}_k$ denotes the matrix obtained by taking the columns $k, k+1, \ldots K$ of $\boldsymbol{H}$, and $\check{\boldsymbol{r}}_k[i]$ is the received vector after the cancellation of previously detected $k-1$ symbols. For each user, the soft estimation $u_k[i]$ is checked by the SAC, which decides whether this decision is reliable according to the metric

$$d_k = \min_{a_f \in \mathcal{A}} \{|u_k[i] - a_f|\}. \tag{3.7}$$

where a_f denotes the constellation point which is the nearest to the soft estimation $u_k[i]$ of the k-th user.

If $d_k > d_{\text{th}}$ where d_{th} is the predefined threshold, we say it is dropped into the shadow area of the constellation map and this decision is determined unreliable as shown in Fig.3.2. In the presence of the SAC, significant additional computational complexity is saved compared to the scheme assumes all the estimates are unreliable. The MF-SIC scheme has a comparable complexity to the conventional SIC scheme, as verified by our studies.

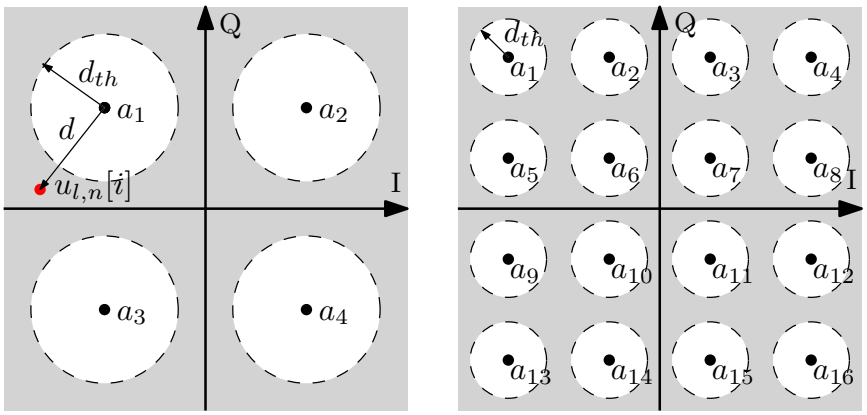

Figure 3.2: The shaded area is the unreliable region for QPSK and 16-QAM constellation. In these figures we assume that a_1 is the nearest constellation point to the soft estimation $u_k[i]$.

Decision Reliable

If the soft estimation $u_k[i]$ is considered reliable, a hard slice will be performed in the same way as in the conventional SIC scheme, the estimated symbol for each data stream $\hat{s}_k$ is obtained by $\hat{s}_k[i] = \mathrm{Q}\{u_k[i]\}$ where $\mathrm{Q}\{\cdot\}$ is signal quantization. The sliced symbol is considered as a reliable decision for user k.

Decision unreliable

If the soft estimation is determined unreliable, a candidate vector is generated.

$$\mathcal{L} = [c_1, c_2, \ldots, c_m, \ldots, c_M] \subseteq \mathcal{A}, \tag{3.8}$$

$\mathcal{L}$ is a selection of the M nearest constellation points to the soft estimation $u_k[i]$. The size of $\mathcal{L}$ can be either fixed or determined by the signal-to-noise ratio (SNR). A higher SNR corresponds to a smaller M which introduces a trade-off between the complexity and the performance. The unreliable decision $\mathrm{Q}\{u_k[i]\}$ is replaced by

$$\hat{s}_k[i] = c_{m_{\text{opt}}}, \tag{3.9}$$

where $c_{m_{\text{opt}}}$ is the optimal candidate selected from the list $\mathcal{L}$.

The benefits provided by the MF algorithm are based on the assumption that the optimal feedback candidate $c_{m_{\text{opt}}}$ is correctly selected. This selection algorithm is described

as follows:

In order to find the optimal feedback, a set of selection vectors $\boldsymbol{b}^1, \ldots, \boldsymbol{b}^m, \ldots, \boldsymbol{b}^M$ is defined, the number of these selection vectors M equals the number of constellation candidates we used for each unreliable decision. For the k-th layer, a $K \times 1$ vector $\boldsymbol{b}^m$ consists of the following elements,

- Previously detected symbols $\hat{s}_1[i], \ldots, \hat{s}_{k-1}[i]$.
- c_m a candidate symbol taken from the constellation for substituting the unreliable decision $\mathrm{Q}\{u_k[i]\}$ in the k-th layer.
- By using the above two terms, the detection of the following layers $k+1, \ldots, q, \ldots, K$-th is performed by the nulling and symbol cancellation which is equivalent to a traditional SIC algorithm.

Therefore, the vector is formed as follows

$$\boldsymbol{b}^m[i] = [\hat{s}_1[i], \ldots, \hat{s}_{k-1}[i], c_m, b^m_{k+1}[i] \ldots, b^m_q[i], \ldots, b^m_K[i]]^T, \tag{3.10}$$

where $b^m_q[i]$ is a potential decision that corresponds to the use of c_m in the k-th layer,

$$b^m_q[i] = \mathrm{Q}\{\boldsymbol{\omega}^H_q \hat{\boldsymbol{r}}^m_q[i]\}, \tag{3.11}$$

where q indexes a certain layer from the $(k+1)$-th to the K-th.

$$\hat{\boldsymbol{r}}^m_q[i] = \check{\boldsymbol{r}}_k[i] - \boldsymbol{h}_k c_m - \sum_{p=k+1}^{q-1} \boldsymbol{h}_p b^m_p[i]. \tag{3.12}$$

For each user, the same MMSE filter vector $\boldsymbol{\omega}_k$ is used for all the candidates, which allows the proposed algorithm to have the computational simplicity of the SIC detection. The proposed algorithm selects the candidates according to

$$m_{\text{opt}} = \arg \min_{1 \le m \le M} ||\boldsymbol{r}[i] - \boldsymbol{H}\boldsymbol{b}^m[i]||^2. \tag{3.13}$$

The $c_{m_{\text{opt}}}$ is chosen to be the optimal feedback symbol for the next layer as well as a more reliable decision for the current user. The algorithm of the proposed MF-SIC is summarized in TABLE 3.1.

Table 3.1: The pseudo-code of the MF-SIC algorithm

0: Initialization $\check{\boldsymbol{r}}_k[i] = \boldsymbol{r}[i]$
1: $\boldsymbol{\omega}_k = (\bar{\boldsymbol{H}}_k \bar{\boldsymbol{H}}_k^H + \sigma_v^2 \boldsymbol{I})^{-1} \boldsymbol{h}_k, k = 1, \ldots, K$
2: **for** $k = 1$ **to** K **do** % For each user
3: $u_k[i] = \boldsymbol{\omega}_k^H \check{\boldsymbol{r}}_k[i]$
4: **if** $d_k > d_{\text{th}}$**, in shadow area**
5: $\boldsymbol{\mathcal{L}} = [c_1, c_2, \ldots, c_m, \ldots, c_M]^T$
6: **for** $m = 1$ **to** M **do** % Multiple Feedback
7: **for** $q = k$ **to** K **do**
8: $\hat{\boldsymbol{r}}_k^m[i] = \check{\boldsymbol{r}}_k[i] - \boldsymbol{h}_k c_m - \sum_{p=k+1}^{q-1} \boldsymbol{h}_p b_p^m[i]$
9: $b_q^m[i] = \mathrm{Q}\{\boldsymbol{\omega}_q^H \hat{\boldsymbol{r}}_q^m[i]\}$
10: **end for**
11: **end for**
12: $\boldsymbol{b}^m[i] = [\hat{s}_1[i], \ldots, \hat{s}_{k-1}[i], c_m, b_{k+1}^m[i], \ldots, b_q^m[i], \ldots, b_K^m[i]]^T$
13: $m_{\text{opt}} = \arg\min_{1 \le m \le M} ||\boldsymbol{r}[i] - \boldsymbol{H}\boldsymbol{b}^m[i]||^2$
14: $\hat{s}_k[i] = c_{m_{\text{opt}}}$
15: **else**
16: $\hat{s}_k[i] = \mathrm{Q}\{u_k[i]\}$
17: **end if**
18: $\check{\boldsymbol{r}}_k[i] = \boldsymbol{r}[i] - \sum_{k=1}^{n-1} \boldsymbol{h}_k \hat{s}_k[i]$
19: **end for**

3.4.2 MF-QRD Detection

As an alternative to the BLAST algorithms, the QR decomposition can also be used to perform the detection in a serial manner. The QR function transforms the channel matrix $\boldsymbol{H}$ as

$$\boldsymbol{H} = \boldsymbol{Q}\boldsymbol{R}, \tag{3.14}$$

where $\boldsymbol{Q}$ is an $N_R \times K$ matrix having orthogonal columns with unit norm and $\boldsymbol{R}$ is a $K \times K$ upper triangular matrix. By combining the received signal $\boldsymbol{r}[i]$, now the sufficient

statistics for detecting $\boldsymbol{s}[i]$ become

$$\tilde{\boldsymbol{r}}[i] = \boldsymbol{Q}^{\boldsymbol{H}}\boldsymbol{r}[i] = \boldsymbol{R}\boldsymbol{s}[i] + \boldsymbol{\eta}[i], \tag{3.15}$$

where the noise vector is $\boldsymbol{\eta}[i] = \boldsymbol{Q}^{\boldsymbol{H}}\boldsymbol{v}[i]$. For the purpose of detecting the signal element $\tilde{s}_k[i]$ in the k-th layer ($k = 1, 2, \ldots, K$) the corresponding soft decision $u_k[i]$ is computed as

$$u_k[i] = \mathrm{Q}\Big\{\frac{\tilde{r}_k[i] - \sum_{\tau=k+1}^{K} y_{k,\tau}\hat{s}_\tau[i]}{y_{k,k}}\Big\}, \tag{3.16}$$

where $y_{k,k}$ are the diagonal entries of $\boldsymbol{R}$ and $\tilde{r}_k[i]$ is the k-th element of $\tilde{\boldsymbol{r}}[i]$. Note that the detection ordering is determined by either SINR ordering or the power of the column norm of the channel of each user (see Chapter 2). The application of column norm based ordering is preferred due to the low complexity cost.

We may also integrate the MF processing with the conventional QR detector mentioned above. The proposed MF-QRD scheme is described in Table 3.2 in which the received signals are recovered from the K-th layer to the first layer. At any k-th layer, the soft decision $u_k[i]$ is calculated by using (3.16) then a decision feedback procedure is carried out as follows:

- A threshold d_{th} is defined.
- For each k-th layer, we compute d_k, the norm of the difference between $u_k[i]$ and its nearest constellation points. The estimate $u_k[i]$ is considered reliable if $d_k < d_{\text{th}}$ otherwise we determine $u_k[i]$ as unreliable.
- In the first case, we obtain $\hat{s}_k[i]$ by $\hat{s}_k[i] = \mathrm{Q}\big\{u_k[i]\big\}$.
- If $u_k[i]$ is decided unreliable, we generate a candidate vector $\boldsymbol{\mathcal{L}} = [c_1, c_2, \ldots, c_m, \ldots, c_M]^T$ that is a selection of M constellation points closest to $u_k[i]$ and M can be either fixed or flexible which leads to distinct complexities.

Based on various c_m at the k-th layer, the estimated signal $\hat{b}_q^m$ from the $k-1$-th layer to the first layer can be computed as

$$\hat{b}_q^m = \frac{1}{y_{q,q}}\big(\tilde{r}_k - y_{k,k}[i]c_m - \sum_{\tau=q+1}^{K} y_{q,\tau}[i]\hat{b}_\tau^m[i]\big), \quad q = k-1, \ldots, 1, \tag{3.17}$$

Table 3.2: The pseudo-code of the MF-QRD algorithm

Initialization:

$\boldsymbol{QR} = \boldsymbol{H}$;

$\tilde{\boldsymbol{r}} = \boldsymbol{Q}^H \boldsymbol{r}$;

Multiple Feedback QRD Detection:

for $k = N_T, \ldots, 1$

$u_k[i] = \big(\tilde{r}_k - \sum_{\iota=k+1}^{N_T} r_{k,\iota}\hat{s}_\iota\big)/r_{k,k}$;

if $u_k[i]$ **is unreliable**

$\boldsymbol{\mathcal{L}} = [c_1, c_2, \ldots, c_m, \ldots, c_M]^T$;

$\tilde{r}'_k = \tilde{r} - \sum_{\iota=k+1}^{N_T} y_{k,\iota}\hat{s}_\iota$;

for $m = 1$ **to** M **do**

for $q = k-1$ **to** 1 **do**

$\hat{b}_q^m = \big(\tilde{r}'_k - y_{k,k}c_m - \sum_{\tau=q+1}^{N_T} y_{q,\tau}\hat{b}_\tau^m\big)/y_{q,q}$;

end for

$\boldsymbol{b}_k^m[i] = \big[\hat{b}_1^m, \ldots, \hat{b}_q^m, \ldots, c_m, \hat{\boldsymbol{s}}_{k+1,N_T}\big]$;

end for

$m_{\text{opt}} = \arg \min_{1 \le m \le M} ||\boldsymbol{r}[i] - \boldsymbol{H}\boldsymbol{b}_k^m[i]||^2$;

$\hat{s}_k[i] = c_{\text{opt}}$;

else

$\hat{s}_k[i] = \mathrm{Q}\big[u_k[i]\big]$;

end if

end for

where $r_k[i]$ is the k-th element of vector $\tilde{\boldsymbol{r}}_k[i]$. Thus, for each c_m we have

$$\boldsymbol{b}_k^m[i] = \big[\hat{b}_1^m[i], \ldots, \hat{b}_q^m[i], \ldots, c_m, \hat{\boldsymbol{s}}_{k+1,K}[i]\big], \tag{3.18}$$

where the row vector $\hat{\boldsymbol{s}}_{k+1,K} = [\hat{s}_{k+1}, \hat{s}_{k+2}, \ldots, \hat{s}_K]$ stands for the existing detected results from the $k+1$-th layer to the K-th layer. Finally, the optimum index m_{opt} is chosen under the ML criterion (3.13), such that the corresponding c_{opt} is determined as $\hat{s}_k[i]$.

3.4.3 MF-SIC with Multi-Branch Processing

This section presents the structure of the proposed MF-SIC with multi-branch processing (MB-MF-SIC). The MB-MF-SIC structure is developed based on the work reported in

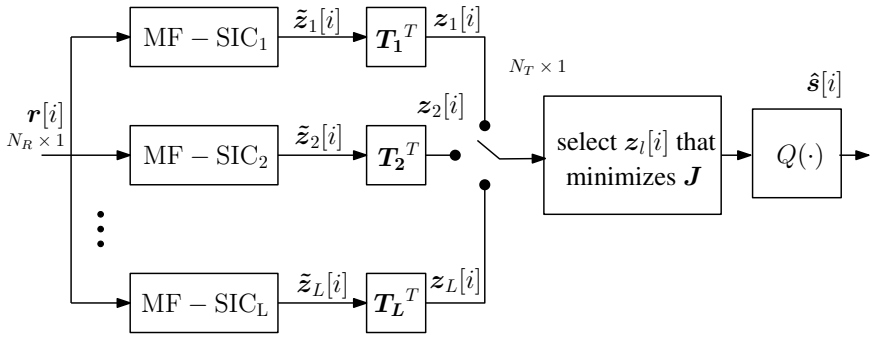

Figure 3.3: Block diagram of the proposed MB-MF-SIC detector.

[76] which contains multiple parallel processing branches of SICs with different ordering patterns as shown in Fig.3.3.

In the l-th branch, the MF-SIC scheme successively computes the detected symbol vector $\hat{\boldsymbol{s}}_l[i]$ as

$$\hat{\boldsymbol{s}}_l[i] = [\hat{s}_{l,1}[i], \hat{s}_{l,2}[i], \ldots, \hat{s}_{l,K}[i]]^T. \tag{3.19}$$

This procedure has been detailed in the previous subsections. The term $\hat{\boldsymbol{s}}_l[i]$ represents the $K \times 1$ ordered estimated symbol vector, which is detected according to the IC ordering pattern $\boldsymbol{T}_l, l = 1, \ldots, L$ for the l-th branch. The IC on the received vector $\check{\boldsymbol{r}}[i]$ is given as follows:

$$\begin{cases} \check{\boldsymbol{r}}_{l,k}[i] = \boldsymbol{r}[i], & k = 1, \\ \check{\boldsymbol{r}}_{l,k}[i] = \boldsymbol{r}[i] - \sum_{j=1}^{k-1} (\boldsymbol{H}')_j \hat{s}_{l,j}[i], & k \geq 2, \end{cases} \tag{3.20}$$

where the transformed channel matrix $\boldsymbol{H}'$ is obtained by

$$\boldsymbol{H}' = \boldsymbol{T}_l \boldsymbol{H}. \tag{3.21}$$

By transforming the channel matrix, the columns of the channel matrix $\boldsymbol{H}$ are permuted. The serial processing from layer $k = 1$ to $k = K$ for each permuted channel $\boldsymbol{H}'$ represents the permuted cancellation order in each branch l [76].

The term $(\boldsymbol{H}')_k$ represents the k-th column of the ordered channel $\boldsymbol{H}'$ and $\hat{s}_{l,k}$ denotes the estimated symbol for each data stream obtained by the MF-SIC algorithm. At the end of each branch we can transform $\hat{\boldsymbol{s}}_l[i]$ back to the original order $\tilde{\boldsymbol{s}}_l[i]$ by using $\boldsymbol{T}_l$ as

$$\tilde{\boldsymbol{s}}_l[i] = \boldsymbol{T}_l^T \hat{\boldsymbol{s}}_l[i]. \tag{3.22}$$

Basically, the MB procedure modifies the original cancellation order in a way that the

detector obtains a group of different estimated vectors. At the end of the MB structure, the algorithm selects the branch with the minimum Euclidean distance according to

$$l_{\text{opt}} = \arg \min_{1 \le l \le L} \boldsymbol{J}(l), \tag{3.23}$$

for each branch,

$$\boldsymbol{J}(l) = ||\boldsymbol{r}[i] - \boldsymbol{H}\tilde{\boldsymbol{s}}_l[i]||^2 = ||\boldsymbol{r}[i] - \boldsymbol{H}'\hat{\boldsymbol{s}}_l[i]||^2. \tag{3.24}$$

In the MB-MF-SIC implementation, the metric $\boldsymbol{J}(l)$ of each MF-SIC branch can be obtained directly from (3.13). The final detected symbol vector is

$$\bar{\boldsymbol{s}}[i] = \tilde{\boldsymbol{s}}_{l_{\text{opt}}}[i] = \boldsymbol{T}^T_{l_{\text{opt}}} \hat{\boldsymbol{s}}_{l_{\text{opt}}}[i]. \tag{3.25}$$

This MB scheme can bring a close-to-optimal performance, however, the exhaustive search of $L = K!$ branches is not practical. To develop an ordering scheme with low complexity, which renders itself to practical implementation, is of great interest. Therefore, a number of branch reduction sub-optimal schemes were reported in [76], namely frequently selected branches (FSB), pre-stored patterns (PSP) and listing patterns approach (LPA). In this thesis, the FSB is used as the sub-optimal solution for selecting the L branches. The FSB algorithm builds a codebook which contains the ordering patterns for the most likely selected branches and the required number of branches to obtain a near-optimal performance is greatly reduced. In order to build FSB codebook, we identify the statistics of each selected branch and construct the codebook with the L most likely selected branches to be encountered. Detailed description of these sub-optimal ordering schemes are included in [76].

3.5 Iterative Processing

The MF aided detector for systems employing channel coding is considered in this section. The IDD receiver structure is described in the first subsection and followed by the introduction of the candidate symbol selection algorithm used in the MF-SIC and the branch selection algorithm with the MB configuration.

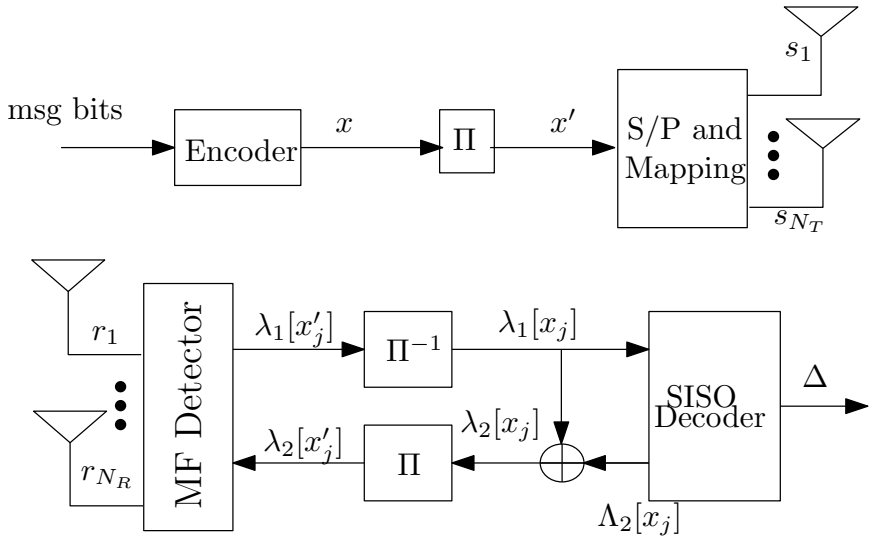

Figure 3.4: Transmitter and receiver structure with iterative detection and decoding. The subscripts "1" and "2" denote the variables associated with the inner SISO component and the outer SISO component respectively. The upper-script $(\cdot)'$ denotes the corresponding bit vector is interleaved.

3.5.1 Iterative Processing with Coded Point-to-Point MIMO Systems

As depicted in Fig.3.4, for each transmission, the message bits are encoded by the channel encoder and interleaved before modulation and multiplexing. The iterative (turbo) receiver consists of two stages: a soft-input soft-output (SISO) detector and a SISO maximum *a posteriori* (MAP) decoder. These stages are separated by interleavers and deinterleavers.

At the output of the SISO detector the interleaved *a posteriori* log-likelihood ratio (LLR) of the j-th encoded bit of the k-th symbol is given by

$$\begin{aligned}\Lambda_1[x'_{k,j}] &= \log \frac{P(x'_{k,j}=+1|\boldsymbol{r},\boldsymbol{H})}{P(x'_{k,j}=-1|\boldsymbol{r},\boldsymbol{H})}, \\ &= \log \frac{P(x'_{k,j}=+1|\boldsymbol{u})}{P(x'_{k,j}=-1|\boldsymbol{u})}.\end{aligned} \tag{3.26}$$

With the MF-SIC processing, we set $\boldsymbol{u} = \boldsymbol{s} + \boldsymbol{v}_{\text{eff}}$, where $\boldsymbol{v}_{\text{eff}}$ is the effective noise factor after the MMSE filtering in each layer. By assuming that the k-th layer $u_k = s_k + v_{\text{eff}}$ is statistically independent from other layers [27], this leads to the approximation

$$\Lambda_1[x'_{k,j}] \approx \log \frac{P(x'_{k,j}=+1|u_k)}{P(x'_{k,j}=-1|u_k)}, \tag{3.27}$$

Using Bayes's rule, the $\Lambda_1[x'_{k,j}]$ can be rewritten as

$$\begin{aligned}\Lambda_1[x'_{k,j}] &= \log \frac{P(u_k|x'_{k,j}=+1)}{P(u_k|x'_{k,j}=-1)} + \log \frac{P(x'_{k,j}=+1)}{P(x'_{k,j}=-1)} \\ &= \lambda_1[x'_{k,j}] + \lambda_2^p[x'_{k,j}]\end{aligned} \tag{3.28}$$

where the term

$$\lambda_2^p[x'_{k,j}] = \log \frac{P(x'_{k,j}=+1)}{P(x'_{k,j}=-1)} \tag{3.29}$$

represents the *a priori* information for the coded bits $x'_{k,j}$, which is obtained by the MAP decoder in the previous iteration. The superscript ^{p} denotes the value is obtained from the previous iteration. For the first iteration we assume $\lambda_2^p[x'_{k,j}] = 0$ for all bits. The first term $\lambda_1[x'_{k,j}]$ denotes the *extrinsic* information which is computed based on the received signal $\boldsymbol{r}$ and *a priori* information $\lambda_2^p[x'_{k,l}]$ where $l \neq j$.

For the detector, the coded bit *extrinsic* LLR for the k-th layer is obtained as

$$\lambda_1[x'_{k,j}] = \log \frac{\sum_{a_c \in \mathcal{A}_{k,j}^+} P(u_k|s_k=a_c)\exp(L_a(a_c))}{\sum_{a_c \in \mathcal{A}_{k,j}^-} P(u_k|s_k=a_c)\exp(L_a(a_c))} \tag{3.30}$$

where $\mathcal{A}_j^+$ and $\mathcal{A}_j^-$ denotes the subsets of constellation $\mathcal{A}$ where the bit x'_j takes the values 1 and 0 respectively. $L_a(a_c)$ denotes the *a priori* symbol probability for symbol a_c. Since

$$P(u_k|s_k=a_c) = \frac{1}{\pi\sigma_{\text{eff}}^2}\exp(\frac{-|u_k-s_k|^2}{\sigma_{\text{eff}}^2}), \tag{3.31}$$

where σ_{eff}^2 represents the variance of effective noise of u_k. We rewrite (3.30) as

$$\lambda_1[x'_{k,j}] = \log \frac{\sum_{a_c \in \mathcal{A}_j^+} \exp(-|u_k-s_k|^2/\sigma_{\text{eff}}^2)\prod_{(l\neq j)} P(x'_{k,l})}{\sum_{a_c \in \mathcal{A}_j^-} \exp(-|u_k-s_k|^2/\sigma_{\text{eff}}^2)\prod_{(l\neq j)} P(x'_{k,l})}, \tag{3.32}$$

where $P(x'_{k,j})$ is *a priori* probability of a bit x'_j and obtained by its *a priori* LLR as [56]

$$P(x'_{k,j}) = \frac{1}{2}[1 + x'_{k,j}\tanh(\frac{1}{2}\lambda_2^p[x'_{k,j}])]. \tag{3.33}$$

Then $\lambda_1[x'_{k,j}]$ is de-interleaved and fed to the MAP decoder of the k-th layer as the *a priori* information. The MAP decoder calculates *a posteriori* LLR of each code bit by using the trellis diagram as [92]

$$\Lambda_2[x_{k,j}] = \lambda_2[x_{k,j}] + \lambda_1^p[x_{k,j}]. \tag{3.34}$$

The output of the MAP decoder is obtained by the *a priori* information $\lambda_1^p[x_{k,j}]$, the *extrinsic* information provided by the decoder. The *a posteriori* LLR of every information

bit is also collected by the MAP decoder which is used to make the decision of the message bit at the last iteration. The *extrinsic* information obtained by the MAP decoder is fed back to the SISO detector as the *a priori* information of all the spatial layers. At the first iteration, λ_1 and λ_2^p are statistically independent and as the iterations are performed they become more correlated until the improvement through iterations diminishes.

We assume that the output of the MMSE filter $u_k[i]$ is Gaussian, therefore, the soft output of the SISO detector for the k-th layer is written as [92]

$$u_k[i] = V_k s_k[i] + \mu_k[i], \tag{3.35}$$

where V_k is a scalar variable which is equal to the k-th layer's signal amplitude and $\mu_k[i]$ is a Gaussian random variable with variance $\sigma^2_{\text{eff},k}$, since

$$V_k[i] = E[s_k^*[i]u_k[i]] \tag{3.36}$$

and

$$\sigma^2_{\text{eff},k} = E[|u_k[i] - V_k[i]s_k[i]|^2]. \tag{3.37}$$

The estimates of $\hat{V}_k[i]$ and $\hat{\sigma}^2_{\text{eff},k}$ can be obtained by time averages of the corresponding samples over the transmitted packet. There are also alternative solutions to obtain the variance value $\sigma^2_{\text{eff},k}$ and we leave these details to the reference [15] and [19].

3.5.2 Iterative Processing with Coded Multiuser MIMO Systems

In this section, we present the proposed MF-SIC detector for coded systems which employ convolutional codes with IDD for the multiuser MIMO systems. We show that a reduced number of turbo iterations can be used with the proposed schemes as compared to previously reported turbo multiuser detectors [19] [20]. This is important to reduce the delay of wireless systems which rely on iterative processing techniques.

Similar to point-to-point configurations, the receiver consists of the following two stages: a SISO detector and a bank of SISO MAP decoders for the corresponding users. These stages are separated by interleavers and deinterleavers. Specifically, the estimated likelihoods of the convolutionally encoded bits are computed by the detector and these estimates are deinterleaved and serve as input to the MAP decoders. The MAP decoder

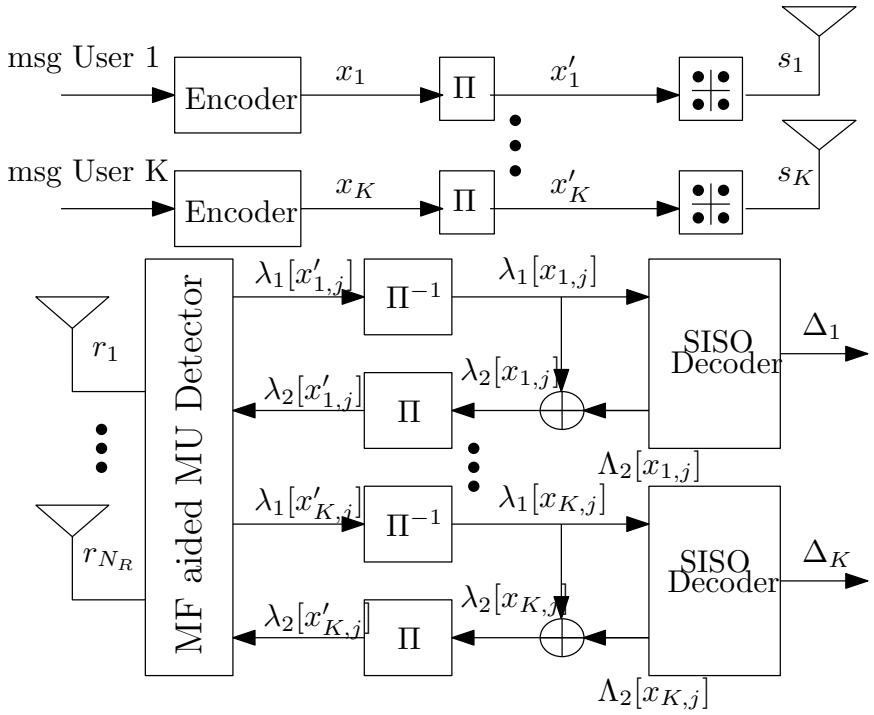

Figure 3.5: Receiver structure with iterative detection and decoding. The multiuser detector separates the data for each user and use the *a priori* information to enhance its performance.

generates *a posteriori* probabilities (APPs) for each user's encoded bits, and therefore the soft estimate of the transmitted symbol is obtained. The procedure discussed above is repeated in an iterative manner. The difference between the point-to-point and multiuser iterative receiver structure is that in the multiuser scenario, each user's message are coded separately but the detection is performed jointly.

At the output of the SISO detector the *a posteriori* log-likelihood ratio (LLR) of the j-th convolutionally encoded bit of the k-th user's block is given by

$$\Lambda_1[x_{k,j}] = \log \frac{P(x_{k,j} = +1|\boldsymbol{r})}{P(x_{k,j} = -1|\boldsymbol{r})}, \tag{3.38}$$

Using Bayes's rule, $\Lambda_1(x_{k,j})$ can be rewritten as

$$\begin{aligned} \Lambda_1[x_{k,j}] &= \log \frac{P(\boldsymbol{r}|x_{k,j} = +1)}{P(\boldsymbol{r}|x_{k,j} = -1)} + \log \frac{P(x_{k,j} = +1)}{P(x_{k,j} = -1)} \\ &= \lambda_1[x_{k,j}] + \lambda_2^p[x_{k,j}], k = 1, \ldots, K. \end{aligned} \tag{3.39}$$

All the terms mentioned in the above functions are similarly defined in the previous subsection. The multiuser detector jointly detect the signals transmitted by all the K users.

For the first iteration we assume $\lambda_2^p[x_{k,j}] = 0$ for all users. The first term $\lambda_1[x_{k,j}]$ is obtained the based on the received signal of the joint detection $\boldsymbol{r}$ and *a priori* information $\lambda_2^p[b_{k,\tau}]$ where $\tau \neq j$. Similar to point-to-point configuration as mentioned in the previous subsection, for the detector, the coded bit *extrinsic* LLR for the k-th user is obtained as

$$\lambda_1[x_{k,j}] = \log \frac{\sum_{a_c \in \mathcal{A}_{k,j}^+} P(u_k|s_k = a_c) \exp(L_a(a_c))}{\sum_{a_c \in \mathcal{A}_{k,j}^-} P(u_k|s_k = a_c) \exp(L_a(a_c))}, \tag{3.40}$$

where $\mathcal{A}_{k,j}^+$ and $\mathcal{A}_{k,j}^-$ denote the subsets of constellation $\mathcal{A}$ where the bit $x_{k,j}$ takes the values 1 and 0, respectively. The quantity $L_a(a_c)$ denotes the *a priori* symbol probability for symbol a_c and the probability density of u_k given s_k has been given in (3.31).

Then $\lambda_1[x_{k,j}]$ is de-interleaved and fed to the corresponding MAP decoder of the k-th user as the *a priori* information. The MAP decoders calculate the *a posteriori* LLR of each code bit by using the trellis diagram as [92]

$$\Lambda_2[x_{k,j}] = \lambda_2[x_{k,j}] + \lambda_1^p[x_{k,j}]. \tag{3.41}$$

The output of the MAP decoder is obtained by the *a priori* information $\lambda_1^p[x_{k,j}]$ and the *extrinsic* information provided by the decoder. The *a posteriori* LLR of every information bit is also collected by the MAP decoder which is used to make the decision of the message bit after the last iteration. The *extrinsic* information obtained by the K MAP decoders is fed back to the SISO detector as the *a priori* information of all users. At the first iteration, λ_1 and λ_2^p are statistically independent and as the iterations are performed they become more correlated until the improvement through iterations diminishes.

The structure of the proposed MF-SIC with soft cancellation (MF-SIC-SC) multiuser detector is described in terms of iterations. In the first iteration, the *a priori* information provided by the decoder is zero which heavily degrades the performance of parallel interference cancellation (PIC) based detection. Therefore, instead of using the PIC based soft cancellation (SC/MMSE) [56] [19], in our approach, the proposed MF-SIC algorithm is used in the first iteration to calculate the *extrinsic* information and to feed it to the MAP decoders for all the users. The soft estimates $u_k[i]$ are used to calculate the LLRs of their constituent bits. We assume $u_k[i]$ is Gaussian, therefore, the soft output of the SISO detector for the k-th user is written as [92]

$$u_k[i] = V_k s_k[i] + \mu_k[i], \tag{3.42}$$

where V_k is a scalar variable which is equal to the k-th users amplitude and $\mu_k[i]$ is a Gaussian random variable with variance σ^2_{eff}, since

$$V_k[i] = E[s_k^*[i]u_k[i]] \tag{3.43}$$

and

$$\sigma^2_{\text{eff}} = E\big[|u_k[i] - V_k[i]s_k[i]|^2\big]. \tag{3.44}$$

The estimates of $\hat{V}_k[i]$ and $\hat{\sigma}^2_{\mu_k}$ can be obtained by time averages of the corresponding samples over the transmitted packet.

After the first iteration, the SC/MMSE performs PIC by subtracting the soft replica of interference components from the received vector as

$$\check{\boldsymbol{r}}[i] = \boldsymbol{r}[i] - \boldsymbol{H}\boldsymbol{z}[i], \tag{3.45}$$

where $\boldsymbol{z}[i] = [u_1[i], \ldots, u_{k-1}[i], 0, u_{k+1}[i], \ldots, u_K[i]]$ and a filter is developed to further reduce the residual interference as

$$\boldsymbol{\omega}_k[i] = \arg\min_{\boldsymbol{\omega_k}} E\{|s_k[i] - \boldsymbol{\omega}_k^H \check{\boldsymbol{r}}[i]|^2\}, \tag{3.46}$$

where the soft output of the filter is also assumed Gaussian. The first and the second-order statistics of the symbols are also estimated via time averages of (3.43) and (3.44). The MF-SIC processing is only applied to the first iteration of the IDD receiver, the proposed MF + selection is introduced in the SIC step to yield refined estimation of symbols. As for MB-MF-SIC-SC, the best MF-SIC-SC branch is selected by ML criterion, in order to provide symbol and bit estimates of the coded information.

3.6 Simulations

In this section, we evaluate the BER performance of the proposed algorithms in both point-to-point MIMO and multiuser MIMO scenarios with and without channel coding. We assume that the cancellation order has been sorted according to a decreasing order of channel column norm. Because SD has the MLD performance, provided the radius is appropriately selected. In the simulations, we only show the curves of the SD instead of both of them. Let us assume the proposed algorithms and all their counterparts operate

on channels with the independent and identically-distributed (i.i.d) random flat fading model and assume that the channel coefficients are taken from complex Gaussian random variables with zero mean and unit variance. We assume QPSK modulated symbols with anti-Gray mapping are transmitted by the antennas/users unless stated otherwise.

3.6.1 Point-to-point MIMO Systems

Fig.3.6 shows the performance of the MF-SIC and MB-MF-SIC with 4×4 and 8×8 configurations. In [76], both the optimum ordering patterns codebook and the frequently selected branches (FSB) codebook were designed to construct the transformation matrices $\boldsymbol{T}_l$. The optimum codebook, which can be obtained using the MATLAB function **PERM**($N_T : -1 : 1$), contains $N_T!$ ordering patterns. The FSB codebook was reported with a smaller size, in this case, the FSB index [1,2,5] for a 4×4 system and [1,2,3,5,4,13,17,21,19] for an 8×8 system. The elements in the FSB codebook indicate the indices of the patterns in the optimum codebook. Other parameters are set as $d_{\text{th}} = 0.5$ for the threshold of SAC and $M = 4$ is the size of MF set $\mathcal{L}$. As for the SD, the radius d_{SD} is chosen to be a scaled version of the noise variance [72]. For an 8×8 system, the SD requires 8×10^4 multiplications per symbol detection, the MB-MF-SIC requires 4.6×10^3 multiplications in $SNR = 12$ dB. When $SNR = 8$ dB is the case, the SD requires 2.4×10^5 multiplications while the proposed MB-MF-SIC scheme requires 5.5×10^3 multiplications. The simulation results indicate that a better performance can be achieved when a larger candidate list $\mathcal{L}$ is considered. The chosen of above parameters are on the basis of simulation trials.

The lattice basis reduction (LR) [79] has been proposed to transform the channel matrix into an equivalent but better conditioned one. The LR aided MMSE SIC detector (LR-SIC) is able to achieve the same diversity order with the optimal detectors as plotted in Fig.3.7. In this figure, we compare the LR aided algorithm with the proposed scheme. The LR aided detection has the ability to obtain the full diversity gain, but with several dB poorer coding gain than optimal ML detection. In our simulation, the LR-SIC outperforms the MF-SIC at high SNR region, however the same curve shows a worse performance in the low SNR region. Furthermore, with the increased number of parallel branches, the MF-SIC significantly outperforms the LR-SIC and the optimal performance

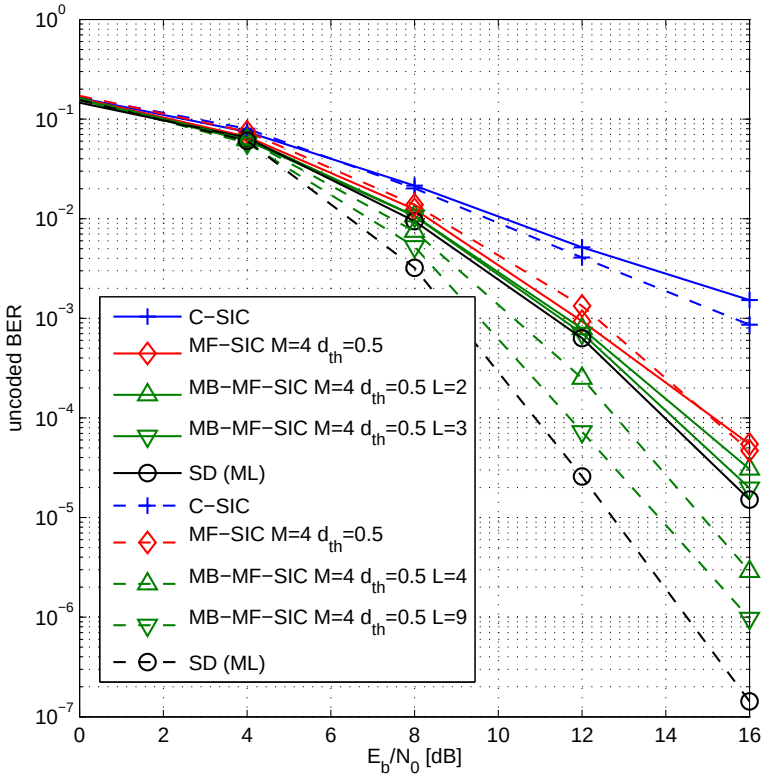

Figure 3.6: Uncoded bit-error-rate with QPSK modulation over flat fading. The proposed schemes approach the performance of SD in both 4×4 (solid line) and 8×8 (dash line) systems while requiring a lower complexity. MF-SIC denotes the multiple feedback detection. MB denotes the multiple branch version, and C-SIC denotes conventional SIC algorithm.

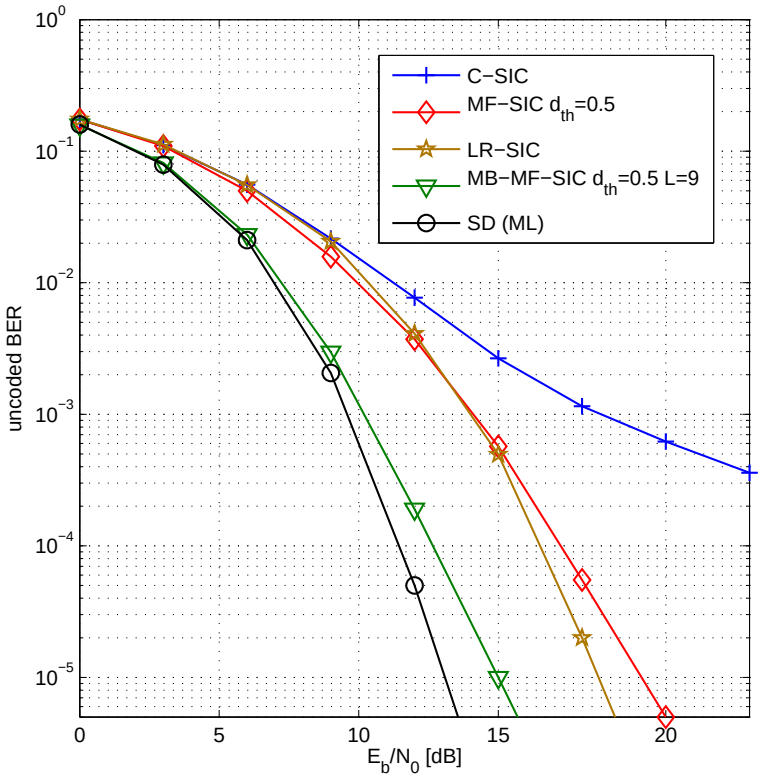

Figure 3.7: Uncoded bit-error-rate of a 6×6 MIMO system with QPSK modulation, MMSE based detection is considered. Complex lattice reduction is adopted with the LR-SIC, the number of constellation candidates M is 4 and threshold d_{th} equals 0.5. MB is incorporated to improve the performance and the number of branches is $L = 9$.

can be obtained within a low SNR region.

The real communication systems usually incorporate with error-control coding in order to lower the SNR requirement. The IDD receiver structure may be introduced to obtain a good performance. For an IDD architecture, we employ a CC with the constraint length equal to 2. A packet with 998 message bits are encoded with a $g = (7, 5)_{oct}$ convolutional encoder and 2000 coded bits are interleaved as a transmitting block. These bits are modulated to 1000 QPSK symbols with anti-Gray coding. Instead of using the perfect channel information in previous results, Fig.3.8 shows the simulation of iterative decoding with imperfect channel information. When a least-squares (LS) algorithm is used, we employ a training sequence with 40 symbols which are known at the receiver to perform channel estimation, and the forgetting factor is $\lambda_{LS} = 0.998$. In this figure,

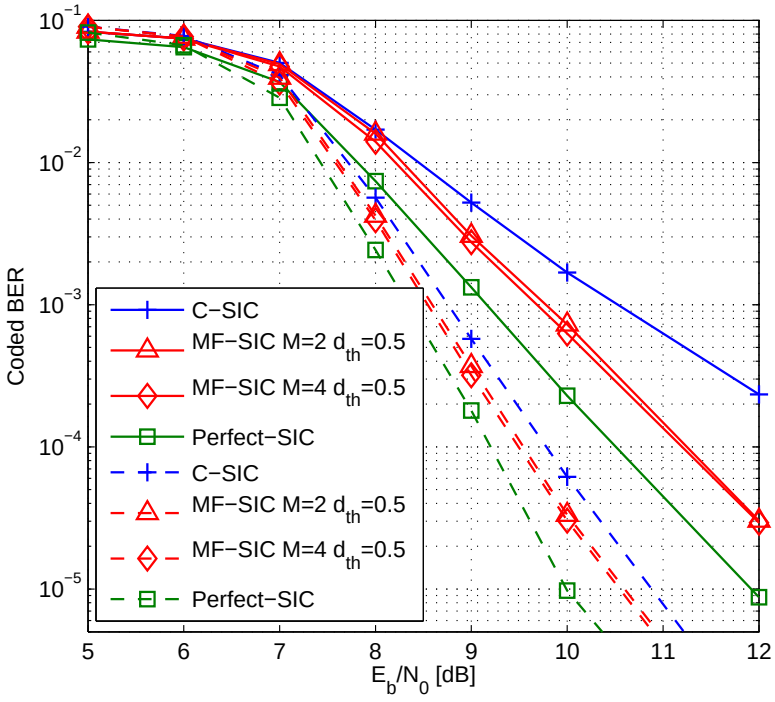

Figure 3.8: Coded bit-error-rate performance of a QPSK 4×4 MIMO system. The MF-SIC ($M = 4$) algorithm outperforms C-SIC in 1st iteration (solid) and 4th iteration (dash) and approaches the SIC detection with perfect symbol cancellation (Perfect-SIC).

we compare the proposed MF-SIC with the conventional SIC (C-SIC) and the SIC algorithm with perfect interference cancellation (Perfect-SIC), with the Perfect-SIC, we mean the transmitted symbol is removed according to the cancellation order before the MMSE filtering. The curves denote that the proposed soft-output MF detector outperforms the C-SIC algorithm with the channel estimation errors and approaches the SIC with perfect cancellation (Perfect-SIC).

3.6.2 Multiuser MIMO Systems

The bit-error-rate (BER) performance of the MF-SIC and MB-MF-SIC is compared with the existing detection algorithms with uncoded systems and a different number of users. For channel coded systems, we simulate the IDD schemes with the PIC based soft cancellation (SC) detector [19] and compare it with the SIC-SC which uses SIC for the first iteration and the SC is performed for the following iterations [21] and MF aided SIC-SC detectors (MF-SIC-SC) as well as its multiple-branch version (MB-MF-SIC-SC). The computational complexity for the proposed detection algorithms is also shown in this section.

Let us consider the proposed algorithms and all their counterparts in the independent and identically-distributed (i.i.d) random flat fading model and the coefficients are taken from complex Gaussian random variables with zero mean and unit variance. As the channel code, we employ a convolutional code with the rate $R = 0.5$ and constraint length 3. For each user, 497 message bits are encoded with a NSC with the polynomial $g = (7, 5)_{\text{oct}}$ and 1000 coded bits are interleaved as a transmitting block, these bits are modulated to 500 QPSK symbols with anti-Gray coding. We also assume that the cancellation order of the conventional SIC and MF-SIC are determined by the channel norm.

Overloaded systems represent a worst case situation for receivers because of the high level of interference. In practice, it is very unlikely to have a sufficient number of receive antennas for decoupling the spatial signal [73]. In Fig.3.9 a system with overloaded transmitting users for uncoded transmission is considered. We use $N_R = 4$ receive antennas in the AP and the $E_b/N_0 = 12$ dB at the receiver end. The FSB codebook [76] was designed to construct the transformation matrices for MB processing. In this case, [1,2] for $L = 2$

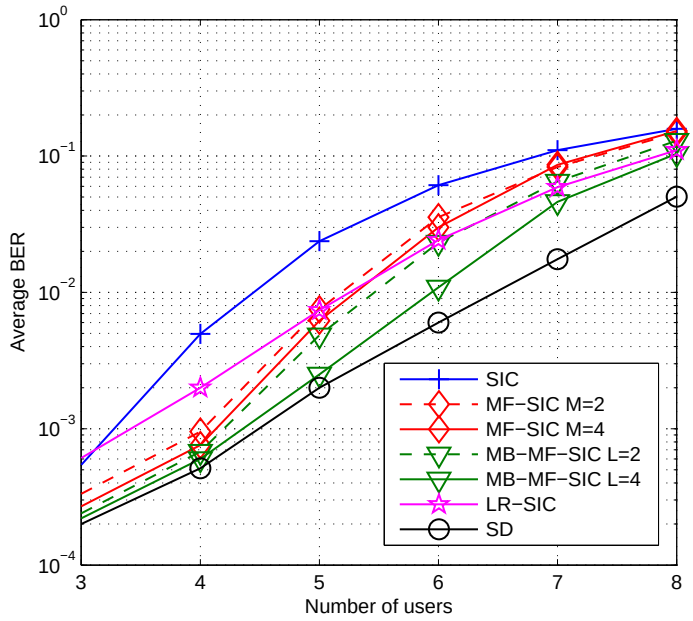

Figure 3.9: Uncoded MU-MIMO system with $E_b/N_0 = 12$dB, $N_R = 4$. The proposed MF-SIC and MB-MF-SIC approach the maximum likelihood performance with 4 users. In the overloaded case, the MB-MF-SIC approaches the SD with small performance loss with 6 users.

and [1,2,3,5] for $L = 4$. Other parameters are set as $d_{\text{th}} = 0.5$, and $M = 4$. As for the SD, we implement the standard SD [77] to achieve the optimal MLD performance, the radius d_{SD} is chosen to be a scaled version of the noise variance [72]. The linear detector (LD) and the lattice-reduction aided SIC (LR-SIC) [79] are also compared in this plot.

Another simulation is carried out with 16-QAM symbols and 4 users. The SNR against BER curves are plotted in Fig.3.10, where we use $M = 2, 4, 8$. The threshold is set to $d_{\text{th}} = 0.05, 0.15, 0.2$ respectively, and we consider a different number of branches $L = 2, 6$ for MB-MF-SIC processing. The proposed MF-SIC detection algorithm is able to achieve a better performance when a smaller threshold distance is selected. The performance of the proposed detector can be further improved when a larger feedback list is selected. Full diversity order can be obtained when a sufficient number of branches are used.

In Fig.3.11, the complexity is given by counting the required complex multiplications as the number of users increases. Each MF-SIC branch has a complexity slightly above

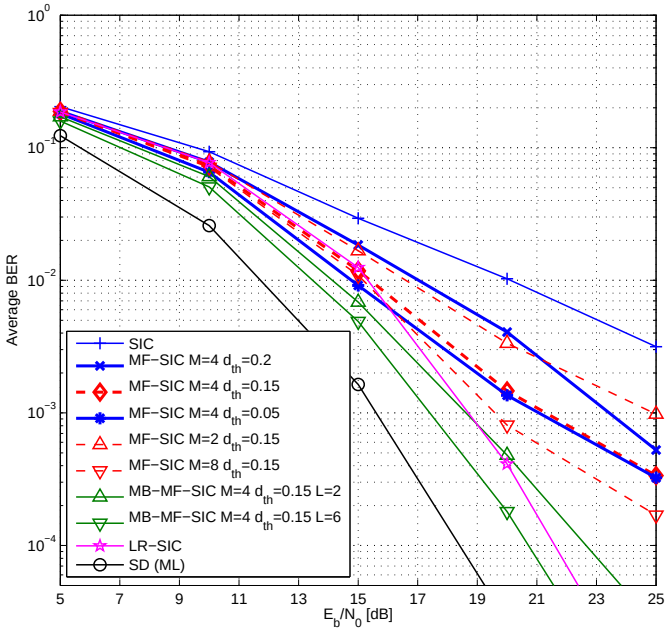

Figure 3.10: Uncoded bit-error-rate against SNR for a 4 user system with 4 receive antennas and 16-QAM modulation over flat fading, the shadow area threshold has an impact on the slope of the curves. Perfect channel information is assumed known at the receiver.

the SIC while it achieves a significant performance improvement. We also compared the complexity in terms of the average number of floating-point operations (FLOPS) required per symbol detection by simulations. A simulation performed with the Lightspeed toolbox [94] and $E_b/N_0 = 12$ dB has shown that for a 16-QAM system with 8 users, the MF-SIC algorithm requires only 2938 FLOPS and a MB-MF-SIC with 9 branches requires 26442 FLOPS while a fixed complexity SD (FSD) [78] requires 75120 FLOPS. It should be noted that FSD is one of the lowest complexity SD algorithms that are known.

For a 4×4 system and $E_b/N_0 = 16$ dB, the MF-SIC employs the SAC procedure, the MF concept and the selection algorithm. This leads to the processing of only 6.1% on average over the layers of the estimated symbol with the MF and selection algorithm, whereas for the remaining symbols, the conventional quantization is performed by $\hat{s}_k[i] = \mathrm{Q}\{u_k[i]\}$. In terms of processing for each layer, the MF-SIC requires processing 13.34% of the symbols in the first layer, followed by 5.21%, 2.51% and 2.15% for the remaining 3 layers, respectively.

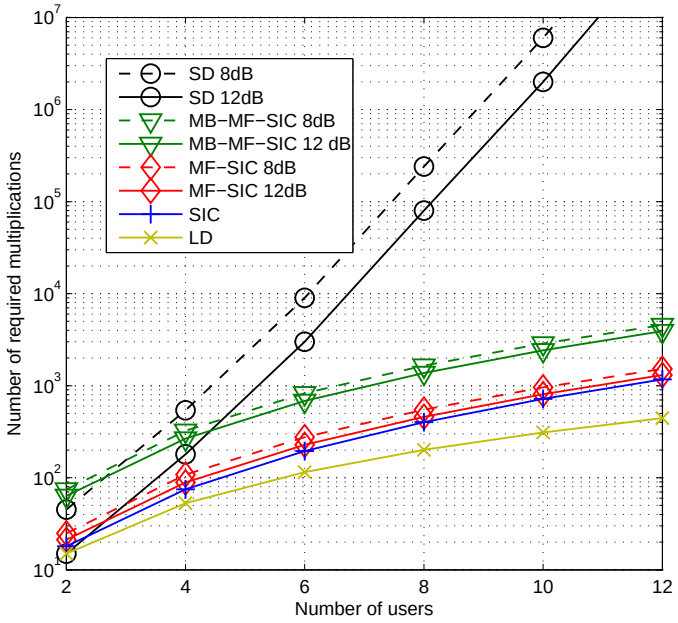

Figure 3.11: Complexity in terms of arithmetic operations against the transmit antennas, the proposed MB-MF-SIC scheme has L times the complexity of the MF-SIC which has a comparable complexity with the conventional SIC. $M = 4$, $d_{\text{th}} = 0.5$, $L = 4$.

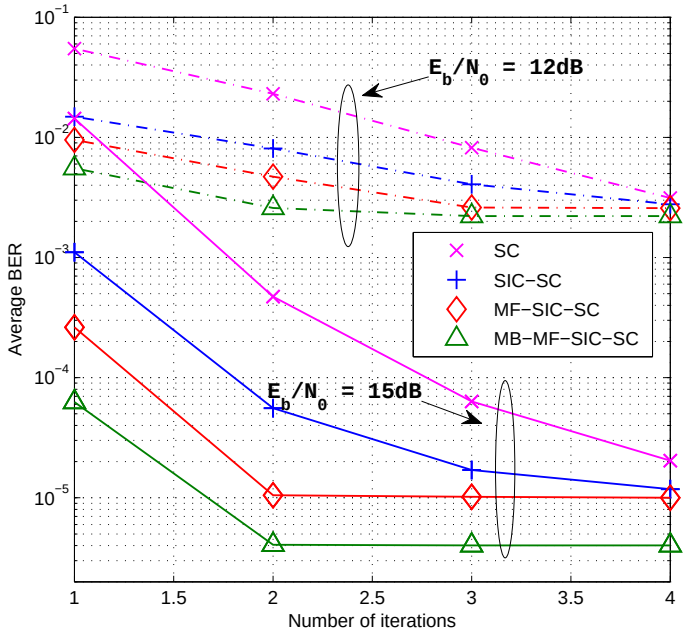

Figure 3.12: Coded MU-MIMO system with $N_R = 8$ and $K = 8$ users. The number of required iterations are saved in obtaining the converged performance with the proposed detectors at both $E_b/N_o = 12$ dB and $E_b/N_o = 15$ dB. $M = 4$, $d_{\text{th}} = 0.5$, $L = 6$.

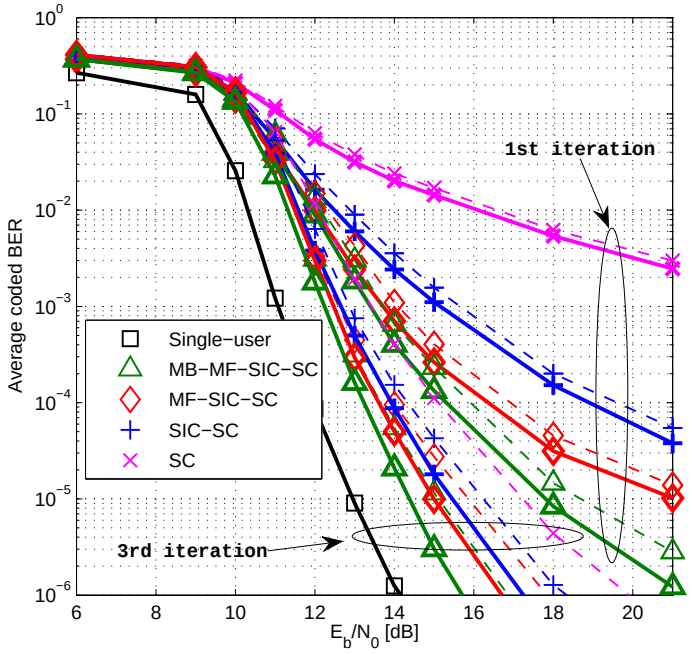

Figure 3.13: Convolutional coded system with $K = 8$ users. The proposed detectors have significant performance gains compared with the SC and SIC-SC detector in their first iteration with both perfect (solid line) and imperfect channel information (dash line).

For coded systems, the BER against the number of iterations is depicted in Fig.3.12. We use $K = 8$ times 500 QPSK symbols transmitted over a Rayleigh fading channel, which are collected by $N_R = 8$ antennas. Compared with the previously reported soft cancellation (SC) and SIC-SC, the proposed MF-SIC-SC and MB-MF-SIC-SC schemes with 2 turbo iterations can obtain a better BER performance than other schemes with 4 iterations, thus the decoding delay is reduced. Fig.3.13 shows the simulation with perfect and imperfect channel estimation, where a least squares (LS) algorithm is used to estimate the channel weights. We employ a training sequence with 40 symbols which are known at the receiver and the forgetting factor is $\lambda_{LS} = 0.998$. The single-user BER performance describes the performance in an interference free scenario. We can see from this plot that after 3 iterations the slope of the MU-MIMO performance curves are almost the same as the single-user curve with 3 dB (MF $d_{\text{th}} = 0.5$ $M = 4$) and 2 dB (MB-MF $L = 6$) performance loss.

3.7 Summary

In this chapter, we discussed the low-complexity detection algorithms and compared the results of various configurations for MIMO systems. A novel MF-SIC receiver for point-to-point and multiuser MIMO systems were proposed. The proposed schemes were also combined with the multiple branch and iterative detection and decoding strategy. It was shown that the new detection schemes significantly outperform existing SIC receivers, mitigate the phenomenon of error propagation with low processing delay.

Chapter 4

Adaptive Decision Feedback Detection with Constellation Constraints for Multi-Antenna Systems

Contents

4.1 Overview

In this chapter, a novel low-complexity decision feedback detection algorithm with constellation constraints (DFCC) is proposed for MIMO systems. Enhanced interference

cancellation is achieved by introducing multiple constellation points as decision candidates. A complexity reduction strategy is also developed to avoid redundant processing with reliable decisions. For time-varying channels, the proposed receiver updates the filter weights using a recursive least squares (RLS) based algorithm. This efficient detector is also incorporated in a multiple branch (MB) structure to achieve a higher detection diversity order. A soft-output DFCC detector is also proposed as a component of an iterative detection and decoding receiver scheme. Simulations show that the proposed DFCC technique has a complexity as low as the adaptive DF detector while it significantly outperforms the ordered successive interference cancellation (OSIC) processing.

4.2 Introduction

Spatially multiplexed MIMO wireless communications have the ability to increase the channel capacity through additional data streams [5]. In order to separate these streams, several detection techniques have been developed. The optimal MLD [12] scheme has exponential complexity with the number of streams and the constellation points, which is impractical for MIMO systems even with a moderate number of transmit antennas. The newly developed sphere decoding algorithms [53] [18] approach the optimal performance with reduced complexity [72], however, they still have a lower bound complexity which is polynomial or exponential depending on the number of streams or SNR [74]. The sub-optimal decision feedback (DF) [75] detection algorithms such as ordered successive interference cancellation (OSIC) or vertical Bell Labs layered space time (V-BLAST) [7], [76] offer a reasonable tradeoff between performance and complexity in MIMO systems.

The DF architecture is able to provide high spectral efficiencies when multiple transmit antennas are deployed, however, the application to systems with time-varying channels is still difficult due to the excessive computational load [81]. The filter vectors required to be updated at each time instance and the channel state information should be tracked, the matrix inversion and other related operations in the time domain need a significant number of computations. To address this drawback, some simpler strategies have been proposed, in [81], the interpolation based channel tracking is deployed and the OSIC detection is updated in a block-wise fashion, and a complexity and performance trade off is therefore

established.

As a promising alternative, adaptive techniques may also be deployed for MIMO systems in time-varying channels [82–86], where the work reported in [86] is a blind algorithm and the others are data-aided techniques. The inter-stream interference introduced by spatial multiplexing can be suppressed by successively detecting the transmitted symbols at each time. In [82], the authors developed a low-complexity data-aided adaptive technique for detecting the time-varying channels based on the so-called generalized decision feedback equaliser GDFE [75] structure, the weight vectors are updated using the recursive least squares (RLS) based algorithm. However, all these above mentioned algorithms have performances far from optimal. In recent work [76], a multiple-branch (MB) based adaptive receiver structure is examined by modifying the nulling and cancellation ordering of the original DF detector in an appropriate way such that the detector obtains a group of L different estimate vectors and then selects the most likely estimates, this method is able to attain a near-optimal performance but the detection complexity is L times higher than the structure with a single branch (SB).

Since the last decade, the invention of turbo codes [17] inspired the development of their associated iterative detection and decoding (IDD) rules. The so called *turbo concept* is applied to many communication systems such as turbo equalization in [87], multi-user detection (MUD) in [88] etc. In such systems, the soft-input soft-output (SISO) detector is required to produce soft-decision values. The optimal maximum *a posteriori* (MAP) detection [89] has an exponential complexity, which triggered an extensive study of low-complexity SISO detectors. In [18] a list version of SD has been used to compute the *a posteriori* bit probabilities by counting selected symbol combinations. Similar techniques are also used in [67] and [27]. On the other hand, the DF SISO detectors such as [90] and [91] have a lower complexity owing to their linear filter structure. However, the performance of these DF detectors is severely limited by the effect of error propagation (EP) [48, 49], [92, 93] and the fact that they only search a small portion of the decision tree.

In this chapter, an innovative DF technique for MIMO detection in time-varying channels is developed. With this novel low-complexity detector, the optimal performance is approached through the introduction of constellation constraints (CC). In each time

instance, the estimates of the symbols made by the filter are refined by a scheme that uses several selected constellation points to produce a number of tentative decisions. The scheme then selects the candidate that yields the minimum Euclidean distance as the replacement. Thanks to this algorithm, 1) an enhanced interference cancellation can be achieved since the feedback symbols are much more reliable than the original; 2) the refined symbol estimation produce better information for updating the adaptive filter weights by the RLS algorithm in each time instance; 3) unlike the SD algorithms which preserve several branches as the tentative decisions, the proposed detector preserves only one branch in the decision tree which prevents the complexity from growing exponentially. For soft-output processing, the proposed detector uses the produced tentative decisions to form a "list" to compute the likelihood for each transmitted bit, the probability of decision errors is significantly reduced. Computer simulations indicate that the proposed decision feedback detection with constellation constraints (DFCC) significantly outperforms the conventional DF schemes (i.e. [82] [83]) and approaches the optimal performance with very low additional detection complexity.

The main contributions of this chapter are:

- A decision feedback based algorithm is developed for detecting the signal transmitted in the time-varying MIMO channels.
- A reliability checking scheme named CC is introduced to improve the efficiency of the detector.
- The MB processing [76] is incorporated into the scheme to achieve a higher detection diversity and obtain a close-to-optimal performance for systems with a larger transmit antenna elements.
- The error performance and the detection complexity of the proposed algorithm are compared with several popular existing detection schemes.
- A soft-output DFCC is developed as a component of an iterative detection and decoding receiver structure.
- Unlike the scheme introduced in the previous chapter, the proposed DFCC algorithm is able to operate on a time-varying MIMO channel. Furthermore, a more

sophisticated CC algorithm is introduced to further improve the efficiency of the detection compared with the SAC algorithm introduced in the previous chapter.

4.3 Data and System Model

The system and data model adopted in this chapter is similar to that defined in Chapter 3, in terms of both point-to-point and multiuser MIMO Systems.

We consider a constellation $\mathcal{A} = \{a_1,\ a_2,\ \ldots,\ a_C\}$, where C denotes the number of constellation points. In this chapter, the symbol vector $\boldsymbol{s}[i]$ is transmitted over time-varying channels $\boldsymbol{H}[i]$ instead of the quasi-static Rayleigh fading channels assumed in Chapter 3. By quasi-static, me mean that the channel is constant within one frame and changes in the next frame such that the channels in successive frames are uncorrelated [15]. In terms of time-vary channels, the channel weights change many times inside a frame time duration and correlation is introduced between the successive channel weights. Jakes model [97] is widely adopted to model this type of channels, because of its simplicity. With Jakes model, a Rayleigh fading channel subject to a given Doppler spectrum is synthesized by a number of sinusoids. The Rayleigh amplitude can be approximated when a larger number of sinusoids are introduced [51]. In this chapter, the Jakes model is applied for simulations, and the variance of channel is subject to the normalized Doppler frequency shift, which is usually denoted as f_dT.

In order to emphasize the problem that interests us, in our point-to-point MIMO system, we assume the antennas transmit symbols simultaneously. On the other hand, in a multiuser MIMO scenario, the K users are assumed perfectly synchronized and transmit their symbols in the same time slot. The synchronization problems may be found in the references such as [33], [85].

In order to reduce the ordering complexity of the decision feedback system, channel norm ordering is applied at the receiver. As introduced in Chapter 2, the order of detecting the signal can be configured corresponding to a decreasing order of $\|\boldsymbol{h}_k\|$ where $k = 1, \ldots, K$.

$$\|\boldsymbol{h}_1\|^2 \geq \|\boldsymbol{h}_2\|^2 \geq \ldots \geq \|\boldsymbol{h}_K\|^2, \tag{4.1}$$

the column norm based ordering requires ordering the channel only once, which has the complexity significantly lower than the SINR based ordering. In the following part of this chapter, this criterion is used to decide the optimal NCO.

4.4 Proposed Decision Feedback Detector

This section is devoted to the description of the proposed DFCC concept and its application in a multi-branch processing framework. In the following parts of this chapter, we only introduce the detection procedure with a point-to-point MIMO system model, the application of a multiuser MIMO system is straightforward.

The structure and the signal processing model of the proposed DFCC detector is depicted in Fig.4.1. The received signal $\boldsymbol{r}[i]$ is filtered by a $N_R \times 1$ forward filter $\boldsymbol{\omega}_{f,k}^H[i]$ which is acting as the nulling vector of the OSIC algorithm. Then for each data stream $k = 1, \ldots, K$, the decisions are accumulated and cancelled by the $(k-1)$-dimensional decision backward filter $\boldsymbol{\omega}_{b,k}^H[i]$. Let $\hat{\boldsymbol{s}}[i] = \left[\hat{s}_1[i], \hat{s}_2[i], \ldots, \hat{s}_K[i]\right]^T$ represent the detected symbol vector and $u_k[i]$ denote the difference between the forward filter output and the backward filter output, which can be described as

$$u_k[i] = \boldsymbol{\omega}_{f,k}^H[i]\boldsymbol{r}[i] + \boldsymbol{\omega}_{b,k}^H[i]\hat{\boldsymbol{s}}_{k-1}[i], \tag{4.2}$$

where $\boldsymbol{\omega}_{b,1}^H = \mathbf{0}$ and the $(k-1)$-dimensional detected symbol vector is defined as

$$\hat{\boldsymbol{s}}_{k-1}[i] = \left[\hat{s}_1[i], \hat{s}_2[i], \ldots, \hat{s}_{k-1}[i]\right]^T. \tag{4.3}$$

For notational convenience, the forward and backward filters can be concatenated together as [82]

$$\tilde{\boldsymbol{\omega}}_k[i] = \begin{cases} \boldsymbol{\omega}_{f,k}[i], & k = 1 \\ \left[\boldsymbol{\omega}_{f,k}^T[i], \boldsymbol{\omega}_{b,k}^T[i]\right]^T, & k = 2, \ldots, K. \end{cases} \tag{4.4}$$

The input can also be concatenated as

$$\tilde{\boldsymbol{r}}_k[i] = \begin{cases} \boldsymbol{r}[i], & k = 1 \\ \left[\boldsymbol{r}^T[i], -\hat{\boldsymbol{s}}_{k-1}^T[i]\right]^T, & k = 2, \ldots, K. \end{cases} \tag{4.5}$$

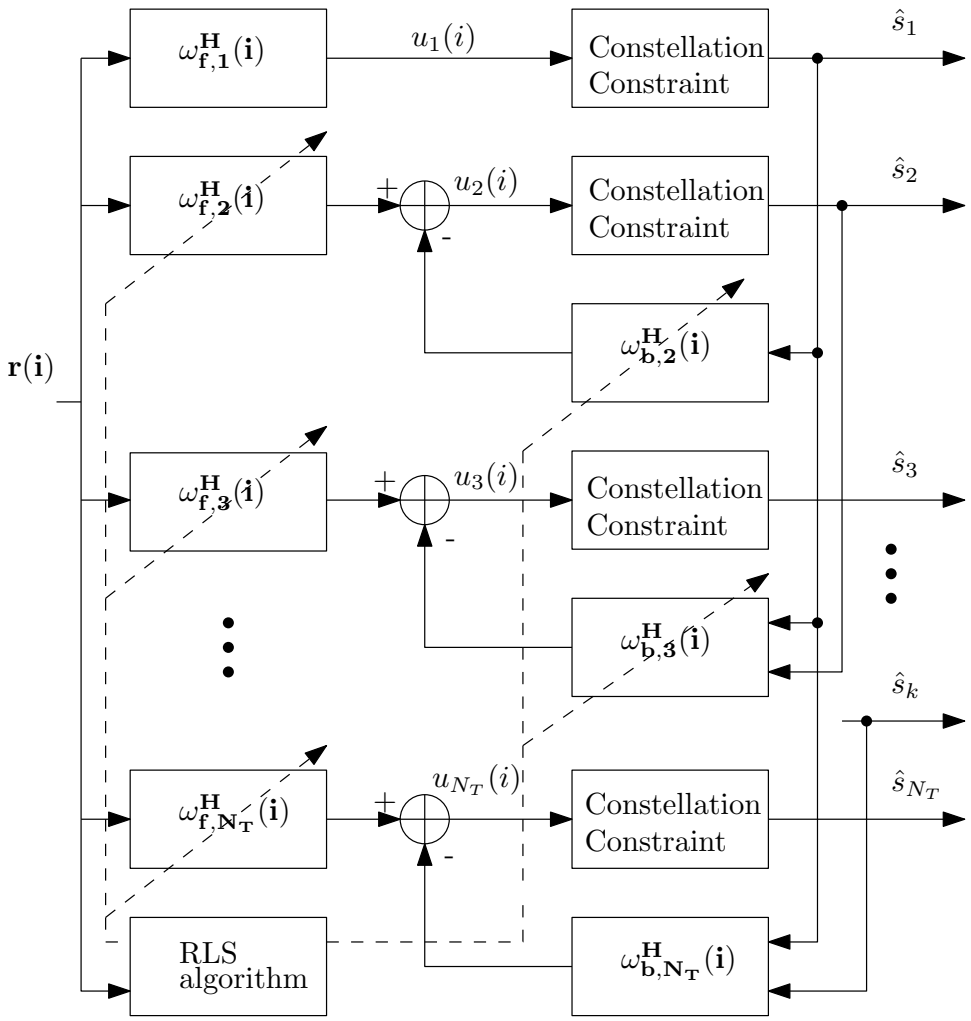

Figure 4.1: Detailed block diagram of the proposed DFCC-MIMO detector. Recursive least squares (RLS) algorithm is introduced to iteratively obtain the filter matrix

Then, we can rewrite (4.2) as

$$u_k[i] = \tilde{\boldsymbol{\omega}}_k^H[i]\tilde{\boldsymbol{r}}_k[i]. \tag{4.6}$$

The weight vector for time-varying channels $\tilde{\boldsymbol{\omega}}_k^H[i]$ can be obtained by solving the standard least squares (LS) problem, the LS cost function with an exponential window is given by

$$\mathcal{J}_k[i] = \sum_{\tau=1}^{i} \lambda^{i-\tau} \left| \hat{s}_k[\tau] - \tilde{\boldsymbol{\omega}}_k^H[i]\tilde{\boldsymbol{r}}_k[\tau] \right|^2 \tag{4.7}$$

where $0 \ll \lambda < 1$ is the forgetting factor. The optimal tap weight minimizing $\mathcal{J}_k[i]$ is given by [75]

$$\tilde{\boldsymbol{\omega}}_k[i] = \boldsymbol{\Phi}_k^{-1}[i]\boldsymbol{p}_k[i] \tag{4.8}$$

where the time-averaged cross correlation matrix is obtained by

$$\boldsymbol{\Phi}_k[i] = \sum_{\tau=1}^{i} \lambda^{i-\tau}\tilde{\boldsymbol{r}}_k[\tau]\tilde{\boldsymbol{r}}_k^H[\tau] \tag{4.9}$$

and the time-averaged cross correlation vector is defined by

$$\boldsymbol{p}_k[i] = \sum_{\tau=1}^{i} \lambda^{i-\tau}\tilde{\boldsymbol{r}}_k[\tau]\hat{s}_k^*[\tau] \tag{4.10}$$

Using the RLS algorithm [43], the optimal weight in (4.8) can be calculated recursively. The RLS is summarised in [76], [82] and described below

$$\boldsymbol{q}_k[i] = \boldsymbol{\Phi}_k^{-1}[i-1]\boldsymbol{r}_k[i] \tag{4.11}$$

$$\boldsymbol{k}_k[i] = \frac{\lambda^{-1}\boldsymbol{q}_k[i]}{1 + \lambda^{-1}\boldsymbol{r}_k^H[i]\boldsymbol{q}_k[i]} \tag{4.12}$$

$$\boldsymbol{\Phi}_k^{-1}[i] = \lambda^{-1}\boldsymbol{\Phi}_k^{-1}[i-1] - \lambda^{-1}\boldsymbol{k}_k[i]\boldsymbol{q}_k^H[i] \tag{4.13}$$

$$\tilde{\boldsymbol{\omega}}_k[i] = \tilde{\boldsymbol{\omega}}_k[i-1] + \boldsymbol{k}_k[i]\xi_k^*[i] \tag{4.14}$$

where

$$\xi_k[i] = \begin{cases} s_k[i] - \tilde{\boldsymbol{\omega}}_k^H[i-1]\tilde{\boldsymbol{r}}_k[i], & \text{Training Mode,} \\ \hat{s}_k[i] - \tilde{\boldsymbol{\omega}}_k^H[i-1]\tilde{\boldsymbol{r}}_k[i], & \text{Decision-directed Mode.} \end{cases} \tag{4.15}$$

This adaptive detection algorithm works in two modes. In the first mode, the filter weights are trained by the known training sequence $\boldsymbol{s}[i]$. After the filter weights converge to a certain point, the algorithm is then switched to the decision-directed mode. In this mode, the detector uses the detected symbols to update the tap weights. In this case, the quality

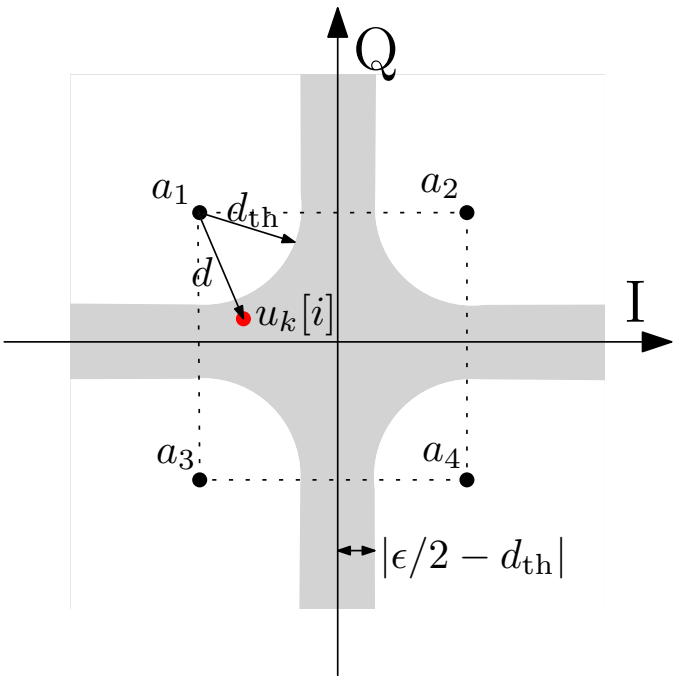

Figure 4.2: The constellation constraints (CC) device. The CC procedure is invoked as the soft estimates $u_k[i]$ dropped into the shaded area. Parameter ϵ denotes the distance between 2 nearest constellation symbols.

of the detected symbols has a significant impact on the performance of this adaptive DF detector. In the following subsection the CC algorithm is introduced to obtain enhanced decisions for each stream and allows this adaptive procedure to achieve a close-to-optimal error performance.

4.4.1 Decision Feedback with Constellation Constraints

The CC structure introduces a number of selected constellation points as the candidate decisions when the filter output $u_k[i]$ is determined unreliable. A selection algorithm is introduced to prevent the search space from growing exponentially. The reliability of the detected symbol is determined by the CC device, which saves the computational complexity by avoiding redundant processing with reliable decisions. In the following, the procedure for detecting $\hat{s}_k[i]$ for the k-th spatial stream is described, and the detection of other streams can be obtained accordingly.

After the system is switched to the decision-directed mode, the concatenated filter

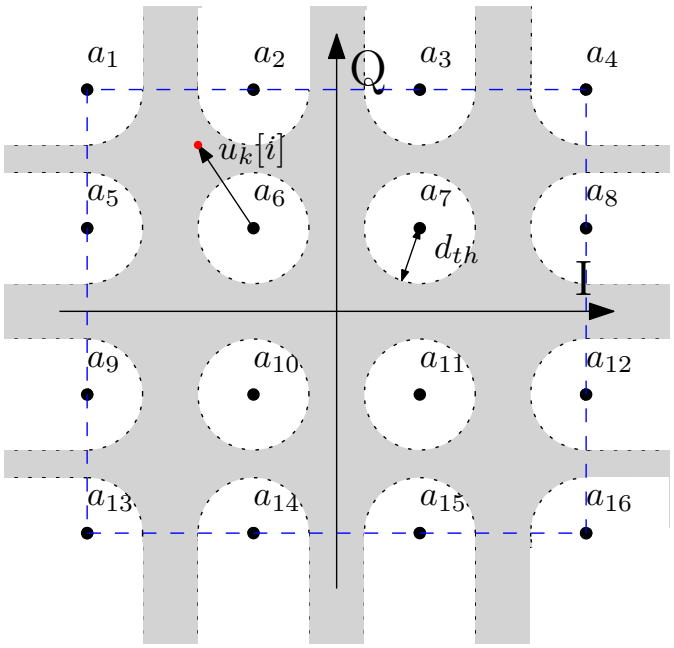

Figure 4.3: The constellation constraints for 16-QAM signals. A number of feedback candidates are invoked as the decision is dropped into the shaded area. Assuming the red dot $u_k[i]$ is the estimated symbol.

output $u_k[i]$ is checked by the CC device which is illustrated in Fig.4.2. The CC structure is defined by the threshold distance d_{th}, which can be a constant or determined in terms of SNR.

We also define two regions for the QPSK constellation map: (1) The region inside the square obtained by connecting four a_c, the a_c are assumed to have the form, $a_c = \Big(\pm \epsilon/2, \pm(\epsilon/2)j \Big)$, where ϵ is the distance between two nearest constellation symbols. The estimation $u_k[i]$ is considered inside the square if the following equations hold

$$\begin{cases} \big|\Re\{u_k[i]\}\big| \leq \epsilon/2 \\ \big|\Im\{u_k[i]\}\big| \leq \epsilon/2. \end{cases} \tag{4.16}$$

where $\Re\{\cdot\}$ and $\Im\{\cdot\}$ denote the real part and the image part of a complex value, respectively.

(2) Otherwise, the estimation is in the region outside the square obtained.

CASE 1 inside the square

In the first case, the estimation $u_k[i]$ is considered as unreliable if the following equation holds,

$$d = \min_{a_c \in \mathcal{A}} \left\{ |u_k[i] - a_c| \right\} > d_{\text{th}}. \tag{4.17}$$

where d denotes the distance between the estimated symbol $u_k[i]$ and its nearest constellation point and a_c is each element of the constellation points. Otherwise, the estimated symbol is closer to the constellations and the decision is considered as reliable.

CASE 2 outside the square

In this case, the equations of (4.16) do not hold, where the estimated symbol $u_k[i]$ is outside the square. In this case, the decision is determined unreliable if the distance from $u_k[i]$ to I(In-phase)-axis and Q(quadrature)-axis is small. Therefore, the estimation is unreliable if any of the following equations holds,

$$\left| \Re\{u_k[i]\} \right| < \epsilon/2 - d_{\text{th}}, \tag{4.18}$$

$$\left| \Im\{u_k[i]\} \right| < \epsilon/2 - d_{\text{th}}. \tag{4.19}$$

Otherwise, the estimated symbol is far away from the axis borders and the estimation is considered as reliable.

This can be further extend to multi-tier constellations (eg.16-QAM see Fig. 4.3) where the outer-tier would be similar to CASE 2, but we should also include two additional equations beside (4.18) and (4.19) which are given as

$$\min \left| \Re\{u_k[i]\} \pm \epsilon \right| < \epsilon/2 - d_{\text{th}}, \tag{4.20}$$

$$\min \left| \Im\{u_k[i]\} \pm \epsilon \right| < \epsilon/2 - d_{\text{th}}. \tag{4.21}$$

where $\left| \Re\{u_k[i]\} \pm \epsilon \right|$ are the distances between $u_k[i]$ and two vertical lines across the points $(0, \pm\epsilon)$, respectively. And $\left| \Im\{u_k[i]\} \pm \epsilon \right|$ are similarly defined as the distances between $u_k[i]$ and two horizontal lines across points $(\pm\epsilon, 0)$, respectively.

Therefore, for 16-QAM constellation, the estimation is considered as unreliable if any one of the four equations above (4.18-4.21) holds.

On the other hand, for the inner-tier constellations, if

$$\min \left| a_k[i] - u_k[i] \right| \geq d_{\text{th}}, \tag{4.22}$$

was true, the estimation is considered as unreliable.

The CC device distinguishes the reliable feedback signals from the unreliable ones, which allows the DFCC to maintain the complexity at the same level of the conventional DF structure and saves the computational complexity by avoiding redundant processing with reliable decisions.

Reliable

If the filter output $u_k[i]$ is dropped into the lighted area of the constellation map, the decision is considered as reliable. A quantization operation $\mathrm{Q}(\cdot)$ is then performed as

$$\hat{s}_k[i] = \mathrm{Q}(u_k[i]). \tag{4.23}$$

This quantized symbol is a reliable decision for the current stream and used to compute $\xi_k[i]$ in the decision-directed mode.

Unreliable

If it is the case that $u_k[i]$ is dropped into the shaded area of the constellation map, the decision is determined as unreliable. The CC processing is invoked and a candidate vector is generated as given by

$$\mathcal{L} = \{c_1, c_2, \ldots, c_m, \ldots, c_M\} \subseteq \mathcal{A}, \tag{4.24}$$

The candidates are constrained by the constellation map and the vector is a selection of the M nearest constellation points to the $u_k[i]$. The size of $\mathcal{L}$ can be either fixed or adaptive

with the channel condition which introduces a trade off between the performance and the energy efficiency. The refined estimate for this unreliable decision is obtained by

$$\hat{s}_k[i] = c_{\text{opt}}, \tag{4.25}$$

where c_{opt} is the optimal candidate selected from $\mathcal{L}$. This refined decision will produce a more accurate $\xi_k[i]$ which minimizes the MSE in (4.11)-(4.14). The benefits provided by the CC algorithm are based on the assumption that the optimal feedback candidate c_{opt} is correctly selected. This selection algorithm is similarly defined in Chapter 3 and given as follows:

In order to find the optimal candidate, a set of tentative decision vectors $\mathcal{B}_k = \left\{\boldsymbol{b}_k^1, \ldots, \boldsymbol{b}_k^m, \ldots, \boldsymbol{b}_k^M\right\}$ is defined, the number of these tentative decision vectors M equals the number of selected constellation candidates. Each vector $\boldsymbol{b}_k^m$ is defined as

$$\boldsymbol{b}_k^m[i] = \left[\hat{s}_1[i], \ldots, \hat{s}_{k-1}[i], c_m, \hat{b}_{k+1}[i], \ldots, \hat{b}_K[i]\right]. \tag{4.26}$$

This $K \times 1$ vector $\boldsymbol{b}_k^m$ consists of the following parts:
(A) $(k-1)$-dimensional detected symbol vector $\hat{\boldsymbol{s}}_{k-1}[i]$ which is used in (4.5).
(B) A candidate symbol c_m taken from $\mathcal{L}$ for substituting the unreliable $\mathrm{Q}(u_k[i])$ in the k-th data stream.
(C) By concatenating (A) and (B) as the previous decisions, the tentative decisions of the following streams $\hat{b}_{k+1}[i], \ldots, \hat{b}_K[i]$ are subsequently obtained by the adaptive detector. Let us define the vector with the candidate constellation point as

$$\check{\boldsymbol{s}}_{k,m}[i] = \left[\hat{s}_1[i], \ldots, \hat{s}_{k-1}[i], c_m\right]^T, \tag{4.27}$$

$$= \left[\hat{\boldsymbol{s}}_{k-1}^T[i], c_m\right]^T. \tag{4.28}$$

Therefore, (4.5) is transformed to

$$\bar{\boldsymbol{r}}_{k+1,m}[i] = \left[\boldsymbol{r}^T[i], -\check{\boldsymbol{s}}_{k,m}^T[i]\right]^T, k = 1, \ldots, K. \tag{4.29}$$

The tentative decision of the $(k+1)$ stream is

$$\hat{b}_{k+1}[i] = \mathrm{Q}\Big\{\tilde{\boldsymbol{\omega}}_{k+1}^H[i]\bar{\boldsymbol{r}}_{k+1,m}[i]\Big\}. \tag{4.30}$$

The CC algorithm selects the best constellation point among M candidates according to the maximum likelihood rule as

$$m_{\text{opt}} = \arg \min_{1 \le m \le M} \left\|\boldsymbol{r}[i] - \boldsymbol{H}\boldsymbol{b}_k^m[i]\right\|^2. \tag{4.31}$$

Table 4.1: The pseudo-code of the DFCC algorithm

Initialization: $i = 0$

for $k = 1$ **to** K **do**
  $\boldsymbol{\Phi}_k^{-1}[0] = \delta^{-1}\boldsymbol{I}$; $\boldsymbol{\omega}_{f,k}[0] = \mathbf{1}$; $\boldsymbol{\omega}_{b,k}[0] = \mathbf{0}$;
end for where δ is a small positive constant.

RLS weight update: $i > 0$

$\boldsymbol{q}_k[i] = \boldsymbol{\Phi}_k^{-1}[i-1]\boldsymbol{r}_k[i]$;
$\boldsymbol{k}_k[i] = \frac{\lambda^{-1}\boldsymbol{q}_k[i]}{1+\lambda^{-1}\boldsymbol{r}_k^H[i]\boldsymbol{q}_k[i]}$;
$\boldsymbol{\Phi}_k^{-1}[i] = \lambda^{-1}\boldsymbol{\Phi}_k^{-1}[i-1] - \lambda^{-1}\boldsymbol{k}_k[i]\boldsymbol{q}_k^H[i]$;

if the system is in the training mode
  $\xi_k[i] = s_k[i] - \tilde{\boldsymbol{\omega}}_k^H[i-1]\tilde{\boldsymbol{r}}_k[i]$;
if the system is in the decision-directed mode
  $\xi_k[i] = \hat{s}_k[i] - \tilde{\boldsymbol{\omega}}_k^H[i-1]\tilde{\boldsymbol{r}}_k[i]$;
end

$\tilde{\boldsymbol{\omega}}_k[i] = \tilde{\boldsymbol{\omega}}_k[i-1] + \boldsymbol{k}_k[i]\xi_k^*[i]$;

Constellation constraints: Decision-directed mode only

for $k = 1, \ldots, K$
$u_k[i] = \tilde{\boldsymbol{\omega}}_k[i-1]^H\boldsymbol{r}[i]$;
if $u_k[i]$ **is unreliable**
  $\boldsymbol{\mathcal{L}} = [c_1, c_2, \ldots, c_m, \ldots, c_M]^T$;
  for $m = 1$ **to** M **do**
    $\check{\boldsymbol{s}}_{k,m}[i] = [\hat{\boldsymbol{s}}_{k-1}^T[i], c_m]^T$;
    for $q = k+1$ **to** K **do**
      $\bar{\boldsymbol{r}}_q[i] = \left[\boldsymbol{r}^T[i], \check{\boldsymbol{s}}_{k,m}^T[i], \hat{b}_{k+1}, \ldots, \hat{b}_{q-1}\right]^T$;
      $\hat{b}_q = \tilde{\boldsymbol{\omega}}_q^H[i]\bar{\boldsymbol{r}}_q[i]$;
    end for
  $\boldsymbol{b}_k^m[i] = \left[\check{\boldsymbol{s}}_{k,m}[i], \hat{b}_{k+1}[i], \ldots, \hat{b}_K[i]\right]$;
  end for
  $c_{\text{opt}} = \arg\min_{1\le m\le M}\left\|\boldsymbol{r}[i] - \boldsymbol{H}\boldsymbol{b}_k^m[i]\right\|^2$;
  $\hat{s}_k[i] = c_{\text{opt}}$;
else
  $\hat{s}_k[i] = \mathrm{Q}(u_k[i])$;
end if

Then c_{opt} is chosen to replace the unreliable decision $u_k[i]$. The same filter weight $\boldsymbol{\omega}_k[i]$ is used to process all the candidates, which allows the proposed algorithm to have the computational simplicity of the adaptive DF detector. The pseudo-code of the proposed DFCC algorithm is summarized in TABLE 4.1.

4.4.2 DFCC with Multiple-Branch Processing

The previous subsection shows that the DFCC solves (4.7) with optimal nulling and cancellation ordering patterns. In this subsection, the proposed DFCC is applied with several parallel branches that are equipped with different ordering patterns. By exploiting a certain ordering pattern, the MB produces a symbol estimate vector. Therefore, a group of symbol estimate vectors are generated at the end of the DFCC-MB structure. This parallel architecture achieves a higher detection diversity order by selecting the branch which yields the estimates with the best performance.

Let us define

$$\boldsymbol{s}'[i] \triangleq \boldsymbol{T}_l \boldsymbol{s}[i] = \left[s_{1,l}[i], s_{2,l}[i], \ldots, s_{K,l}[i]\right]^T, \tag{4.32}$$

a permutation of the transmitted symbol set $\boldsymbol{s}[i]$, ordered by the transformation matrix $\boldsymbol{T}_l, l = 1, \ldots, L.$, where each row and each column of $\boldsymbol{T}_l$ contain only one "1". We also define $\hat{\boldsymbol{s}}'_l[i] = \left[\hat{s}_{1,l}[i], \hat{s}_{2,l}[i], \ldots, \hat{s}_{K,l}[i]\right]^T$ as the detected symbol vector and $u_{k,l}[i]$ denotes the output of k-th forward filter for the l-th branch which exploits the order $\boldsymbol{T}_l$. It is worth noting that the estimates of the permuted transmitted symbol can be transferred back to the original order by using $\boldsymbol{T}_l$ as

$$\hat{\boldsymbol{s}}_l[i] = \boldsymbol{T}_l^T \hat{\boldsymbol{s}}'_l[i]. \tag{4.33}$$

The optimal ordering scheme conducts an exhaustive search of $L = K!$ branches. For a practical implementation, a number of sub-optimal schemes are used to design the transformation matrices $\boldsymbol{T}_l$ codebook, these approaches are proposed in [76]. In this chapter, the FSB (see Section 3.3.3) is applied in the receiver.

For the branch l, the filter output is given by

$$u_{k,l}[i] = \boldsymbol{\omega}'^H_{f,k}[i]\boldsymbol{r}[i] + \boldsymbol{\omega}'^H_{b,k}[i]\hat{\boldsymbol{s}}'_{k-1,l}[i], \tag{4.34}$$

where the $(k-1)$-dimensional detected symbol vector is defined as

$$\hat{\boldsymbol{s}}'_{k-1}[i] = \left[\hat{s}_{1,l}[i], \hat{s}_{2,l}[i], \ldots, \hat{s}_{k-1,l}[i]\right]^T, \tag{4.35}$$

and each entry is obtained by l-th DFCC branch. The forward filter $\boldsymbol{\omega}'_{f,k}[i]$ and backward filter $\boldsymbol{\omega}'_{b,k}[i]$ correspond to the permuted channel

$$\boldsymbol{H}' \triangleq \boldsymbol{T}_l \boldsymbol{H}. \tag{4.36}$$

The filters can be concatenated together as

$$\tilde{\boldsymbol{\omega}}'_k[i] = \begin{cases} \boldsymbol{\omega}'_{f,k}[i], & k = 1, \\ \left[\boldsymbol{\omega}'^T_{f,k}[i], \boldsymbol{\omega}'^T_{b,k}[i]\right]^T, & k = 2, \ldots, K. \end{cases} \tag{4.37}$$

the input can also be concatenated as

$$\tilde{\boldsymbol{r}'}_k[i] = \begin{cases} \boldsymbol{r}[i], & k = 1, \\ \left[\boldsymbol{r}^T[i], -\hat{\boldsymbol{s}}'^T_{k-1}[i]\right]^T, & k = 2, \ldots, K. \end{cases} \tag{4.38}$$

Then, we simplify (4.34) as

$$u_{k,l}[i] = \tilde{\boldsymbol{\omega}'}^H_k[i]\tilde{\boldsymbol{r}'}_k[i]. \tag{4.39}$$

The LS cost function for the l-th branch is written by

$$\mathcal{J}_{k,l}[i] = \sum_{\tau=1}^{i} \lambda^{i-\tau} \left| \hat{s}_{k,l}[\tau] - \tilde{\boldsymbol{\omega}'}^H_k[i]\tilde{\boldsymbol{r}'}_k[\tau] \right|^2 \tag{4.40}$$

4.4.3 Channel estimation

As we discussed in the previous sections, the MIMO channel state information is required for selecting the CC candidates (4.31) and for generating the cancellation ordering codebook for MB processing (4.36). The LS channel estimation algorithm has been investigated in [80]. Based on a weighted average of error squares, the estimated channel minimizes the cost function whose expression at time instant i is defined as

$$\mathcal{J}_{\hat{\boldsymbol{H}}}[i] = \sum_{\tau=1}^{i} \lambda^{i-\tau} \left| \boldsymbol{r}[\tau] - \hat{\boldsymbol{H}}[i]\boldsymbol{s}[\tau] \right|^2, \tag{4.41}$$

where $\hat{\boldsymbol{H}}[i]$ is the channel matrix estimate at time instant i. The quantities $\boldsymbol{r}[\tau]$ and $\boldsymbol{s}[\tau]$ are received signal and pilot symbol vectors at the time instant τ, respectively.

To minimise the cost function, the gradient of the cost function with regard to the estimated channel matrix should be equated to a zero matrix as

$$\nabla_{\hat{\boldsymbol{H}}[i]} \mathcal{J}_{\hat{\boldsymbol{H}}}[i] = \mathbf{0}_{N_R,K}. \tag{4.42}$$

By solving the above equation, the LS estimate of the channel matrix is obtained as

$$\begin{aligned}\hat{\boldsymbol{H}}[i] &= \Big(\sum_{\tau=1}^{i}\lambda^{i-\tau}\boldsymbol{r}[\tau]\boldsymbol{s}^{H}[\tau]\Big)\Big(\sum_{\tau=1}^{i}\lambda^{i-\tau}\boldsymbol{s}[\tau]\boldsymbol{s}^{H}[\tau]\Big)^{-1} \\ &= \boldsymbol{D}[i]\boldsymbol{\Phi}^{-1}[i].\end{aligned} \tag{4.43}$$

In order to avoid the matrix inversion operation $(\cdot)^{-1}$, a recursive algorithm is developed. Let us define

$$\boldsymbol{\Phi}^{-1}[i] = \boldsymbol{P}[i], \tag{4.44}$$

where $\boldsymbol{D}[i]$ can be obtained iteratively by

$$\boldsymbol{D}[i] = \lambda\boldsymbol{D}[i-1] + \boldsymbol{r}[i]\boldsymbol{s}[i]^{H} \tag{4.45}$$

and $\boldsymbol{P}[i]$ is calculated iteratively by using the matrix inversion lemma,

$$\boldsymbol{P}[i] = \lambda^{-1}\boldsymbol{P}[i-1] - \frac{\lambda^{-2}\boldsymbol{P}[i-1]\boldsymbol{s}[i]\boldsymbol{s}[i]^{H}\boldsymbol{P}[i-1]}{1+\lambda^{-1}\boldsymbol{s}[i]^{H}\boldsymbol{P}[i-1]\boldsymbol{s}[i]}. \tag{4.46}$$

The initial state of the parameters are set as $\boldsymbol{D}[0] = \boldsymbol{0}_{N_R,K}$ and $\boldsymbol{P}[0] = \delta_c^{-1}\boldsymbol{I}$, where δ_c is a small constant.

4.5 Detection Complexity

The computational complexity of the proposed DFCC and its MB version is given in this section. Essentially, we detail the complexity of the DFCC procedure with a single branch (SB), and the complexity of the DFCC-MB can be obtained by multiplying the complexity of the DFCC by the number of branches L. The detailed computational complexity is shown in terms of the averaged number of required complex multiplications and floating-point operations (FLOPS) per symbol detection.

In terms of complex multiplications, the proposed algorithms and other existing schemes are represented in TABLE. 4.2, $N = K = N_R$ is the number of transmit and receive antenna elements. The parameter M denotes the number of candidates in $\mathcal{L}$ when decisions are determined unreliable, and C denotes the number of constellation points that correspond to the modulation type. The complexity of the SD is associated with C, the k-dimensional sphere radius d_{SD} is chosen to be a scaled version of the variance of

Table 4.2: Computational complexity of algorithms

Algorithms	**Required complex multiplications**
Non-Adaptive OSIC	$2N^3 + N^2 + N$
LMMSE –RLS	$4N^2 + 4N$
DF –RLS	$\frac{28}{3}N^2 - \frac{4}{3}$
DFCC –RLS WORST	$(\frac{28}{3}N^2 - \frac{4}{3}) + M(\frac{5}{2}N^2 - \frac{3}{2}N)$
DFCC –RLS BEST	same as "DF –RLS"
DFCC MB –RLS	L times "DFCC –RLS"
Standard SD [67]	$\sum_{k=1}^{N} \frac{Ck\pi^{k/2}}{\Gamma(k/2+1)} d_{SD}^{k} + 2N^2$

the noise [67]. The proposed DFCC has the worst case and the best case complexities situated at the same level of the conventional DF algorithm [82]. In the worst case, all N decisions are considered unreliable, which means the $\mathcal{L}$ is generated for every stream and the CC selection is invoked N times which brings $M(5/2N^2 - 3/2N)$ multiplications on top of the DF algorithm. Thanks to the CC scheme, we can see from TABLE. 4.3 that when $SNR = 16$ dB, only a small division of the decisions are considered unreliable across the stream layers. The probability of unreliable estimates is decreased as the detection diversity increases. This leads to the processing of 6.1%, 4.65%, 3.59% on average over the streams of the estimated symbol for $N = 2, 4, 8$ antennas, respectively. For the remaining symbols, the conventional quantization is performed. The decreased probability of invoking the CC selection suggests that the DFCC may be suitable for a MIMO system with a larger number of data streams.

According to TABLE. 4.2, the worst DFCC–RLS complexity is $(\frac{28}{3}N^2 - \frac{4}{3}) + M(\frac{5}{2}N^2 - \frac{3}{2}N)$ while the first term $(\frac{28}{3}N^2 - \frac{4}{3})$ is the complexity for a conventional adaptive DF scheme. The second term denotes the additional complex multiplications on top of the conventional schemes. The additional complexity is obtained as follows:

Table 4.3: The percentage that the estimate is considered as unreliable.

Layers k	**1**	**2**	**3**	**4**	**5**	**6**	**7**	**8**
2×2 **16dB**	7.6	4.6	-	-	-	-	-	-
4×4 **16dB**	10.1	4.5	1.9	2.1	-	-	-	-
8×8 **16dB**	15.0	6.6	2.1	1.7	1.1	0.6	0.5	0.4
2×2 **12dB**	14.9	16.6	-	-	-	-	-	-
4×4 **12dB**	22.1	12.8	11.9	14.7	-	-	-	-
8×8 **12dB**	26.6	21.4	16.4	13.4	11.1	10.47	10.0	9.1

- If u_1 is unreliable, (by omitting the time index $[i]$) we replace $\mathrm{Q}(u_1)$ with $c_m, m = 1, \ldots, M$ and the Line.18 - Line.21 of the pseudo-code table 4.1 needs to repeat M times for the different c_m. The involved number of the complex multiplication is $M \times \sum_{q=1}^{K-1} q$.
- If u_2 is unreliable, similar to above, the number of involved number of the complex multiplication is $1 + M \times \sum_{q=1}^{K-2} q$.
- If u_3 is unreliable, the involved number of the complex multiplication is $2 + M \times \sum_{q=1}^{K-3} q$. ...
- By summing across K antennas we have:

$$\sum_{k=1}^{K}(k-1) + M\sum_{q=1}^{K-k} q. \tag{4.47}$$

The overall additional complexity can be obtained by summing the above number with the complexity inducted by maximum likelihood selection and reliability checking algorithm. Fig.4.4 attached below will help to obtain the conclusion above.

In addition, Fig.4.5 depicts the number of required complex multiplications per symbol detection. The plots compare the required operations as the number of antennas in-

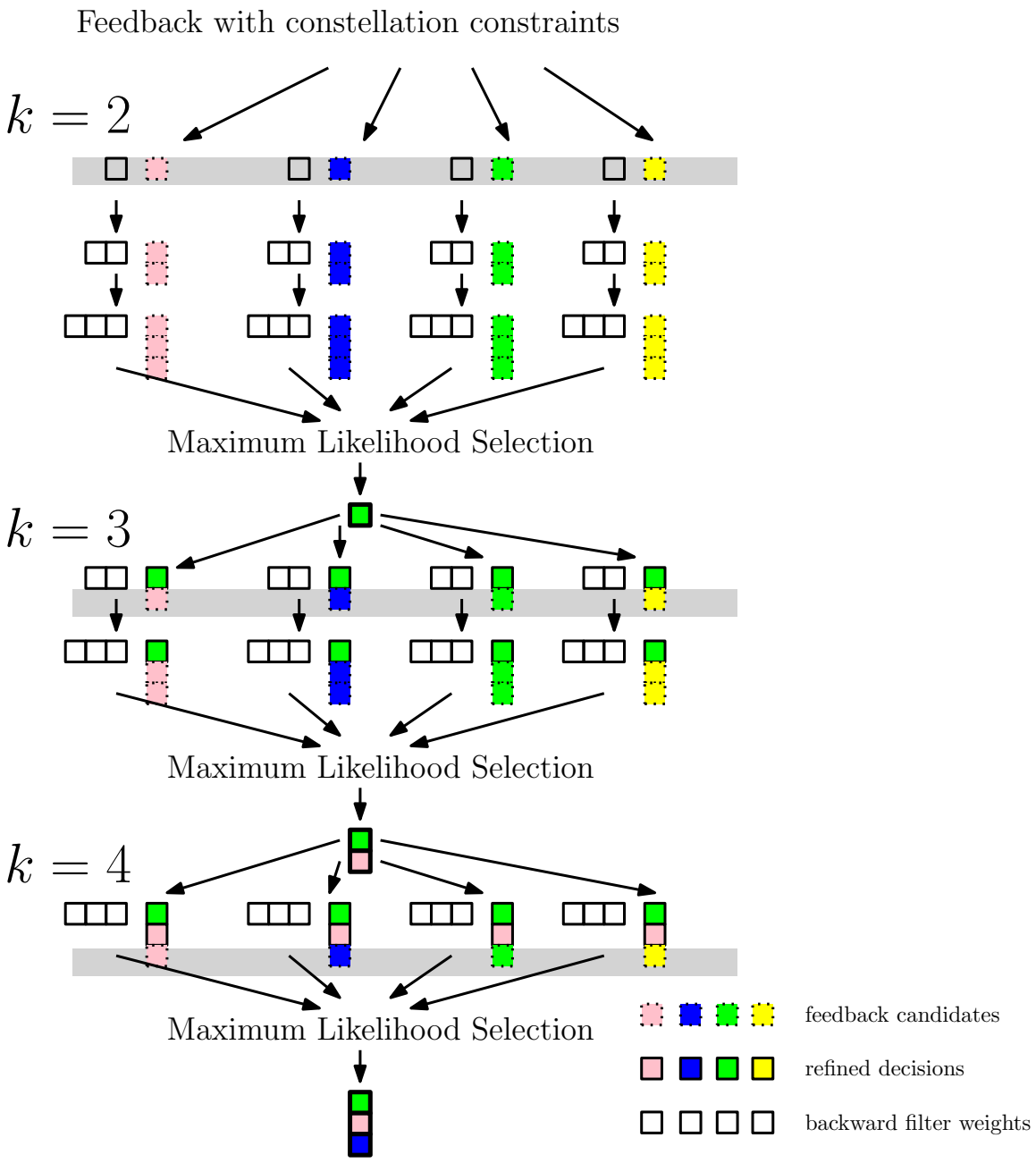

Figure 4.4: The blank squares denote the complex elements in the decision backward filter $\boldsymbol{\omega}_{b,k}^{H}$, and the coloured squares denote the feedback candidates c_m. Dotted squares represent tentative decisions while the solid squares represent reliable decisions.

creases. Each DFCC branch has a complexity slightly above the conventional DF-RLS while it achieves a significant performance gain over the DF-RLS. The DFCC-RLS represented here has the configuration of $M = 4, d_{\text{th}} = 0.5$ and the DFCC MB-RLS has $L = 10$ branches in QPSK modulation. The low complexity of the DFCC algorithm provides an opportunity to deploy the MB structure with low computational cost, especially for systems with large transmit antenna arrays. The result also indicated that as $K = N_R$ increases, more branches are need to be applied to prevent more performance degradation from the SD. This issue was first mentioned in [76], the optimal ordering scheme conducts an exhaustive search of $L = N!$ branches, where ! is the factorial operator. This means that for the optimal solution, L needs to be proportional to $N!$. For example, for a $4\times$ 4 MIMO system, there are $L = 4! = 24$ ordering patterns in the optimal ordering scheme. The detection with the optimal number of branches is not a practical implementation, therefore, three approaches were introduced in [76], namely Pre-stored patterns (PSP), Frequently selected branches (FSB) and Listing patterns approach (LPA). These algorithms are able to find a smaller number of selected branches and keep a near-optimal performance. A discussion of these alternative solutions is beyond the scope of this thesis. In this work, we use the FSB as the sub-optimal solution to demonstrate that the algorithm has the ability to attain a near-optimal performance. It is not easy to know if the number of the needed branches has to be proportional to N (or N^2 or N^3). However, a series of studies indicate that the near-optimal FSB requires L branches and L is related to N instead of N^2 or N^3 .

The average overall detection complexity of the proposed scheme is also measured in terms of the average number of FLOPS used. The simulations were performed with the Lightspeed toolbox [94], in which the number of FLOPS equals 2 for a complex addition and 6 for a complex multiplication. Fig.4.6 depicts the number of required FLOPS per symbol detection. The SD has the highest complexity while the Non-Adaptive OSIC and lattice reduction aided OSIC (LR-OSIC) have complexities many times higher than the DF–RLS detector. The proposed DFCC–RLS requires a negligible number of additional FLOPS compared with the DF–RLS detector. The proposed DFCC significantly improves the overall performance of the conventional DF detection, especially when the time-varying channel is tracked. The single-branch DFCC has a performance sensitive to $K = N_R = N$, a higher number of N requires more parallel branches to maintain a comparable level of performance of SD. With any given N , the proposed algorithm provides a

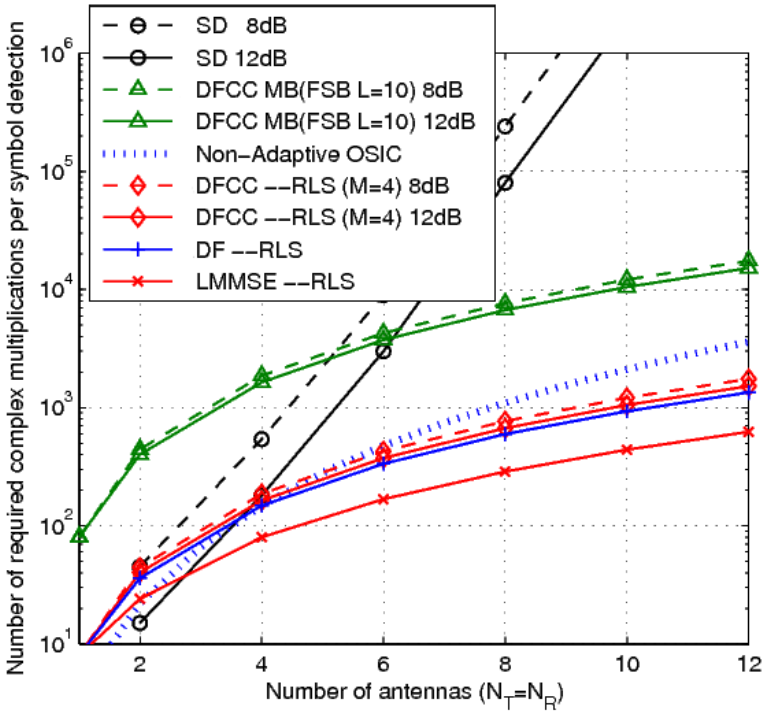

Figure 4.5: Detection complexity in terms of required number of arithmetic operations per symbol detection against the number of antennas. The proposed DFCC-MB algorithm has L times the complexity of DFCC which has a similar complexity with the DF scheme.

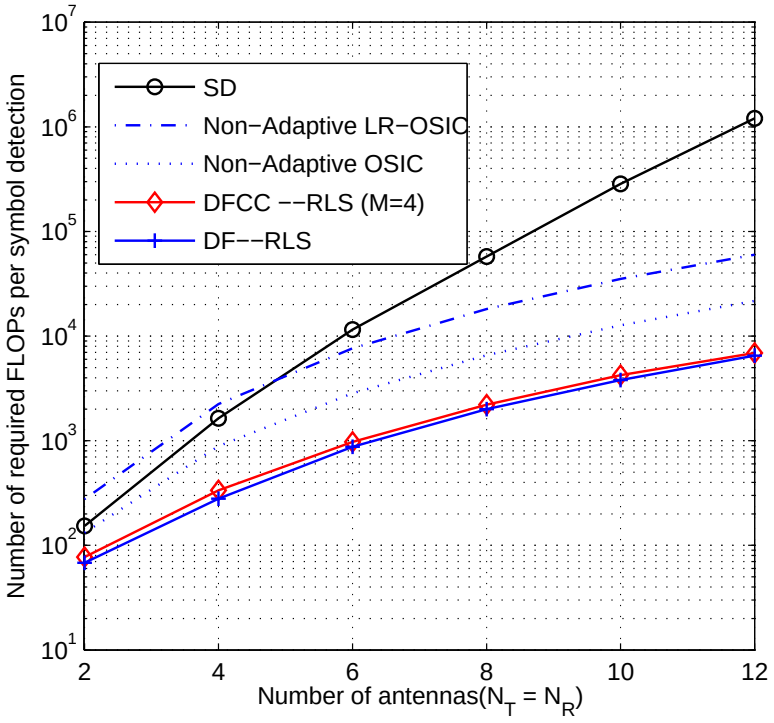

Figure 4.6: Detection complexity in terms of required FLOPS per symbol detection, DFCC with $d_{\text{th}} = 0.5$ has the complexity as low as DF detector at $E_b/N_0 = 8dB$

complexity benefit at high SNR levels, the estimates of the transmitted symbols are more reliable. Therefore, for most of the time, a single feedback is needed, and the complexity approaches the conventional DF detector. Fig.4.7 demonstrates the complexity benefit in terms of SNR. The complexity is sensitive to the SNR, thanks to the reliability checking scheme, many redundant processing can be avoided in higher SNR region. For the higher SNR, the estimated symbols have a higher probability to be considered reliable. There is a constant 42 FLOPS gap when $SNR > 25$ dB, which is generated by the reliable checking operations of each estimated symbol. A 4×4 MIMO system is adopted with QPSK transmitted signal we also set the threshold equals to d_{th} = 0.5.

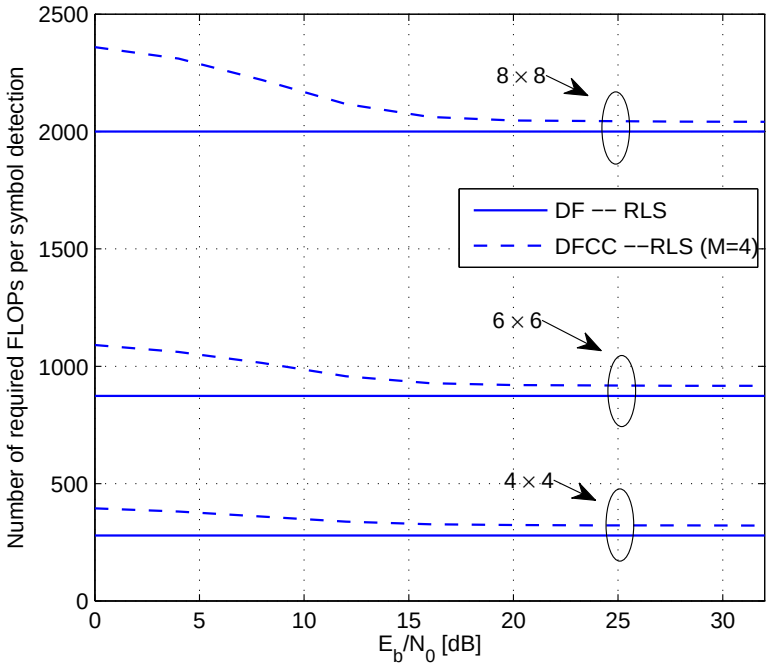

Figure 4.7: Complexity in terms of required FLOPS per symbol detection, DFCC $(M = 4, L = 1)$ has a decreasing complexity as the SNR increases.

4.6 Iterative Processing Constellation Constraints with Soft-output

In the following, a soft-output detector with the CCDF architecture is described to improve the performance with error control coding. Let $b_{k,j}$ be the j-th bit of the constellation symbol and $(j = 1, 2, \ldots, J)$ where $J = \log_2 C$ is the constellation size. We also denote $L[b_{k,j}]$ as the log-likelihood ratio (LLR) value for the coded bits $b_{k,j}$ which is defined as

$$L[b_{k,j}] = \ln P(b_{k,j} = 1) - \ln P\left(b_{k,j} = 0\right). \tag{4.48}$$

Thus, we define *a priori* LLR of the coded bits $b_{k,j}$ as $L[b_{k,j}^{(p1)}]$ and *a posteriori* LLR as

$$L[b_{k,j}^{(a1)}] = \ln P(b_{k,j} = 1|\boldsymbol{r}) - \ln P\left(b_{k,j} = 0|\,\boldsymbol{r}\right). \tag{4.49}$$

The detection processing is performed block-by-block. The soft-input soft-output MIMO detector computes the *extrinsic* LLR as

$$L[b_{k,j}^{(e1)}] = L[b_{k,j}^{(a1)}] - L[b_{k,j}^{(p1)}]. \tag{4.50}$$

The *extrinsic* information is obtained by subtracting the dependency on $L[b_{k,j}^{(p1)}]$ and (4.50) is re-written as [90]

$$L[b_{k,j}^{(e1)}] = \ln \frac{\mathrm{P}\left(b_{k,j}=1\middle|\boldsymbol{r}\right)}{\mathrm{P}\left(b_{k,j}=0\middle|\boldsymbol{r}\right)} - \ln \frac{\mathrm{P}\Big(b_{k,j}=1\Big)}{\mathrm{P}\Big(b_{k,j}=0\Big)}, \tag{4.51}$$

$$= \ln \frac{\sum_{\boldsymbol{s}\in\mathcal{X}_{k,j}^{1}} \mathrm{P}\big(\boldsymbol{r}\big|\boldsymbol{s}\big)\exp\big(f(\boldsymbol{s})\big)}{\sum_{\boldsymbol{s}\in\mathcal{X}_{k,j}^{0}} \mathrm{P}\big(\boldsymbol{r}\big|\boldsymbol{s}\big)\exp\big(f(\boldsymbol{s})\big)}. \tag{4.52}$$

and $\mathcal{X}_{k,j}^{1}$ is the set of all symbol vectors that consist of bits satisfying $b_{k,j}=1$ and $\mathcal{X}_{k,j}^{0}$ is similarly defined but satisfying $b_{k,j}=0$. The joint probability density in (4.51) is obtained by [91]

$$\mathrm{P}\big(\boldsymbol{r}\big|\boldsymbol{s}\big) \propto \exp\Big(-\frac{1}{\sigma_v^2}\|\boldsymbol{r}-\boldsymbol{H}\boldsymbol{s}\|^2\Big), \tag{4.53}$$

and

$$f(\boldsymbol{s}) = \frac{1}{2}(2\boldsymbol{b}_{[k,j]}^{T}-1)\boldsymbol{L}[b_{k,j}^{(p1)}], \tag{4.54}$$

where $\boldsymbol{b}_{[k,j]}$ is a length $K\log_2 C$ column vector comprised of $b_{k,j}$ except its (k,j)-th element is replaced by 0, and $\boldsymbol{L}[b_{k,j}^{(p1)}]$ is the *a priori* LLR values obtained form the outer channel decoder. All the entries of $\boldsymbol{L}[b_{k,j}^{(p1)}]$ are set to zeros in the first pass as the initial probability of the symbol transmission is equal. The *extrinsic* LLRs of the coded bits are deinterleaved and used as the *a priori* LLRs and delivered to the channel decoder which performs the decoding algorithms as BCJR [65] or Max-log-MAP [95]. The soft decision obtained from the decoder is then interleaved and fed back to the detector to complete an iteration. The computational complexity of this MAP detector is high as the size of the summation increases exponentially with K and C, which implies that too much complexity is required for processing LLR for each bit using (4.51). We now discuss how the bit-level LLR can be obtained using the complexity-reduced DFCC detector.

In this complexity-reduced detection, the probability density for all the possible transmitted vectors (4.53) are not available. A small set of vectors can be found by deploying the DFCC detection, the ML vector may still be found in the list of tentative decisions. Since only a small set of symbol vectors is considered, the DFCC performance is worse than that of MAP detection when the soft-output is required. However, by appropriately selecting the tentative decisions, the DFCC performance can approach the MAP detector

performance. Let $\mathcal{B}$ denote the set of tentative decisions obtained from the DFCC detector

$$\tilde{\mathcal{B}} = \mathcal{B}_1 \cup \mathcal{B}_2 \cup, \ldots, \cup \mathcal{B}_K, \tag{4.55}$$

If $L > 1$, we have

$$\mathcal{B} = \tilde{\mathcal{B}}_1 \cup \tilde{\mathcal{B}}_2 \cup, \ldots, \cup \tilde{\mathcal{B}}_L, \tag{4.56}$$

and the *extrinsic* information is obtained by

$$L[b_{k,j}^{(e1)}] = \ln \frac{\sum_{\boldsymbol{s} \in \mathcal{X}_{k,j}^1 \bigcap \mathcal{B}} \mathrm{P}\big(\boldsymbol{r}\big|\boldsymbol{s}\big) \exp\big(f(\boldsymbol{s})\big)}{\sum_{\boldsymbol{s} \in \mathcal{X}_{k,j}^0 \bigcap \mathcal{B}} \mathrm{P}\big(\boldsymbol{r}\big|\boldsymbol{s}\big) \exp\big(f(\boldsymbol{s})\big)}. \tag{4.57}$$

In the case that the intersection of the MAP set and the candidate vector set is empty,

$$\mathcal{X}_{k,j}^1 \cap \mathcal{B} = \emptyset \qquad \text{or} \qquad \mathcal{X}_{k,j}^0 \cap \mathcal{B} = \emptyset. \tag{4.58}$$

the LLR for that specific bit can be filled with an arbitrary number with a large magnitude. The algorithm of the soft-output DFCC detection is summarized in the following algorithm table.

4.7 Simulations

4.7.1 Point-to-point MIMO Systems

In this section, several numerical examples are used to demonstrate the overall system performance of using our algorithms. The performance is measured in terms of bit error rate (BER), obtained by 10^4 Monte Carlo runs. In our simulations, the SNR per transmitted information bit is defined as

$$\frac{E_b}{N_0}\Big|_{\mathrm{dB}} = 10 \log_{10} \Big(\frac{N_R}{R \log_2 C} \cdot \frac{\sigma_s^2}{\sigma_v^2} \Big). \tag{4.59}$$

The total transmitted power $E_s = K \cdot \sigma_s^2$ which is evenly distributed to K transmit antennas. The N_R receive antennas collect a total power of $N_R E_s$ which carries $K \log_2 C$ coded bits or $RK \log_2 C$ information bits. $R \leq 1$ is the channel coding rate which introduces information redundancy. The coding rate $R = 1$ is assumed for the simulations without channel coding.

Algorithm 1 Algorithm soft-output log-Max-DFCC Detection

Require: $\boldsymbol{r} \in \mathcal{C}^{N_R \times 1}$, $\boldsymbol{H} \in \mathcal{C}^{N_R \times K}$, constellation set $\mathcal{A}$, σ_v^2, $n \leftarrow 0$, $\boldsymbol{L}(b_{k,j}^{p1})$, TI.

1. Find the set of symbol vectors $\mathcal{X}_{k,j}^1 \cap \mathcal{B}$ and $\mathcal{X}_{k,j}^0 \cap \mathcal{B}$
2. **for** $lo \leftarrow TI$ {Turbo Iteration} **do**
3. **for** $k \leftarrow 1, \ldots, K$ **do**
4. **for** $j \leftarrow 1, \ldots, J$ **do**
5. **for** $\boldsymbol{s} \in \mathcal{X}_{k,j}^1 \cap \mathcal{B}$ **do**
6. $\boldsymbol{b} \leftarrow \text{demap}(\boldsymbol{s})$, $\boldsymbol{b}_{k,j} \leftarrow 0$
7. $\text{P}(\boldsymbol{x}) \leftarrow \frac{1}{2}(2\boldsymbol{b}_{[k,j]} - 1)\boldsymbol{L}(b_{k,j}^{(p1)})$ {*Symbol probability*}
8. $\lambda_n^1 \leftarrow \ln \text{P}(\boldsymbol{x}) - \frac{\|\boldsymbol{r} - \boldsymbol{H}\boldsymbol{s}\|^2}{\sigma_v^2}$
9. **end for**
10. **for** $\boldsymbol{s} \in \mathcal{X}_{k,j}^0 \cap \mathcal{B}$ **do**
11. $\boldsymbol{b} \leftarrow \text{demap}(\boldsymbol{s})$, $\boldsymbol{b}_{k,j} \leftarrow 0$
12. $\text{P}(\boldsymbol{x}) \leftarrow \frac{1}{2}(2\boldsymbol{b}_{[k,j]} - 1)\boldsymbol{L}(b_{k,j}^{(p1)})$ {*Symbol probability*}
13. $\lambda_n^0 \leftarrow \ln \text{P}(\boldsymbol{x}) - \frac{\|\boldsymbol{r} - \boldsymbol{H}\boldsymbol{s}\|^2}{\sigma_v^2}$
14. **end for**
15. $L(b_{k,j}^{(e1)}) \leftarrow \max\{\lambda_n^1, n = 1, \ldots, |\mathcal{X}_{k,j}^1 \cap \mathcal{B}|\} - \max\{\lambda_n^0, n = 1, \ldots, |\mathcal{X}_{k,j}^0 \cap \mathcal{B}|\}$
16. **end for** {Antenna stream}
17. **end for** {*Bit Label*}
18. Deinterleave *extrinsic* $\boldsymbol{L}(b_{k,j}^{(e1)})$
19. Perform BCJR decoding and compute $\boldsymbol{L}(b_{k,j}^{(e2)})$
20. Interleaving *extrinsic* $\boldsymbol{L}(b_{k,j}^{(e2)})$ and feedback to detector.
21. **end for** {*Turbo Iteration*}
22. Decision of systematic bit is obtained via sign$\{\boldsymbol{L}(m_k)\}$

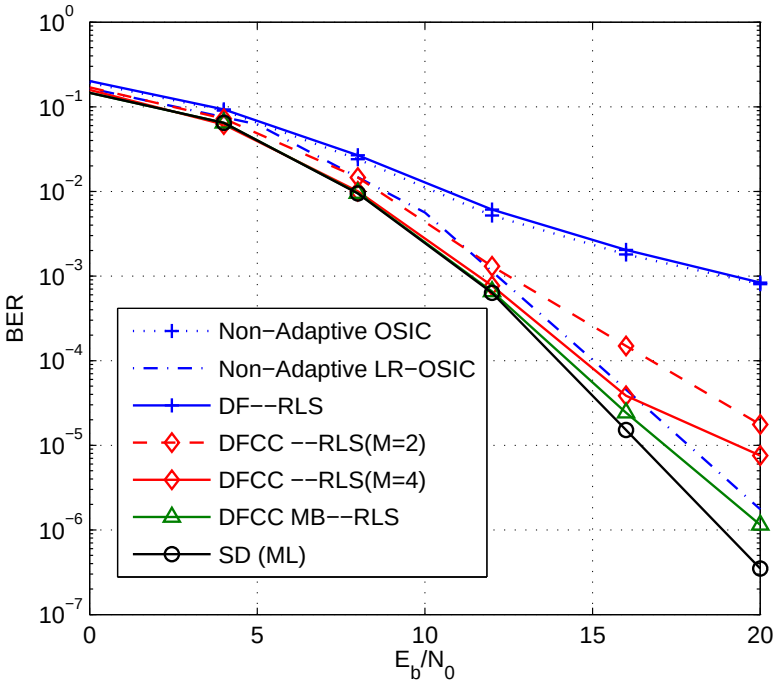

Figure 4.8: BER vs. E_b/N_0 with QPSK symbols. The proposed DFCC detection achieves a near optimal performance in a 4×4 system configuration with single branch. The number of candidate constellation points M introduces a trade off between the performance and the complexity. Number of training vectors $I = 50$.

In the following simulations, unless otherwise stated, we consider that the proposed algorithms and all their counterparts operate with a channel with independent and identically-distributed (i.i.d) block fading model. The channel model is of Rayleigh random fading and the coefficients are taken from complex Gaussian random variables with zero mean and unit variance. The QPSK modulation is used; The transmitted vectors $\boldsymbol{s}[i]$ are grouped into frames consisting of 500 vectors where the first $\boldsymbol{s}[1], \ldots, \boldsymbol{s}[I]$ vectors are training vectors. In each frame, the channel between a transmit and receive antenna pair is fixed and a single path is assumed. We also assume that the original detection order of streams has been sorted according to the optimal order as discussed in Section. II.

Fig.4.8 shows the BER against E_b/N_0. Assume the channel is known, the DF-RLS detector ($\lambda = 0.998$) proposed in [82] exhibits a similar performance to the Non-adaptive OSIC detector. The DF-RLS detector has about 7dB performance loss when the target BER equals 10^{-3} compared with the performance of SD. A lattice reduction aided MMSE OSIC detection (LR-OSIC) [96] is also compared in this plot, and it shows a 2dB loss to

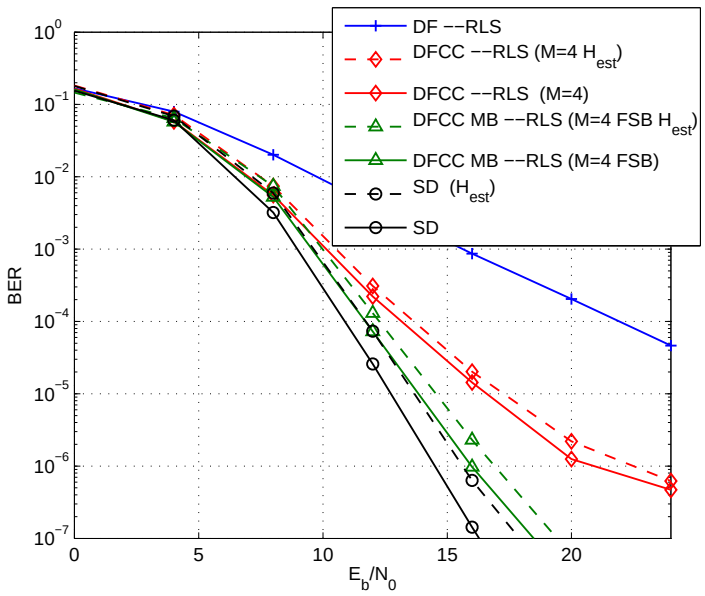

Figure 4.9: BER vs. E_b/N_0. The DFCC algorithm achieves a significant performance gain compared with the DF detector. The optimal performance can be approached by employing MB in an 8×8 system configuration with perfect (solid) and imperfect channel estimation (dash). QPSK symbols are transmitted on a Rayleigh fading channel. Number of training vectors $I = 50$.

the optimal performance. As for the SD, with a sufficiently large sphere radius selected, the SD can always produce an ML solution. With 4 constellation constrained candidates and $d_{\text{th}} = 0.5$, the proposed DFCC-RLS ($\lambda = 0.998$) algorithm shows a near-optimal BER performance at the target BER equal to 10^{-3}. By introducing more branches, the DFCC MB-RLS can further improve the performance at high SNR regions. In [76], both the optimum ordering patterns codebook and the FSB codebook were designed to construct the transformation matrices $\boldsymbol{T}_l$, the FSB codebook was reported with a smaller size in this case (FSB $L = 2$).

The BER against E_b/N_0 plot for a system with 8×8 antennas is demonstrated in Fig.4.9. DFCC has a 8 dB performance gain compared to the DF at the target BER 10^{-4}. The channel is assumed unknown and LS channel estimation is applied to all the detectors indexed by H_{est}. By introducing MB (FSB $L = 6$), the proposed DFCC MB achieves a performance with about 1 dB loss from optimal at the target BER 10^{-4}.

In order to investigate the convergence behaviour of the DF-RLS and DFCC-RLS al-

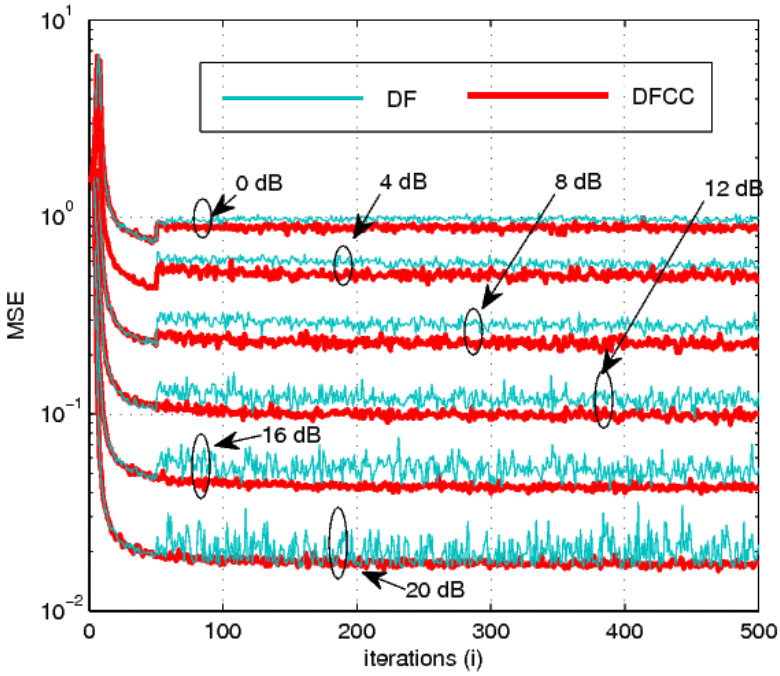

Figure 4.10: MSE for filter output in terms of RLS iterations, with 4×4 antennas and QPSK symbols. After 50 training vectors transmitted, the decision-directed mode is switched on.

gorithms, the MSE of the filter output against the number of update iterations is shown in Fig.4.10 for QPSK modulation and Fig.4.11 for 16-QAM constellation. Thanks to the CC scheme, DFCC has a lower converged MSE and the variance of $\xi_k[i]$ in the decision-directed mode is significantly reduced.

In order to demonstrate the tracking ability of the proposed detectors in the time-varying channels, Fig.4.12 and Fig.4.13 present the comparison of BER performance for various normalized Doppler frequency f_dT. In these simulations, each channel between a transmit and receive antenna pair is varied based on the Jakes model [97]. LS channel estimation is applied to the unknown channel. The length of the training sequence is $I = 50$ and (FSB $L = 3$, 4×4) and (FSB $L = 3$, 8×8) for DFCC MB detector. The simulation results show that even with a single-branch (SB), the performance of the SD with channel tracking can be approached.

Fig. 4.14 demonstrate the MSE for the symbol estimation across all K streams in terms of RLS iterations, with 4×4 antenna configuration and QPSK modulation.

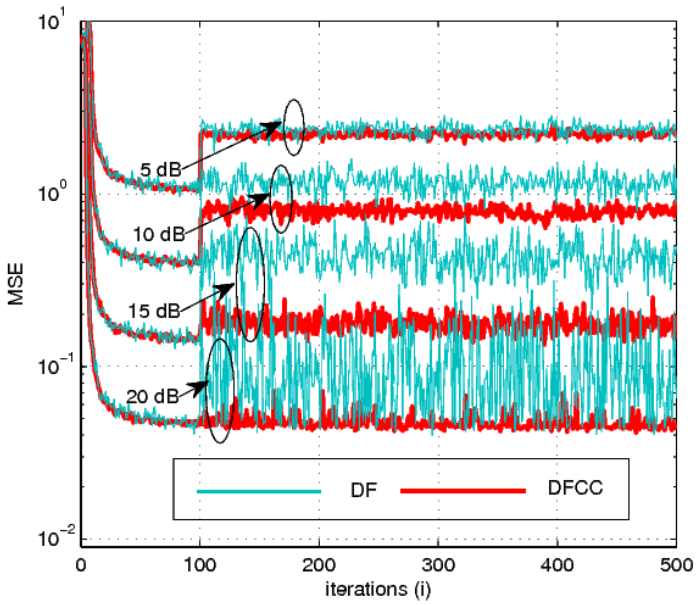

Figure 4.11: MSE for filter output in terms of RLS iterations, with 4×4 antennas and 16-QAM symbols. After 100 training vectors transmitted, the decision-directed mode is switched on.

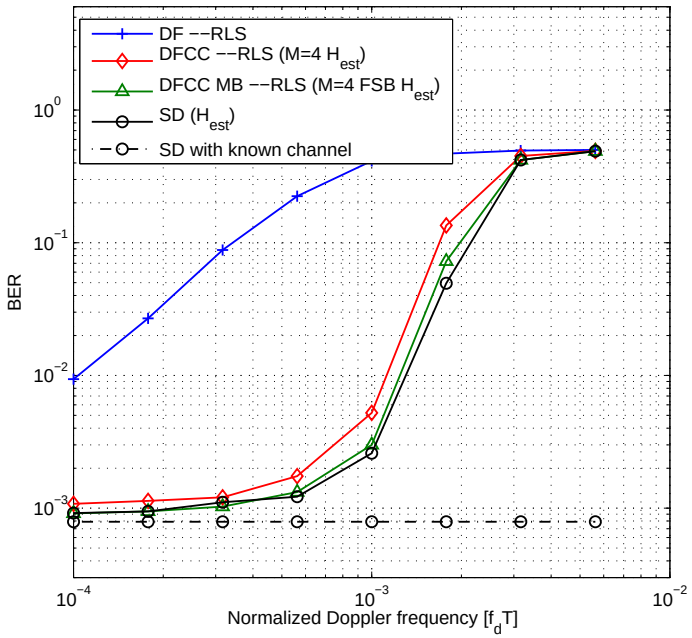

Figure 4.12: Comparison of BER performance for various normalized Doppler frequency f_dT when $K = N_R = 4$ and E_b/N_0 = 14 dB, QPSK modulation.

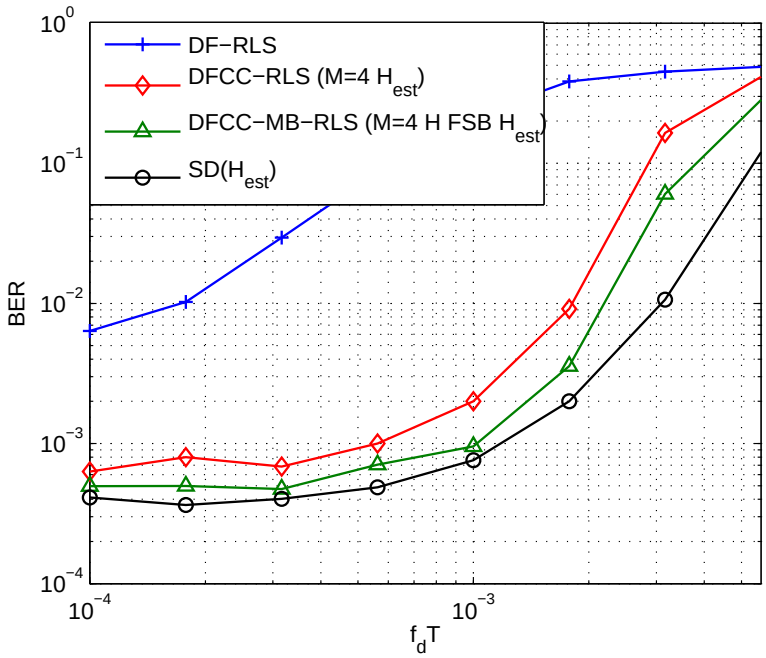

Figure 4.13: Comparison of BER performance for different detectors with various values of the normalized Doppler frequency f_dT when $K = N_R = 8$ with QPSK modulation.

$E_b/N_0 = 14dB$, and the normalized Doppler frequency f_dT equals to $10^{-2.5}$, $10^{-2.75}$, 10^{-3} respectively. With various values of f_dT, the proposed DFCC scheme shows the improvement in terms of MSE. From the figure we can see that the DFCC also has the ability to track the fading channel with $f_dT = 10^{-3}$.

In Fig.4.15, we describe the soft input and output behaviour of the detection algorithms through *extrinsic* information transfer (EXIT) chart [69] analysis. In this plot, QPSK modulation with 4×4 system are considered. The E_b/N_0 is set to 7 dB. I_A and I_E represent the mutual information at the input and output of the detector. With a SB, the proposed DFCC is able to achieve a higher capacity compared to the DF algorithm. With the increased branches, more tentative decisions are included in the limited vector set $\mathcal{B}$. The MAP behaviour can be approached by using the number of branches equal to $L = 4$ and $L = 18$.

The curves in Fig.4.16 are given for convolutionally coded BER performance on a Rayleigh block fading channel. The proposed SB DFCC with $M = 4$ candidates and $d_{\text{th}} = 0.5$ improves the conventional DF detection performance about 4 dB at target coded BER equals 10^{-4}. The number of branches L incorporated in the scheme introduces a

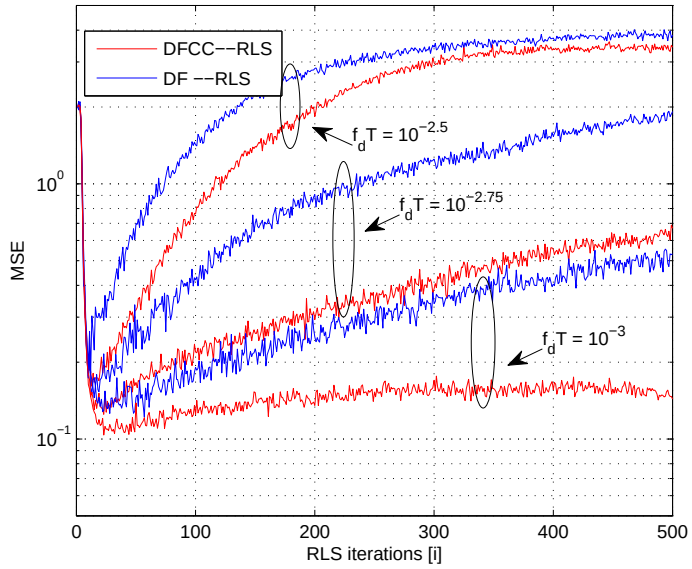

Figure 4.14: MSE of the estimated symbols in terms of RLS iterations, with 4×4 MIMO antennas. After 10 training vectors transmitted, the decision-directed mode is switched on. The MSE across the 4 layers is significantly reduced.

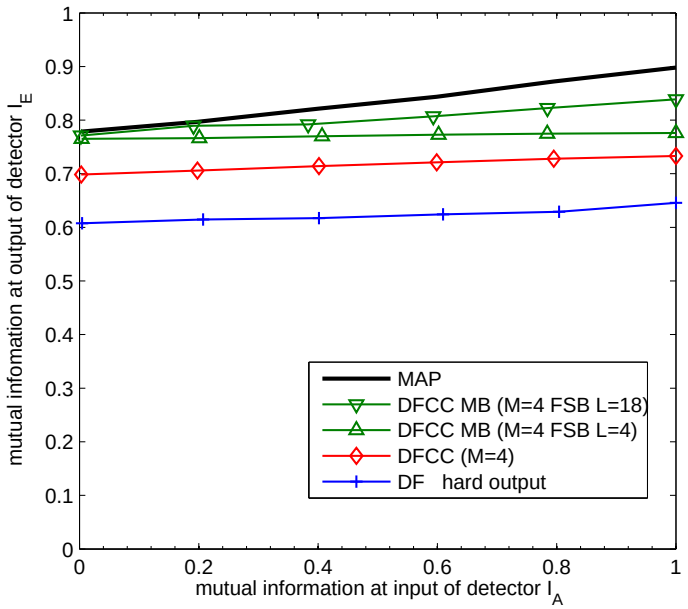

Figure 4.15: EXIT chart for the 4×4 system at SNR of 7dB. QPSK transmission is considered.

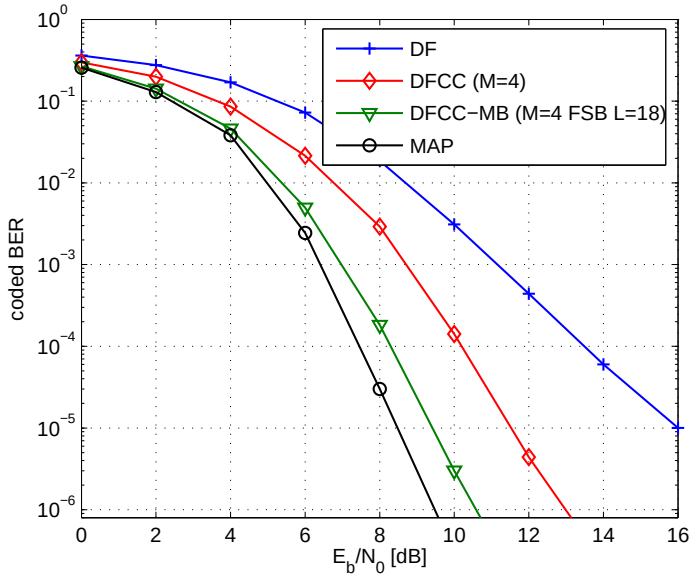

Figure 4.16: Coded BER curves of QPSK over 4×4 MIMO channels; block size 1000 message bits, code rate $R = 1/2$, memory 2 convolutional code with polynomial $[7, 8]_{\text{oct}}$.

trade off between complexity and performance. With (FSB L = 18) branches, the DFCC MB detector approaches the optimal MAP detection performance with only 0.35 dB performance loss when coded BER = 10^{-4}.

4.7.2 Multiuser MIMO Systems

In this subsection, simulations are presented to demonstrate the system performance of the proposed adaptive multiuser DFCC (AMUDFCC) detection algorithm. We consider Rayleigh random fading and QPSK modulation. The transmitted vectors $\boldsymbol{s}[i]$ are grouped into frames consisting of 500 symbol vectors where the first 10 symbol vectors are training data. Also, a column norm based detection ordering is employed.

The computational complexity is shown in terms of floating-point operations (FLOPS) per symbol detection. The simulations are performed with the Lightspeed toolbox [94], in which the number of FLOPS equals 2 for a complex addition and 6 for a complex multiplication. In Fig.4.17, with block fading where the channel coefficients are taken from complex Gaussian random variables having zero mean and unit variance. The BER performances of all schemes improve while the number of receive antenna N_R grows

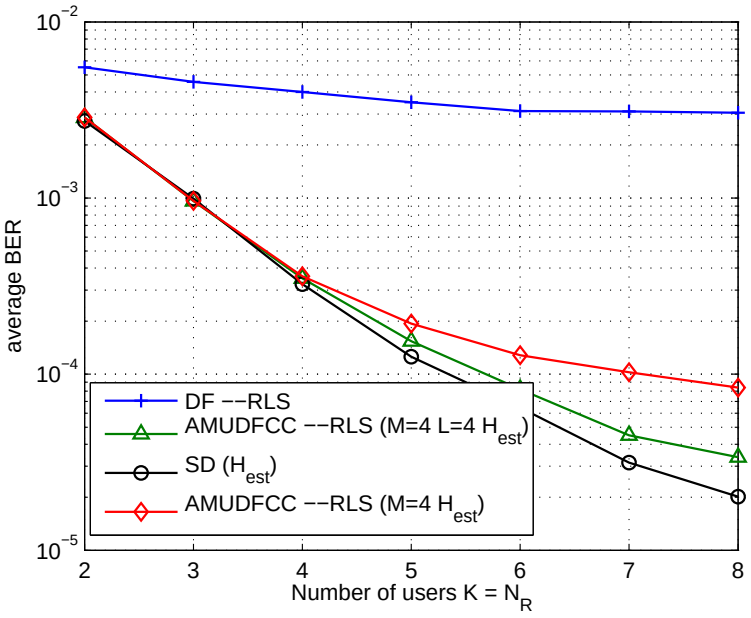

Figure 4.17: Performance with $E_b/N_0 = 13$ dB, adaptive multi-user decision feedback with constellation constraints (AMUDFCC) with $d_{\text{th}} = 0.5$ and LS channel estimation. AMUDFCC has a superior performance to the conventional DF scheme and is not far from the MLD.

with the number of users K. More importantly, the proposed detector offers a significant performance gain over the DF-RLS detector at a small extra computational cost as shown in Fig.4.18. By adding more complexity, the performance can be further improved by introducing L parallel branches.

For a coded system with LS channel estimation, the BER performance against the average SNR across all users is shown in Fig.4.19, the receiver structure is discussed in section 4.6, the proposed AMUDFCC detector has performance gains as compared to the conventional DF scheme. By increasing the number of branches with different NCO, the SD performance can be approached.

4.8 Summary

In this chapter, we have developed an adaptive decision feedback based detector for MIMO transmission systems with varying channels. In this context, we have presented

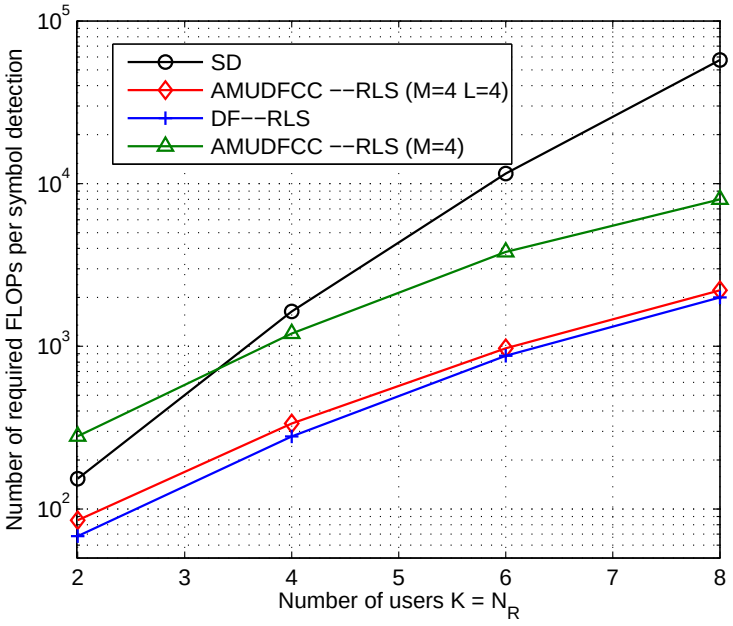

Figure 4.18: Performance with $E_b/N_0 = 13$ dB, AMUDFCC with $d_{\text{th}} = 0.5$ and LS channel estimation. The proposed scheme has a similar cost to the conventional DF structure.

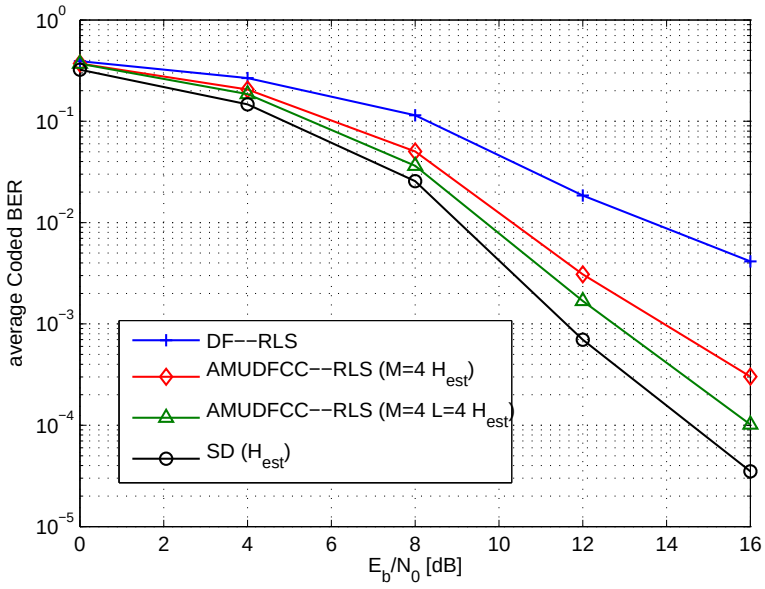

Figure 4.19: $K = 6$ users are separately coded by the $g = (7, 5)_o$, rate $R = 1/2$, memory 2 convolutional code and we use the block size equals 500 vectors, $M = 4$ candidates and $d_{\text{th}} = 0.5$. The number of turbo iterations between the detector and the decoder is 3.

a novel way to improve the BER performance by using the feedback with constellation constraints. This approach has the ability to effectively address the error propagation problem in decision driven interference cancellation techniques while maintaining the low complexity of adaptive detectors.

Chapter 5

Distributed Iterative Detection with Reduced Message Passing for Networked MIMO Cellular Systems

Contents

5.1 Overview

There are primarily two aspects in distributed base station cooperation (BSC) strategies: The network-wide optimization of information exchange and the network decentralized implementation. We are interested in the latter one, where the concept of *distributed iterative detection* (DID) was introduced. This chapter considers BSC for the uplink of a multiple-user multiple-cell wireless system. We propose a distributed iterative detection

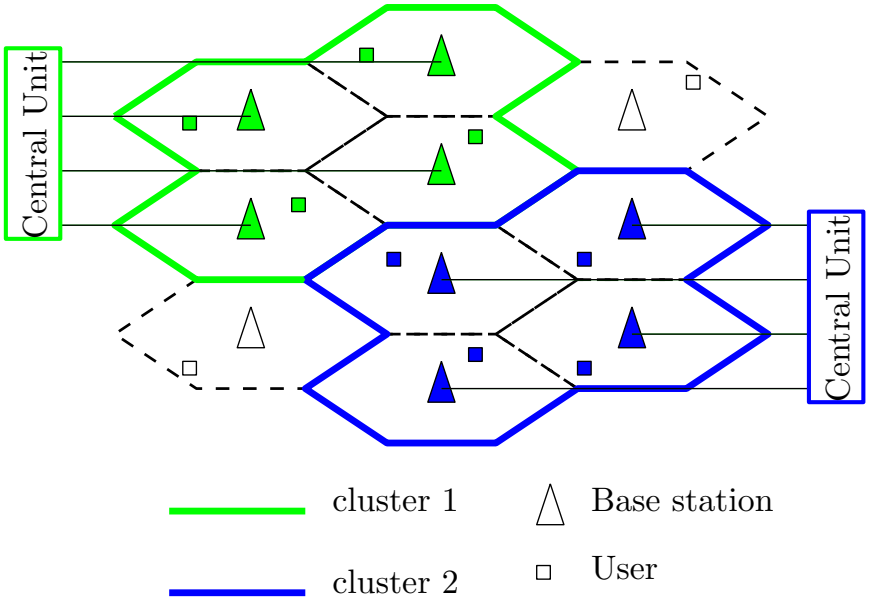

Figure 5.1: Base stations cooperating to perform JMD, each cluster has 4 BSs and 4 users.

strategy with reduced signalling requirement. We adopt the basic system model which was introduced by Mayer et al. [22] and Khattak et al. [26] and compare the proposed distributed detection strategy with the existing ones. The motivation of the work is to achieve an inter-cell-interference (ICI) suppression with low backhaul traffic and detection complexity.

5.2 Introduction

Apart from the traditional voice and text message services, the growing demand for broadband mobile multimedia applications requires higher data rates and reliable links between base stations and mobile users. Since the available spectrum is limited, the improvement of system capacity can be achieved by introducing a higher frequency reuse and the micro cell planning. In such a network configuration, a higher spectral efficiency is obtained, however, the ICI will become dominant at the cell edges, especially in an aggressive frequency reuse scenario (such as full frequency reuse). The application of interference mitigation techniques is necessary in these systems to prevent a restricted data rate of the users located at the cell edge and improve the system fairness.

The strategies to deal with the ICI in the system uplink including the joint multiuser

detection (JMD) [60] and distributed iterative detection (DID) [23]. In terms of JMD, the BSs for each cell make the received signals available to all cooperating cells. With this set up, the receivers not only use the desired signal energy but also the energy from the interferers leading to much improved received SINR. Both array and diversity gains are obtained resulting in substantial increase in system capacity [23]. Despite the optimality of JMD, it needs to exchange all the quantized received signals between the cooperative BSs via a wired backbone network and brings about huge data traffic. To reduce the backhaul, clusters are introduced to the network applying JMD, where a group of BSs form a cluster and the JMD is performed in a central unit as Fig. 5.1. Since the receive antennas are away from each other and located in each cell and the signals are joint processed at single central unit, this method is named *distributed antenna system* (DAS) [23] and therefore a virtual MIMO system is formed [60]. In this structure, the information is exchanged within the cluster which reduces the backhaul and the detection complexity in each JMD. Even with the benefits mentioned above, the restrictions of DAS are listed below:

- By assuming unlimited backhaul capacity, the performance of the DAS is optimal for an isolated cluster. However the performance degrades in a large network with many clusters, especially at the boundaries of the clusters.
- The central units are required to support a large number of users in the cluster with many cells which introduce huge complexity even taking into account that the central units usually have high computational power.
- It requires transmission of quantized received signals over the wired network to the central unit which causes the data traffic to become many times higher than that in conventional cellular systems. [26]
- In the implementation aspect, the organization of cells and clusters is a complex task which requires additional scheduling and signalling information to be transferred via backhaul.

The above problems can be partially addressed by reducing the number of cells in each cluster and by introducing advanced interference mitigating techniques for the detection in each central unit at the cost of additional backhaul traffic between the clusters. In the

extreme case, each cluster has a single cell and therefore a DID is reported as an alternative of JMD. With the DID configuration, iterative signal processing is performed at the network level. The receiver detects each user stream at its corresponding cell and iteratively refines the estimate of the transmitted symbol with the help of the information provided by other cooperating cells. Each BS detects the desired user/stream only, the other interfering signal is treated as noise. The output of the decoder is used to reconstruct the transmitted symbol and this estimate is spread to the cooperating BSs. Each BS has an interface to exchange the estimation result to the neighbours, the reconstructed interferers are cancelled from the received signal and the power of interference reduces as more iterations are performed. As for the JMD, the complexity of computing *extrinsic* information is exponential in both the number of transmit antennas and the number of cells. With the DID, for each cell, the complexity of the search required to compute the ML solution is restricted to the number of data streams in the cell, this results in a significant reduction in complexity [23]. Although with the advantages, the restrictions of DID are listed below:

- The DID scheme does not benefit from array gain and diversity gain since the energy received from the cooperating BSs are cancelled without utilization, the performance is bounded by an isolated single-user single-cell system.
- The iterative interference cancellation is performed in the network scale, which requires additional backhaul traffic between interfering BSs. A number of iterations is required to achieve an acceptable performance and may result in detection delay that must be minimised.

The first problem mentioned above can be partially addressed by forming a cluster adopting a small number of cells with highly correlated users, a small sized virtual MIMO system is created in each cluster and array/diversity gain can be achieved inside the cluster. With this configuration, the interference mitigation with the DID is performed among the clusters. By varying the number of cells in each cluster, we can establish a tradeoff as illustrated in Fig.5.2.

Many works in the literature have been reported based on the DAS configuration and we leave the description of such systems to the references [60–62]. In the remaining part

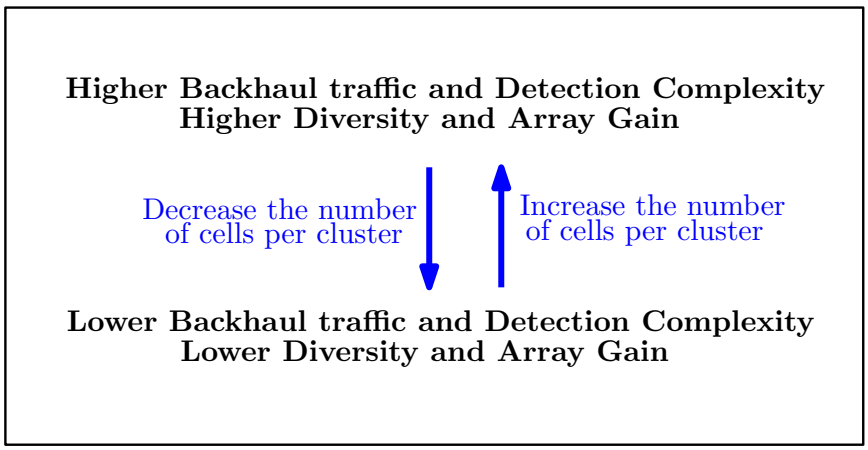

Figure 5.2: Tradeoff between the diversity/array gain and backhaul/complexity.

of this chapter, we focus on the interference mitigation techniques dealing with the multiuser multicell detection through base station cooperation (BSC) in uplink, interference-limited, aggressive frequency reuse scenario (Frequency reuse factor 1). In the proposed DID with reduced message passing (DID-RMP) algorithm, the cooperating BSs exchange the information while performing single or multi-user detection. Instead of exchanging the soft estimates introduced in [23, 56], the proposed algorithm generates a sorted list containing the probability of the constellation symbols given the channel information. The indices of the constellation symbols with high probability are exchanged via the backhaul link. A selection unit (SU) is also proposed in the network to choose the best candidates on the list. The indices are exchanged among the BSs in an iterative manner and the system improves the estimate of the desired signal with each iteration pass. The indexed interference at the cooperating BSs is subtracted from the received signal resulting in a reduced interference level and more reliable estimates of data. The simulation results show that the proposed DID-RMP scheme is able to obtain a performance better than the soft symbol cancellation technique described in [23, 26] while requiring less backhaul traffic.

5.3 Data Model of a Networked MIMO Cellular System

In this chapter, we are interested in an asymmetric multiuser detection scenario of a networked MIMO cellular system. We assume the cellular network can detect groups of users that are strongly received by several cooperating BSs. We consider that several cells

ϕ are grouped into one cluster, the diversity gains and array gains can be obtained inside the cluster, the interference among the clusters is mitigated through the application of DID and the proposed schemes. Since we are generally interested in mitigating the inter-cluster interference, in order to clarify our description, in this section we only consider the special case $\phi = 1$, where each cell represents a cluster. The applications with more cells in the cluster $\phi > 1$ are straightforward.

Let us consider an idealized synchronous uplink single-carrier narrowband cellular network that is aiming at capture most of the features of a realistic wireless system with respect to the interference and the need for backhaul use. We define M as the number of cooperating BSs and K as the number of users in the cooperating cells, and assume the users and BSs have a single transmit antenna. Extensions to multiple antennas are straightforward. In cooperating systems, a limited number of cells can work together in order for the backhaul overhead to be affordable [98]. In this system, the transmitted data of each user is protected by the error control coding separately. A message vector $\boldsymbol{m}_k$ from user k is encoded by a channel codes before a bit interleaving operation. The resulting bit-sequence $\boldsymbol{b}_k$ has Q entries and $k = 1, 2, \ldots, K$ are indices of the interfering users. The sequence is then divided into groups of J bits each, which are mapped to a complex symbol vector as the output of the user k, this operation is denoted as $\boldsymbol{s}_k = [s_{k,1}, \ldots, s_{k,Q_s}] = \text{map}(\boldsymbol{b}_k)$ where $Q_s = Q/J$ and each entry of $\boldsymbol{s}_k$ is taken from a complex constellation $\mathcal{A}$, with $E\{|s_{k,j}|^2\} = \sigma_s^2$.

A $K \times 1$ symbol vector $\boldsymbol{s}[i] = \left[s_1[i], s_2[i], \ldots, s_K[i]\right]^T$ is transmitted simultaneously by all K users. At base station m, the received symbols $r_m[i]$ are given by

$$r_m[i] = \boldsymbol{g}_m[i]\boldsymbol{s}[i] + v_m[i], \qquad 1 \leq i \leq Q_s. \tag{5.1}$$

where $[i]$ is the time index and $v_m[i]$ denotes the additive zero mean complex Gaussian noise with variance $E\{v[i]v[i]^*\} = \sigma_v^2$.

The entries of the $1 \times K$ row vector $\boldsymbol{g}_m$ are the element-wise product of $h_{m,k}$ and $\sqrt{\rho_{m,k}}$, where $h_{m,k}$ is the complex channel realization from the k-th user to the m-th BS with i.i.d $\mathcal{CN}(0, 1)$. The coefficients $\rho_{m,k}$ reflect the path loss with respect to BS m and user k. Similarly to [26], we further separate $r_m[i]$ into four terms,

$$\begin{aligned} r_m[i] &= g_{m,d}s_d[i] + \sum_{n\in\mathcal{C}_m} g_{m,n}s_n[i] + \sum_{n\in\hat{\mathcal{C}}_m} g_{m,o}s_o[i] + v[i], \\ &= \sqrt{\rho_{m,d}}h_{m,d}s_d[i] + \sqrt{\rho_{m,n}}\sum_{n\in\mathcal{C}_m} h_{m,n}s_n[i] + \\ &\quad \sqrt{\rho_{m,o}}\sum_{n\in\hat{\mathcal{C}}_m} h_{m,o}s_o[i] + v[i]. \end{aligned} \tag{5.2}$$

where the first term denotes the desired signal (indexed by $_d$), the second and the third terms denote the strong interference and the weak interference (indexed by $_n$ and $_o$, respectively). The coefficients ρ_n and ρ_o characterize the channel gains with strong and weak interferers, separately. The set of indices of all strongly received interference at BS m is denoted as $\mathcal{C}_m$ and the weakly received interference is denoted as $\hat{\mathcal{C}}_m$.

As indicated in [16], the strongest interferer dominates the total received ICI, in this model, we assume the number of strongly received signal $m_n \leq 5$. For example, for a system with $K = M = 4$ and $\zeta = 2$ as the number of strong interferers, we assume the weak interference $\rho_{m,o}$ is zero and $\rho_{m,d} = 1$, and the coupling matrix is formed as

$$\boldsymbol{P} = \begin{bmatrix} 1 & \rho_{m,n} & \rho_{m,n} & 0 \\ 0 & 1 & \rho_{m,n} & \rho_{m,n} \\ \rho_{m,n} & 0 & 1 & \rho_{m,n} \\ \rho_{m,n} & \rho_{m,n} & 0 & 1 \end{bmatrix}. \tag{5.3}$$

In this configuration, we assume the BSs have the ability to know which cells are the interfering signals coming from. The BS in the desired cell then notifies the BS of the interfering cells and obtains the estimated transmit signal from that cell to perform the interference cancellation. The exchanged interfering information is transmitted via a wired backhaul which connects all the base stations in the network.

The signal-to-noise ratio (SNR) is defined as the ratio of the desired signal power at the receiver side and the noise power, which is mathematically described as

$$\left.\frac{E_s}{N_0}\right|_{\text{dB}} := 10\log_{10}\frac{E\{\|h_{m,d}s_d\|^2\}}{E\{v^2\}}. \tag{5.4}$$

Let us also denote the average signal-to-interference ratio (SIR) of the desired user k as

$$SIR_k := 10\log_{10}\frac{E\{\|g_{m,d}s_d\|^2\}}{\sum_{n\in\mathcal{C}_m} E\{\|g_{m,n}s_n\|^2\} + \sum_{n\in\hat{\mathcal{C}}_l} E\{\|g_{m,o}s_o\|^2\}}. \tag{5.5}$$

5.3.1 Data Model for Users and BSs Equipped with Multiple Antennas

In this part, a data model for networked MIMO systems in which the users and BSs are equipped with multiple antennas is discussed. The scalar $r_m[i]$ and vector $\boldsymbol{g}_m[i]$ in (5.1) are now described in the vector $\boldsymbol{r}_m[i]$ and matrix $\boldsymbol{G}_m[i]$ forms respectively, as given by,

$$\boldsymbol{r}_m[i] = \boldsymbol{G}_m \boldsymbol{z}[i] + \boldsymbol{v}_m[i], \tag{5.6}$$

where $\boldsymbol{r}_m \in \mathbb{C}^{N_R \times 1}$ is the received vector for the m-th BS and $\boldsymbol{G}_m \in \mathbb{C}^{N_R \times KN_T}$ is the combined channel matrix with

$$\boldsymbol{G}_m = \left[\boldsymbol{G}_{m,1}, \ldots, \boldsymbol{G}_{m,k}, \ldots, \boldsymbol{G}_{m,K}\right], \tag{5.7}$$

where $\boldsymbol{G}_{m,k} \in \mathbb{C}^{N_R \times N_T}$ denotes the channel between user k and BS m. Note that each user has N_T transmit antennas and each BS has N_R receive antennas. The quantity $\boldsymbol{z} \in \mathbb{C}^{KN_T \times 1}$ is the collection of the data streams from the K users $\boldsymbol{z} = [\boldsymbol{s}_1^T, \ldots, \boldsymbol{s}_K^T]^T$ and $\boldsymbol{s}_k \in \mathbb{C}^{N_T \times 1}$.

The equation (5.2) can be rewritten as

$$\begin{aligned} \boldsymbol{r}_m[i] &= \boldsymbol{G}_{m,d}\boldsymbol{s}_d[i] + \sum_{n \in \mathcal{C}_m} \boldsymbol{G}_{m,n}\boldsymbol{s}_n[i] + \sum_{n \in \hat{\mathcal{C}}_m} \boldsymbol{G}_{m,o} s_o[i] + \boldsymbol{v}_m[i], \\ &= \sqrt{\rho_{m,d}}\boldsymbol{H}_{m,d}\boldsymbol{s}_d[i] + \sqrt{\rho_{m,n}} \sum_{n \in \mathcal{C}_m} \boldsymbol{H}_{m,n}\boldsymbol{s}_n[i] + \\ &\quad \sqrt{\rho_{m,o}} \sum_{n \in \hat{\mathcal{C}}_m} \boldsymbol{H}_{m,o}\boldsymbol{s}_o[i] + \boldsymbol{v}_m[i], \end{aligned} \tag{5.8}$$

where we assume the N_T antennas for each user have same channel gain coefficients ρ_n and ρ_o. The coupling matrix given in (5.3) and the definition of SNR and SIR can be generalized accordingly.

Although using multiple antennas in both users and BS receiver is promising, it requires additional signal processing power to decode the inter-antenna interference introduced by the same user. In order to simplify the description of the proposed structure and its traditional counterparts, we employ the single antenna case $N_T = N_R = 1$ in the following sections.

5.4 Iterative Detection with Reduced Message Passing

In this section, the decision-aided DID structure is described in detail, in the first subsection the distributed iterative signal processing in an interference limited cellular network is reviewed [24]. In the following two subsections, the soft and hard parallel interference cancellation algorithms are based on the quantized estimates from the cooperating BSs is given. The last subsection is devoted to the description of the proposed DID-RMP.

5.4.1 Decision-aided Distributed Iterative Detection

The setup for performing the distributed detection with the information exchange between base stations is shown in Fig.5.3. The K users' data are separately coded and modulated to complex symbols after the bit-interleaving. At each BS, the received signal $r_m[i]$ is the collection of the transmitted signal and the Gaussian noise.

In addition, each BS equip a communication interface for exchanging information with the cooperating BSs. The information is in the form of a bit sequence that represents the quantized soft estimates. The interface is capable of transmitting and receiving information. Via these interfaces, each cooperating BS is connected to a device, namely the selection unit (SU), and is ready to receive and transmit the cooperating information. The proposed SU has very limited computational power and it can be integrated with BSs in the network.

In each BS, a block of received signals $r_m[i]$ is used by the MAP demapper to compute the *a posteriori* probability in the form of log-likelihood-ratios (LLRs), which are given by

$$\Lambda_1^p[b_{j,k}[i]] = \log \frac{P[b_{j,k}[i] = +1 | r_m[i]]}{P[b_{j,k}[i] = -1 | r_m[i]]}, \tag{5.9}$$

where the equation can be solved by using Bayes' theorem and we leave the details to the references [18, 56]. The detector and decoder are serially concatenated to form a "turbo" structure, the *extrinsic* information is exchanged by the two soft-input soft-output components. We denote the *intrinsic* information provided by the decoder as $\Lambda_2^p[b_{j,k}[i]]$

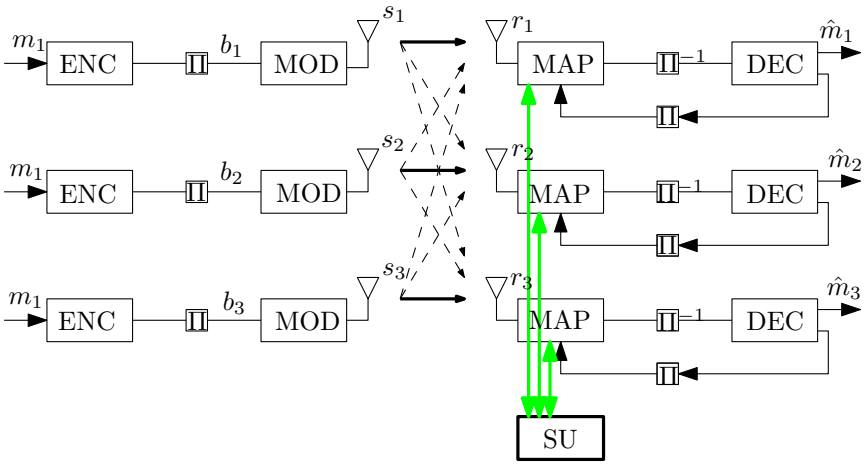

Figure 5.3: An example configuration showing a cooperating 3-cell network. The dashed lines between the transmitter and receiver denote the ICI while the solid lines denote the desired signal.

and the bit probability is obtained as

$$P[b_{j,k}[i]] = \log \frac{P[b_{j,k}[i] = +1]}{P[b_{j,k}[i] = -1]}. \tag{5.10}$$

From [56], the bit-wise probability is obtained by

$$\begin{aligned} P[b_{j,k}[i] = \bar{b}_j] &= \frac{\exp\left(\bar{b}_j \Lambda_2^p[b_{j,k}[i]]\right)}{1 + \exp\left(\bar{b}_j \Lambda_2^p[b_{j,k}[i]]\right)}, \\ &= \frac{1}{2}\left[1 + \bar{b}_j \tanh\left(\frac{1}{2}\Lambda_2^p[b_{j,k}[i]\right)\right]. \end{aligned} \tag{5.11}$$

where $\bar{b}_j = \{+1, -1\}$. Let us simplify the notation $P\big[s_k[i]\big] := P\big[s_k[i] = c_q\big]$ where c_q is an element chosen from the constellation $\mathcal{A} = \{c_1, \ldots, c_q, \ldots, c_A\}$. The symbol probability $P[s_k[i]]$ is obtained from the corresponding bit-wise probability, and assuming the bits are statistically independent, we have

$$\begin{aligned} P\big[s_k[i]\big] &= \prod_{j=1}^{J} P\big[b_{j,k}[i] = \bar{b}_j\big], \\ &= \frac{1}{2^J} \prod_{j=1}^{J} \left[1 + \bar{b}_j \tanh\left(\frac{1}{2}\Lambda_2^p[b_{j,k}[i]]\right)\right]. \end{aligned} \tag{5.12}$$

From (5.11) and (5.12) we can conclude that $\sum_{|\mathcal{A}|} P\big[s_k[i]\big] = 1$.

5.4.2 Soft Interference Cancellation

The soft interference cancellation has first been used in an iterative multiuser CDMA systems by Wang *et al* in [56]. In this algorithm [22], the soft replicas of ICI are constructed and subtracted from the received signal vector as

$$\tilde{r}_{m,k}[i] = r_m[i] - \boldsymbol{g}_m \tilde{\boldsymbol{u}}_k[i] \tag{5.13}$$

and

$$\tilde{\boldsymbol{u}}_k[i] = \Big[\tilde{s}_1[i], \ldots, \tilde{s}_{k-1}[i], 0, \tilde{s}_{k+1}[i], \ldots, \tilde{s}_K[i]\Big]^T, \tag{5.14}$$

where

$$\tilde{s}_k[i] = E\{s_k[i]\} = \sum_{c_q \in \mathcal{A}} c_q P\big[s_k[i] = c_q\big]. \tag{5.15}$$

The first-order and second-order statistics of the symbols are obtained from the symbol a priori probabilities as

$$\begin{aligned} \sigma^2_{\text{eff}} &= \text{var}\{s_k[i]\} = E\Big\{\big|s_k[i]\big|^2\Big\} - \big|\tilde{s}_k[i]\big|^2, \\ E\Big\{\big|s_k[i]\big|^2\Big\} &= \sum_{c_q \in \mathcal{A}} |c_q|^2 P\big[s_k[i] = c_q\big]. \end{aligned} \tag{5.16}$$

Users and BSs equipped with Multiple Antennas

In the case that the users and BSs are equipped with multiple antennas, then equation (5.13) can be reformulated by

$$\tilde{\boldsymbol{r}}_{m,k}[i] = \boldsymbol{r}_m[i] - \boldsymbol{G}_m \tilde{\boldsymbol{u}}_k[i], \tag{5.17}$$

the soft interference cancellation may be deployed in two cases. For example (i) user-based cancellation

$$\tilde{\boldsymbol{u}}_k[i] = \Big[\tilde{\boldsymbol{s}}_1^T[i], \ldots, \tilde{\boldsymbol{s}}_{k-1}^T[i], \boldsymbol{0}, \tilde{\boldsymbol{s}}_{k+1}^T[i], \ldots, \tilde{\boldsymbol{s}}_K^T[i]\Big]^T, \tag{5.18}$$

where $\boldsymbol{0} \in \mathcal{Z}^{N_T \times 1}$. The remaining signal is the combination of all the data streams transmitted from user k. (ii) In this situation, all the interfering links are mitigated and the stream-based interference cancellation is performed with the cancellation vector

$$\tilde{\boldsymbol{u}}_k[i] = \Big[\tilde{\boldsymbol{s}}_1^T[i], \ldots, \tilde{\boldsymbol{s}}_{k-1}^T[i], \tilde{\boldsymbol{s}'}_k^T[i], \tilde{\boldsymbol{s}}_{k+1}^T[i], \ldots, \tilde{\boldsymbol{s}}_K^T[i]\Big], \tag{5.19}$$

where

$$\tilde{\boldsymbol{s}'}_k^T[i] = \left[\tilde{s}_1[i], \ldots, \tilde{s}_{n_t-1}[i], 0, \tilde{s}_{n_t+1}[i], \ldots, \tilde{s}_{N_T}[i]\right]^T. \tag{5.20}$$

This soft interference cancellation based algorithm generally outperforms hard interference cancellation since it considers the reliability of the cancellation procedure. However, the performance heavily depends on the quantization level [26]. Exchanging the quantized soft bits or LLRs convey reliability information among BSs and involves a large amount of backhaul data per cell per iteration, which make soft interference cancellation unattractive [23, 24].

5.4.3 Hard Interference Cancellation

With the hard interference cancellation, the estimates of the interfering symbols are the constellation symbols. In this case, the quantization is performed for each estimated symbol. The equation (5.14) is rewritten as

$$\hat{\boldsymbol{u}}_k[i] = \left[\mathrm{Q}(\tilde{s}_1[i]), \ldots, \mathrm{Q}(\tilde{s}_{k-1}[i]), 0, \mathrm{Q}(\tilde{s}_{k+1}[i]), \ldots, \mathrm{Q}(\tilde{s}_K[i])\right]^T, \tag{5.21}$$

where $\mathrm{Q}(\cdot)$ is the slicing function that depends on the constellation adopted. The constellation indices are exchanged among the cooperating BSs. Since no reliability information is included, the cooperation procedure requires significantly less backhaul traffic as compared with the soft interference procedure. All the detected information symbols are exchanged in the initial iteration, and in the subsequent iterations, only the symbols with the constituent bits that have flopped between the iterations are exchanged. The indexed constellation symbols are reconstructed at the neighbouring BSs and subtracted from the received signal, the residual noise is considered equal to zero and $\sigma^2_{\text{eff}} = \sigma^2_v$. In the hard interference cancellation configuration, the backhaul traffic can be further brought down by introducing a reliability check of the symbols, and only the reliable symbols are exchanged [24].

5.4.4 Distributed Iterative Detection with Reduced Message Passing

By organizing the probabilities obtained by (5.12) in decreasing order of values, a list of tentative decisions of $s_k[i]$ is obtained in each BS as given by

$$\mathcal{L}_k[i] \triangleq \{c_1, c_2, \ldots, c_\tau\}_k, \tag{5.22}$$

where $1 \leq \tau \leq |\mathcal{A}|$ and

$$Pr[c_1] \geq Pr[c_2] \geq \ldots, Pr[c_\tau], \tag{5.23}$$

where

$$Pr[c_q] \triangleq P\big[s_k[i] = c_q \big| r_m\big]. \tag{5.24}$$

For the sake of simplicity, we remove any symbol with $P\big[s_k[i]\big] \leq \rho_{\text{th}}$ from the list. The threshold ρ_{th} may be fixed or varied in terms of SINR.

For each user, we generate a tentative decision list $\mathcal{L}_k$. By listing all the combinations of the elements across K users, a length Γ tentative decision list is formed. Each column vector on the list denotes a possible transmission symbol vector $\boldsymbol{s}'_l$ where $l = 1, \ldots, \Gamma$. The size of the list is obtained by

$$\Gamma = \prod_{k=1}^{K} |\mathcal{L}_k|, \qquad 1 \leq \Gamma \ll |\mathcal{A}|^K, \tag{5.25}$$

where $|\cdot|$ denotes cardinality. In order to obtain an improved performance, the maximum likelihood (ML) rule can be used to select the best among the Γ candidate symbol vectors. The cost function for the ML criterion, which is equivalent to the minimum Euclidean distance criterion and the selected vector is given by

$$\boldsymbol{s}'_{\text{ML}} = \arg \min_{l=1,\ldots,\Gamma} \big\|\boldsymbol{r}[i] - \boldsymbol{G}\boldsymbol{s}'_l[i]\big\|^2, \tag{5.26}$$

where $\boldsymbol{r}[i] = [r_1[i], \ldots, r_m[i], \ldots, r_M[i]]^T$ and $\boldsymbol{G} = [\boldsymbol{g}_1^T, \ldots, \boldsymbol{g}_m^T, \ldots, \boldsymbol{g}_M^T]^T$ are received signals and the user channels for all cooperating cells.

In the above expression, the knowledge of $\boldsymbol{g}_m$ and the received signal $r_m[i]$ for each cell is required to be passed to the SU, which may lead to high backhaul traffic. However, we may distribute the norm operation to each cell. In a complex space $\mathcal{C}^K$, the common norm is

$$\|\boldsymbol{d}\| \triangleq \sqrt{|d_{1,m}|^2 + \cdots + |d_{K,m}|^2}. \tag{5.27}$$

where $\boldsymbol{d} = \boldsymbol{r}[i] - \boldsymbol{G}\boldsymbol{s}'_l[i]$ and $d_{k,m} = r_m[i] - \boldsymbol{g}_m \boldsymbol{s}'_l[i]$. For each BS, we separately calculate the minimum partial weights by

$$l_m^{\min} = \arg\min_l |r_m[i] - \boldsymbol{g}_m \boldsymbol{s}'_l[i]|^2. \tag{5.28}$$

The index $l_m^{\min}$ is obtained by the SU via backhaul and an enhanced detection is obtained. In each iteration, the received signal is subtracted by

$$\tilde{r}_k[i] = r_k[i] - \boldsymbol{h}_k \tilde{\boldsymbol{u}}_k^{\text{ML}}[i], \tag{5.29}$$

where the hard symbol cancellation vector consists of

$$\tilde{\boldsymbol{u}}^{\text{ML}} = \left[\tilde{s}_1^{\text{ML}}, \ldots, \tilde{s}_{k-1}^{\text{ML}}, 0, \tilde{s}_{k+1}^{\text{ML}}, \ldots, \tilde{s}_K^{\text{ML}}\right]. \tag{5.30}$$

With this multiple candidate structure, an enhanced ICI suppression is obtained. The indices of the symbols on the tentative decision list $\mathcal{A}_k$ are propagated among the neighbouring BSs which require a reduced backhaul traffic compared with that of the soft signal cancellation algorithm. Additionally, as more cancellation iterations are performed, the size of the list reduces as the recovered bits are more reliable. This further decreases the backhaul traffic with the following iterations which is not the case with the approach that adopts a soft interference cancellation strategy.

5.5 Simulations

In the simulations, we assume $\rho_{m,o}$ is zero, $\rho_{m,d} = 1$ and strongly received interference have $\rho_{m,n} = 0.5$. All BSs are assumed to have the same signal-to-noise ratio (SNR) and the interfering BSs are also assumed to have the same signal-to-interference ratio (SIR). In order to evaluate the performance of the distributed turbo system, we select a rate R = 1/2 convolutional code with polynomial $[7, 5]_{\text{oct}}$. The coded bits are modulated as QPSK symbols before transmission. The decoding is performed by a max-log-MAP decoder and the block length is set to 1024. The number of detector and decoder iterations is fixed to 10. The loop of interference cancellation performed by the network stops with iteration 4 and the number of cells in each cluster is $\phi = 1$, if not otherwise stated. In the soft interference cancellation [22] [56], a uniform quantizer is applied in order to quantize the

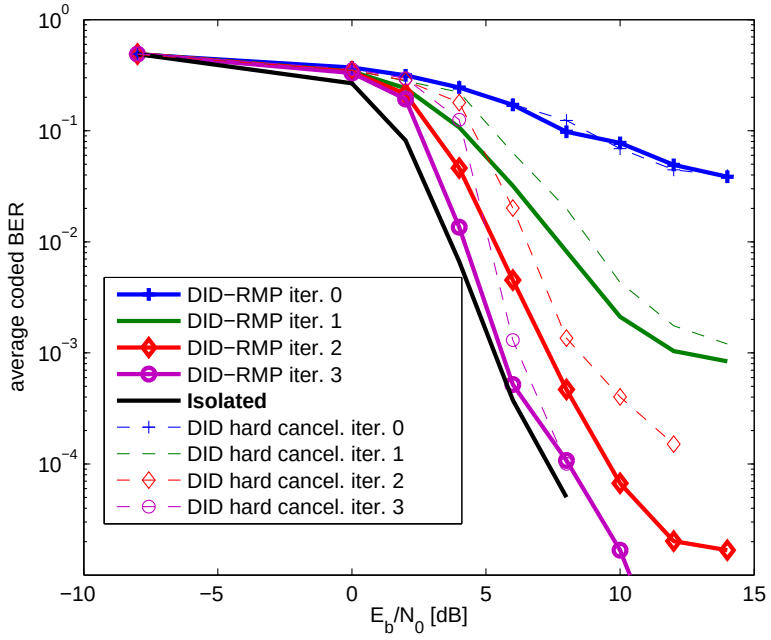

Figure 5.4: The solid lines denote a cooperating 4-cell network with $\zeta = 2$ strong interferers per cell. The dashed lines denote a cooperating network with a 9-cell network with $\zeta = 3$ strong interferers per cell.

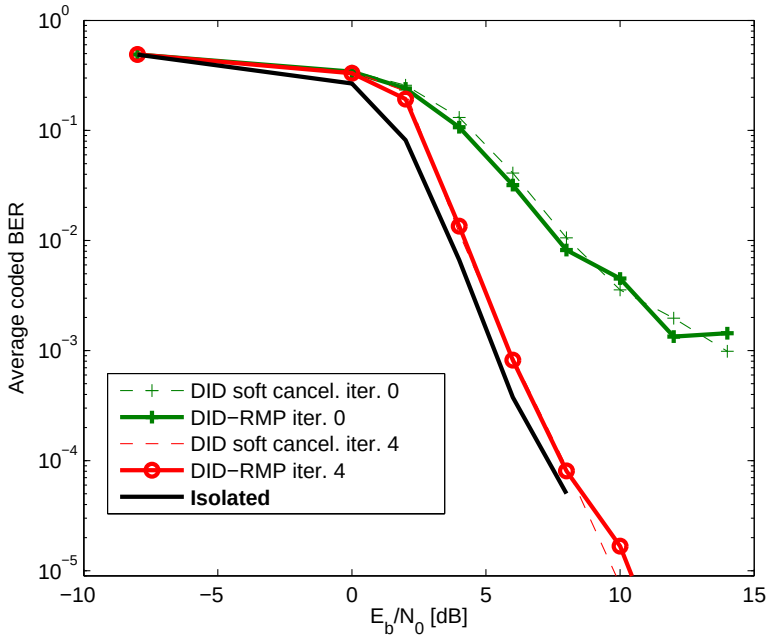

Figure 5.5: The DID is applied on a cooperating 4-cell network with $\zeta = 2$ strong interferers per cell.

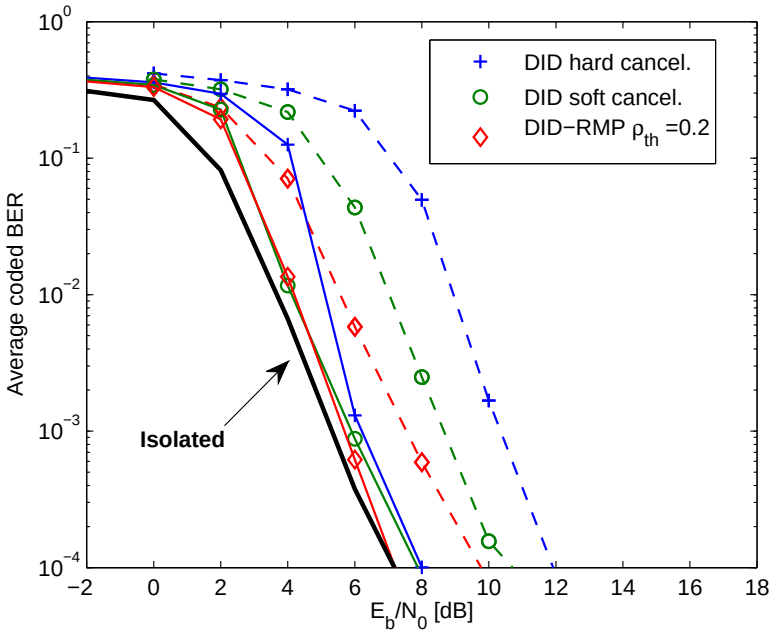

Figure 5.6: The solid lines denote a cooperating 4-cell network with $\zeta = 2$ strong interferers per cell. The dashed lines denote a cooperating network with 9 cells with $\zeta = 3$ strong interferers per cell.

soft estimates. Without significant information loss compared with the unlimited backhaul performance, 6 quantization bits per real dimension backhaul traffic is assumed [24].

Fig. 5.4 and Fig. 5.5 compares the performance of the proposed DID-RMP algorithm with that of DID based on hard and soft information exchange in terms of parallel interference cancellation iterations, respectively. By applying the RMP algorithm, the proposed DID has a similar performance as compared with the soft cancellation scheme and outperforms the DID with hard cancellation by about 2 dB in each iteration.

In Fig. 5.6 the proposed DID-RMP outperforms the soft interference cancellation scheme, the improvement increases with a higher number of strong interferers ζ. With $\zeta = 3$ interferers, the proposed scheme achieves about 3 dB gain as compared with the system using hard cancellation at the target BER $= 10^{-3}$.

Fig. 5.7 illustrate the backhaul traffic as function of the number of strong interferers ζ. As QPSK modulation is used, 2 bits are required to index the constellation symbols to perform hard interference cancellation. The plots indicate that increasing the number of

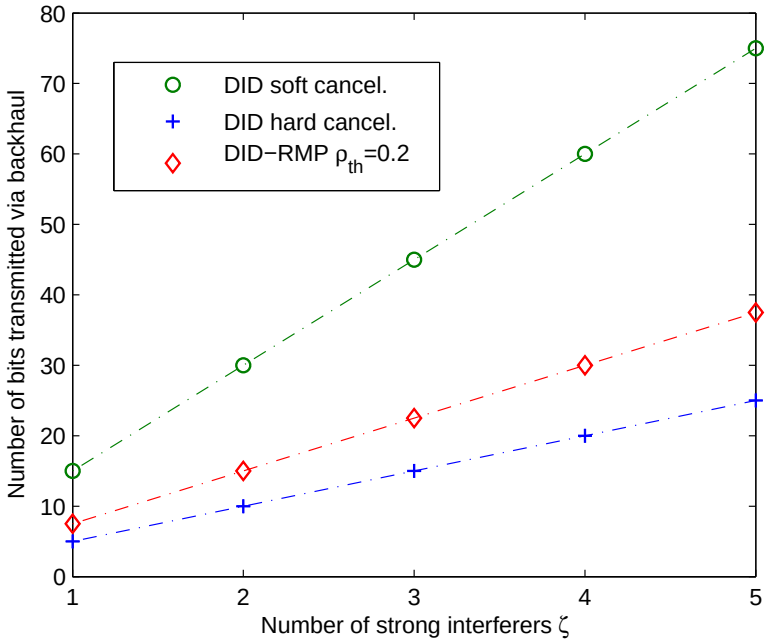

Figure 5.7: Number of bits exchanged per symbol detection in a 9-cell network.

strong interferers for each cell leads to the rise of the backhaul traffic.

In Fig. 5.8, the averaged number of tentative decision in the network is depicted. The number of tentative decisions Γ decreases as more iterations are performed. In the proposed scheme, only indices are exchanged, the backhaul traffic becomes lower in each iteration due to the fact that Γ is getting smaller. On the other hand, the soft interference cancellation scheme does not benefit from the iterations due to the requirement of updating the soft estimates. We can also see from the plots that the average number of candidates quickly converges to 1, which means low additional detection complexity is required for each BS. Compared with Fig. 5.6, the target BER region from 10^{-3} to 10^{-4} and the corresponding SNR is ranged 8 to 10 dB. The average number of tentative decisions per symbol is below 3 for $\zeta = 3$. In case of two strong interferers, we can see that negligible additional backhaul overhead is required.

All the DID in the above simulations are bounded by the isolated cell performance, since $\phi = 1$ and there is only one pair of receive and transmit antennas available in each cluster, no array gain and diversity can be obtained. However, in Fig. 5.9 we assume a cooperating 4-cell network with $\zeta = 2$ strong interferers per BS, we group the four cells into two clusters and $\phi = 2$. A 2×2 distributed MIMO system is created in each cluster

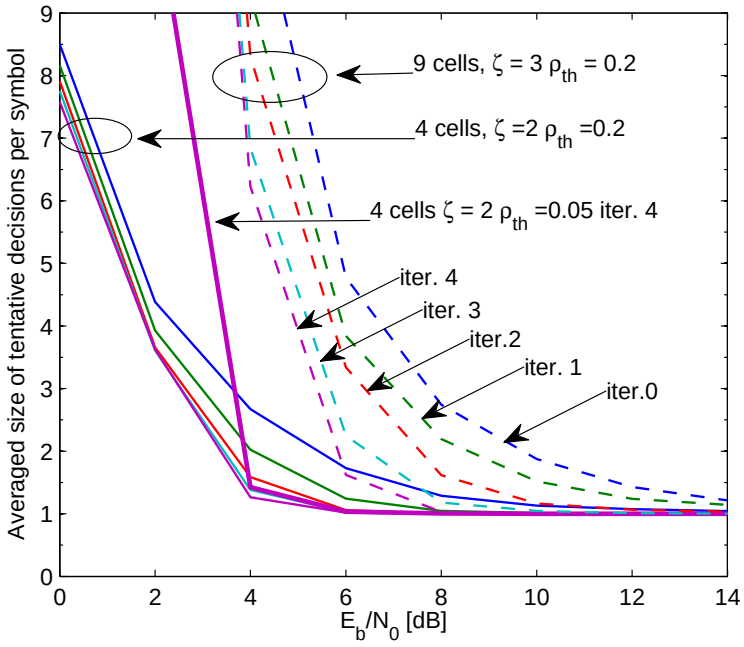

Figure 5.8: The number of tentative decisions Γ decreases as the increase of SNR. With a smaller threshold ρ_{th} selected, more decision candidates are generated, especially in the low SNR region.

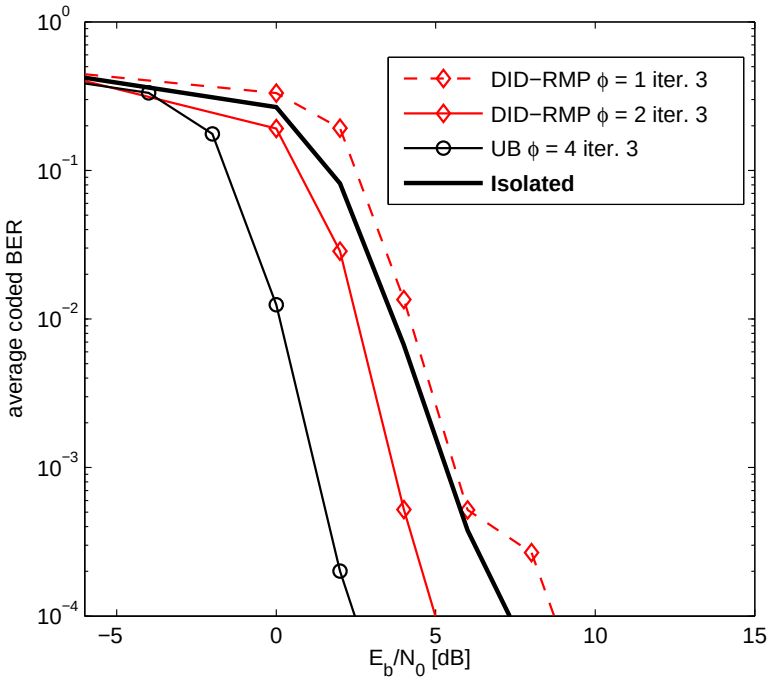

Figure 5.9: Performances of a cooperating 4-cell network with $\zeta = 2$ strong interferers per BS, we group the four cells into two clusters $\phi = 2$ and single cluster $\phi = 4$.

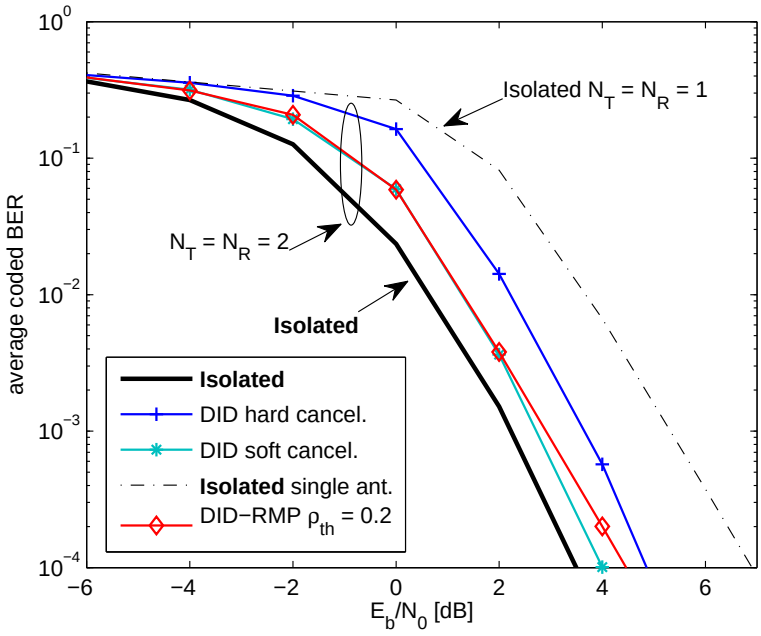

Figure 5.10: Performances of a cooperating 2-cell network with $\zeta = \{1, 1\}$ strong interferers per BS in which we assume a single cell for each cluster $\phi = 1$ and $N_R = N_T = 2$ antennas for each BS and user.

and the interference is mitigated between two clusters. We also investigate a single cluster system with $\phi = 4$, assuming unlimited backhaul (UB), a 4×4 distributed MIMO system is created and high diversity and array gain are obtained.

Fig. 5.10 illustrated a system model with multiple antenna equipped users and BSs, we build a two cell network where each cell has a single user which has $N_T = 2$ transmit antennas. The BSs for the cells also have $N_R = 2$ antennas ready for detection. Each BS receives the desired signal as well as the interference from the adjacent cell. Due to the fact that 2 data stream is seen as interfering signal, we use $\zeta = \{1, 1\}$ to discriminate from the single antenna case. In this figure, we use two isolated bounds as the reference and with 4 iterations, the soft cancellation performance can be achieved by using RMP algorithm with $\rho_{\text{th}} = 0.2$.

5.6 Summary

We have discussed the multiuser multicell detection through base station cooperation in an uplink, high frequency reuse scenario. Distributed iterative detection has been introduced as an interference mitigation technique. In this chapter, we have compared the soft and hard information exchange and cancellation schemes and proposed a novel hard information exchange strategy based on RMP. The proposed algorithm significantly reduces the backhaul data compared with the soft information exchange while it obtains a better bit error performance.

Chapter 6

Conclusions and Future Work

6.1 Summary and Conclusions

In this thesis, we have investigated interference mitigation based detection algorithms and their application to point-to-point, multiuser, and multicell MIMO systems. Various interference suppression techniques such as multiple feedback successive interference cancellation (Chapter 3), adaptive decision feedback detection with constellation constraints (Chapter 4) and distributed iterative detection with reduced message passing (Chapter 5) have been proposed, investigated and compared with the traditional technologies such as successive interference cancellation, decision feedback detection as well as the optimal maximum likelihood detection and sphere decoders.

In the following, we summaries the work in the thesis in terms of the content of chapters.

In Chapter 2, the capacity of MIMO systems has been reviewed in both deterministic and random channels. The analysis shows that the capacity grows linearly as more antenna pairs are equipped in the system. Spatial multiplexing gains provided by the MIMO systems stimulated the investigation of various detectors which are summarised in the second part of the chapter. In the latter sections of Chapter 2, channel codes have been introduced to bring information redundancy and protect the message bits. At the receiver

side, an iterative detection and decoding structure has been described and an analytical tool named extrinsic transfer chart has been reviewed.

The well known successive interference cancellation detection algorithm has the ability to separate the spatially multiplexed signals on a MIMO channel. However, the sub-optimal algorithm has significant performance loss compared with the optimal maximum likelihood detection and sphere decoding algorithms. In Chapter 3, we have proposed a multiple feedback algorithm to enhance the performance of the conventional successive interference cancellation detection, where reliability checking is introduced and the unreliable estimates are replaced by a feedback candidate selected based on the channel information and the received vector. Soft-output detection is obtained by using the MMSE estimated symbols in each spatial layer and therefore the bit likelihood information can be obtained and the iterative detection and decoding can be performed in both the point-to-point and multiuser MIMO systems.

The successive interference cancellation introduced in Chapter 3 has a relatively low detection complexity by assuming that the channel is varied frame by frame. The MMSE filter can be used repeatedly within the frame and the channel matrix inversion is computed at the beginning of each frame. However, if it is the case that the channels are fading rapidly, the conventional detection algorithms generally bring about expensive complexity in the time domain since the filter vectors required to be update accordingly. In order to address this problem, a decision feedback algorithm has been introduced in Chapter 4, where a recursive least squares based adaptive algorithm has been developed to update the forward and backward filters. The proposed constellation constraints aided detector replaces the unreliable estimates with the constellation symbols which effectively mitigate the error propagation in the decision feedback loops.

In Chapter 5, the base station cooperation is considered in a multicell, high frequency reuse scenario, a number of distributed iterative detection are studied based on previously reported literatures. The optimal distributed detections exchange all the soft detection estimates with all the adjacent base stations. Since a large amount of information need to be transmitted via a wired backhaul, the exchanging of hard bit information is preferred, however, the performance degradation is experienced. In Chapter 5, we consider a message passing technique in which each base station generates a detection list with the

probabilities for the desired symbol that are sorted according to the calculated probability density. Then, the network selects the best ones from the lists and conveys the index of the constellation points among the cooperating cells. The proposed distributed iterative detection with the reduced message passing introduce low backhaul traffic overhead compared with the hard bit exchange and outperforms the previously reported hard/soft information exchange algorithms.

6.2 Future Work

On one hand, all the techniques described above assume that there is a single propagation path between the transmit and receive antenna pairs. The channel may be generalized to a multipath channel in which equalization is required by the receiver. The interference mitigation techniques developed in Chapter 3 and Chapter 4 may be incorporated in the equalizer design. On the other hand, the receivers discussed in Chapters 2 - 5 are operated in narrowband systems and can be naturally extended to the broadband communications by using orthogonal frequency division multiplexing techniques.

Some suggestions on the possible future work based on this thesis are given below:

- To consider multicell MIMO systems with cooperative signal relaying [13].
- By applying the techniques introduced in the previous chapters to help solve the synchronization problem in communication networks [33].
- In terms of error control coding, stronger codes such as turbo codes and LDPC can be used to replace the convolutional codes used in the thesis [67].
- The interference cancellation developed in Chapter 3 and Chapter 5 may be applied with physical layer network coding to increase the network throughput.
- Resource allocation may be applied to the network introduced in Chapter 5 and therefore increase the per-cell capacity.
- Hardware implementation of the multiple feedback receiver structure proposed in Chapter 3.

- The massive MIMO and reduced-rank techniques can be applied for parameters detection and estimation [99, 100].

Appendix

Since

$$\boldsymbol{v}_{\text{MMSE}} = (\boldsymbol{H}^H\boldsymbol{H} + \frac{\sigma_v^2}{\sigma_s^2}\boldsymbol{I})^{-1}\boldsymbol{H}^H\boldsymbol{v}, \tag{1}$$

by using singular value decomposition (SVD), the MMSE post-detection noise power is expressed as

$$\begin{aligned}
\|\boldsymbol{v}_{\text{MMSE}}\|^2 &= \left\|(\boldsymbol{H}^H\boldsymbol{H} + \frac{\sigma_v^2}{\sigma_s^2}\boldsymbol{I})^{-1}\boldsymbol{H}^H\boldsymbol{v}\right\|^2 \\
&= \left\|\left(\boldsymbol{V}\boldsymbol{\Sigma}\boldsymbol{V}^H + \frac{\sigma_v^2}{\sigma_s^2}\boldsymbol{I}\right)^{-1}\boldsymbol{V}\boldsymbol{\Sigma}\boldsymbol{U}^H\boldsymbol{v}\right\|^2 \\
&= \left\|\left(\boldsymbol{V}\boldsymbol{\Sigma}^2\boldsymbol{V}^H + \frac{\sigma_v^2}{\sigma_s^2}\boldsymbol{I}\right)^{-1}\left(\boldsymbol{\Sigma}^{-1}\boldsymbol{V}^H\right)^{-1}\boldsymbol{U}^H\boldsymbol{v}\right\|^2 \\
&= \left\|\left(\boldsymbol{\Sigma}\boldsymbol{V}^H + \frac{\sigma_v^2}{\sigma_s^2}\boldsymbol{\Sigma}^{-1}\boldsymbol{V}^H\right)^{-1}\boldsymbol{U}^H\boldsymbol{v}\right\|^2.
\end{aligned} \tag{2}$$

From the above equations we can conclude that the performance of linear detection is directly related to the power of the MMSE effective noise. The noise enhancement which is calculated as

$$\begin{aligned}
E\{\|\boldsymbol{n}_{\text{MMSE}}\|^2\} &= E\left\{\left\|\left(\boldsymbol{H}^H\boldsymbol{H} + \frac{\sigma_v^2}{\sigma_s^2}\boldsymbol{I}\right)^{-1}\boldsymbol{H}^H\boldsymbol{v}\right\|^2\right\} \\
&= E\left\{\left\|\left(\boldsymbol{\Sigma} + \frac{\sigma_v^2}{\sigma_s^2}\boldsymbol{\Sigma}^{-1}\right)^{-1}\boldsymbol{U}^H\boldsymbol{v}\right\|^2\right\} \\
&= \text{tr}\left(\left(\boldsymbol{\Sigma} + \frac{\sigma_v^2}{\sigma_s^2}\boldsymbol{\Sigma}^{-1}\right)^{-1}\boldsymbol{U}^H E\{\boldsymbol{v}\boldsymbol{v}^H\}\boldsymbol{U}\left(\boldsymbol{\Sigma} + \frac{\sigma_v^2}{\sigma_s^2}\boldsymbol{\Sigma}^{-1}\right)^{-1}\right) \\
&= \text{tr}\left(\frac{\sigma_v^2}{\sigma_s^2}\left(\boldsymbol{\Sigma} + \frac{\sigma_v^2}{\sigma_s^2}\boldsymbol{\Sigma}^{-1}\right)^{-2}\right) \\
&= \sum_{k=1}^{N_T}\frac{\sigma_v^2}{\sigma_s^2}\left(\sigma_k + \frac{\sigma_v^2/\sigma_s^2}{\sigma_k^2}\right)^{-2} \\
&= \sum_{k=1}^{N_T}\frac{\sigma_k^2(\frac{\sigma_v}{\sigma_s})^2}{(\sigma_k^2 + (\frac{\sigma_v}{\sigma_s})^2)^2}.
\end{aligned} \tag{3}$$

Glossary

AMUDFCC	**A**daptive **M**ultiple **U**ser **D**ecision **F**eedback detection with **C**onstellation **C**onstraints
AP	**A**ccess **P**oint
APP	**A** **P**osteriori **P**robabilities
AWGN	**A**dditional **W**hite **G**aussian **N**oise
BER	**B**it-**E**rror-**R**ate
BICM	**B**it **I**nterleaved **C**oded **M**odulation
BLAST	**B**ell **LA**b **S**pace **T**ime
BPSK	**B**inary **P**hase **S**hift **K**eying
BS	**B**ase **S**tation
BSC	**B**ase **S**tation **C**ooperation
CC	**C**onstellation **C**onstraints
CCI	**C**o **C**hannel **I**nterference
CDMA	**C**ode **D**ivision **M**ultiple **A**ccess
CSI	**C**hannel **S**tate **I**nformation
C-SIC	**C**onventional **SIC**
DAS	**D**istributed **A**ntenna **S**ystem
dB	Decibel
DF	**D**ecision **F**eedback
DFCC	**D**ecision **F**eedback detection with **C**onstellation **C**onstraints
DID	**D**istributed **I**terative **d**etection
EXIT	**EX**trinsic **I**nformation **T**ransfer
FEC	**F**orward **E**rror **C**orrection
FLOPS	**FL**oating point **O**perations **P**er **S**econd
FSB	**F**requently **S**elected **B**ranches
JMD	**J**oint **M**ultiple-user **D**etection
Hz	**H**ert**z**
IAI	**I**nter **A**ntenna **I**nterference
IC	**I**nterference **C**ancellaton
ICI	**I**nter **C**ell **I**nterference

ISI	**I**nter-**S**ymbol **I**nterference
LD	**L**inear **D**etection
LDPC	**L**ow **D**ensity **P**arity **C**heck
LLR	**L**og-**L**ikelihood **R**atio
LPA	**L**isting **P**atterns **A**pproach
LR	**L**attice **R**eduction
LS	**L**east **S**quares
LTE	**L**ong **T**erm **E**volution
MAP	**M**aximum **A** **P**osteriori
MB	**M**ultiple **B**ranch
MF-SIC	**M**ultiple **F**eedback **S**uccessive **I**nterference **C**ancellation
MIMO	**M**ultiple-**I**nput **M**ultiple-**O**utput
ML	**M**aximum **L**ikelihood
MMSE	**M**inimum **M**ean **S**quare **E**rror
MSE	**M**ean **S**quare **E**rror
MSEW	**M**aximum **S**quared **E**uclidean **W**eight
MUI	**M**ultiple **U**ser **I**nterference
NCO	**N**ulling and **C**ancellation **O**rder
NSC	**N**on-**S**ystematic **C**onvolutional
OFDM	**O**rthogonal **F**requency **D**ivision **M**ultiplexing
OSIC	**O**rdered **SIC**
PCI	**P**erfect **C**hannel **I**nformation
PDF	**P**robability **D**ensity **F**unction
PIC	**P**arallel **I**nterference **C**ancellation
PSK	**P**hase-**S**hift **K**eying
PSP	**P**re- **S**tored **P**atterns
QAM	**Q**uadrature **A**mplitude **M**odulation
RLS	**R**ecursive **L**east **S**quares
RMP	**R**educed **M**essage **P**assing
RSC	**R**ecursive **S**ystematic **C**onvolutional
S/P	**S**erial to **P**arallel
SAC	**S**hadow **A**rea **C**onstraints
SB	**S**ingle **B**ranch

SC	**S**oft **C**ancellation
SD	**S**patial **D**iversity
SD	**S**phere **D**ecoder
SIC	**S**uccessive **I**nterference **C**ancellation
SINR	**S**ignal to **I**nerference plus **N**oise **R**atio
SIR	**S**ignal to **I**nterference **R**atio
SISO	**S**oft-**I**nput **S**oft-**O**utput
SISO	**S**ingle-**I**nput **S**ingle-**O**utput
SM	**S**patial **M**ultiplexing
SNR	**S**ignal to **N**oise **R**atio
SOVA	**S**oft **O**utput **V**iterbi **A**lgorithm
SP	**S**et **P**artitioning
SPIC	**S**oft **P**arallel **I**nterference **C**ancellation
STBC	**S**pace-**T**ime **B**lock **C**odes
STTC	**S**pace-**T**ime **T**rellis **C**odes
SU	**S**election **U**nit
SVD	**S**ingular **V**alue **D**ecomposition
WiMAX	**W**orldwide **i**nteroperability for **M**icrowave **A**ccess
ZF	**Z**ero **F**orcing

Bibliography

[1] D. Martín-Sacristán, J. F. Monserrat, J. Cabrejas-Peñuelas, D. Calabuig, S. Garrigas, N. Cardona, "On the way towards forth-generation mobile: 3GPP LTE and LTE-Advanced," *EURASIP Journal on Wireless Communications and Networking*, vol. 2009, p. 10, Sept. 2009.

[2] "IEEE Standard for Information Technology–Telecommunications and information exchange between systems–Local and metropolitan area networks–Specific requirements Part 11: Wireless LAN Medium Access Control (MAC) and Physical Layer (PHY) specifications Amendment 10: Mesh Networking," *IEEE Std 802.11s-2011* , vol., no., pp.1-372, Sept. 10 2011.

[3] "IEEE Standard for Local and metropolitan area networks Part 16: Air Interface for Broadband Wireless Access Systems Amendment 3: Advanced Air Interface," *IEEE Std 802.16m-2011 (Amendment to IEEE Std 802.16-2009)* , vol., no., pp.1-1112, May 5 2011.

[4] TR36.913, "Requirements for further advancement for Evolved Universal Terrestrial Radio Access (E-UTRA) (LTE-Advanced)," 3GPP, Tech. Rep., 2008.

[5] I. E. Telatar, "Capacity of multi-antenna Gaussian channels," *Eur. Trans. Telecommun.*, vol.10, pp. 585-595, Nov. 1999.

[6] G. J. Foschini, "Layered space-time architecture for wireless communication in a fading environment when using multielement antennas," *Bell Labs Tech. Journal*, vol. 1, no. 2, pp. 4159, 1996.

[7] P. W. Wolniansky, G. J. Foschini, G. D. Golden, R. A. Valenzuela, "V-BLAST: an architecture for realizing very high data rates over the rich-scattering wireless channel," *URSI ISSSE'98*, Pisa, Italy, pp. 295-300. Oct. ,1998.

[8] V. Tarokh, N. Seshadri, A. R. Calderbank, "Space-time codes for high data rate wireless communication: performance criterion and code construction," *IEEE Transactions on Information Theory*, vol. 44, no. 2, pp. 744-765, Mar 1998.

[9] S. M. Alamouti, "A simple transmit diversity technique for wireless communications ," *IEEE Journal on Selected Areas in Communications* , vol. 16, no. 8, pp. 1451-1458, Oct 1998.

[10] L. Zheng, D.N.C. Tse, "Diversity and multiplexing: a fundamental tradeoff in multiple-antenna channels," *IEEE Transactions on Information Theory*, vol. 49, no. 5, pp. 1073- 1096, May 2003.

[11] D. Tse and P. Viswanath. *Fundamentals of Wireless Communications.* Cambridge University Press, 2005.

[12] S. Verdú, *Multiuser Detection*, Cambridge University Press, 1998.

[13] A. Papadogiannis, "System and Techniques for Multicell-MIMO and Cooperative Relaying in Wireless Networks," *PhD thesis*, TELECOM ParisTech, 2009.

[14] L. Isaksson, "Seamless communications, seamless handover between wireless and cellular networks with focus on always best connected", *PhD thesis*, Blekinge Institute of Technology. 2007.

[15] D. Chen, "Precoding for MIMO Systems," *PhD thesis*, The University of York, 2010.

[16] B. Hagerman, "Single-User Receiver for Partly Known Interference in Multi-User Environments," *PhD thesis,* Royal Institute of Technology, Sweden, Sept 1995.

[17] C. Berrou and A. Glavieux, "Near optimum error-correcting coding and decoding: turbo-codes," *IEEE Transactions on Communications*, vol. 44, pp 1261-1271, Oct. 1996.

[18] B. Hochwald and S. T. Brink, "Achieving near-capacity on a multiple-antenna channel," *IEEE Transactions on Communications*, vol. 51, pp. 389-399, Mar. 2003.

[19] T. Matsumoto, "Iterative (turbo) signal processing techniques for MIMO signal detection and equalization," in Smart Antennas in Europe - State-of-the-Art, EURASIP Book Series, 2005.

[20] J. Karjalainen, N. Veselinovic, K. Kansanen, T. Matsumoto, "Iterative Frequency Domain Joint-over-Antenna Detection in Multiuser MIMO," *IEEE Transactions on Communications*, vol.6, no.10, pp.3620-3631, Oct. 2007.

[21] G. Woodward, R. Ratasuk, M. L. Honig, P.Rapajic, "Minimum mean-squared error multiuser decision-feedback detectors for DS-CDMA," *IEEE Transactions on Communications*, vol. 50, no. 12, Dec. 2002.

[22] T. Mayer, H. Jenkac, and J. Hagenauer, "Turbo base-station cooperation for intercell interference cancellation, *IEEE International Conference on Communications*, vol. 11, pp. 4977 4982. June 2006.

[23] S. Khattak, G. Fettweis, "Low Backhaul Distributed Detection Strategies for an Interference Limited Uplink Cellular System," *IEEE Vehicular Technology Conference, 2008. VTC Spring 2008*. pp.693-697, 11-14 May 2008

[24] S. Khattak, G. Fettweis, "Distributed Iterative Detection in an Interference Limited Cellular Network," *IEEE 65th Vehicular Technology Conference, 2007-Spring,* pp. 2349-2353, 22-25 April 2007.

[25] S. Khattak, G. Fettweis, A. U. Khan, "Performance Comparison of Iterative Multiuser Detection Techniques In Interference Limited Cellular Networks," *International Conference on Emerging Technologies, 2006. ICET '06.* pp. 480-485, 13-14, Nov. 2006.

[26] S. Khattak, W. Rave, G. Fettweis, "Distributed Iterative Multiuser Detection through Base Station Cooperation," *EURASIP Journal on Wireless Communications and Networking*, vol. 2008, pp. 15, 2008.

[27] C. Studer, "Iterative MIMO decoding: algorithms and VLSI implementation aspects," *PhD thesis* Hartung-Gorre Publisher, 2009.

[28] Y. Cai, "Advanced interference suppression techniques for spread spectrum systems, " *PhD thesis*, The University of York, 2009.

[29] M. F. Demirkol, M. A. Ingram, "Power-controlled capacity for interfering MIMO links," *IEEE VTS 54th Vehicular Technology Conference 2001 Fall*, vol. 1, pp. 187-191, 2001.

[30] L. Wang, "Array signal processing algorithms for beamforming and direction finding," *PhD thesis*, The University of York, Dec. 2009.

[31] E. Visotsky, U. Madhow, "Space-time transmit precoding with imperfect feedback," *IEEE Transactions on Information Theory*, vol. 47, no. 6, pp. 2632-2639, Sep 2001.

[32] M. V. Clark, T. M. Willis. III, L. J. Greenstein, A. J. Rustako, V. Erceg, R. S. Roman, "Distributed versus centralized antenna arrays in broadband wireless networks," *IEEE VTS 53rd Vehicular Technology Conference, 2001 Spring*, vol. 1, pp. 33-37, 2001.

[33] F. Simoens, H. Wymeersch, H. Steendam and M. Moeneclaey, "Synchronization for MIMO systems", in Smart Antennas in Europe - State-of-the-Art, EURASIP Book Series, 2005.

[34] W. E. Ryan, S. Lin, "Channel Codes Classical and Modern," Cambridge University Press, 2009.

[35] C. Berrou, A. Glavieux, P. Thitimajshima, "Near Shannon limit error-correcting coding and decoding: Turbo-codes," *IEEE International Conference on Communications* vol. 2, pp. 1064-1070 vol. 2, 23-26, Geneva, May 1993.

[36] A. D. Liveris, Z. Xiong, C. N. Georghiades, "Compression of binary sources with side information at the decoder using LDPC codes," *IEEE Communications Letters*, vol. 6, no. 10, pp. 440- 442, Oct 2002.

[37] V. Tarokh, H. Jafrakhani, A. R. Calderbank, "Space-time block codes from orthogonal designs," *IEEE Transactions on Information Theory*, 45(5), 14561467, 1999.

[38] A. Paulraj, R. Nabar, D. Gore, Introduction to Space-Time Wireless Communications. Cambridge, UK; Cambridge University Press, 2003.

[39] S. Sanhdu, A. Paulraj, "Space-time block codes: a capacity perspective," IEEE Communications Letters, 4(12), 384386. 2000.

[40] JJ. van de Beek, O. Edfors, M. Sandell, S. K. Wilson, P. O. Borjesson, "On channel estimation in OFDM systems," *IEEE VTC95*, vol. 2, pp. 815819. July 1995.

[41] F. Tufvesson, T. Maseng, "Pilot assisted channel estimation for OFDM in mobile cellular systems," *IEEE VTC97*, vol. 3, pp. 16391643. May 1997.

[42] Z. Ding, Y. Li, "Blind Equalization and Identification," New York: Marcel Dekker. 2001.

[43] S. Haykin, Adaptive Filter Theory, 4th edn, PHIPE. 2001.

[44] V. Tarokh, N. Seshadri, A. R. Calderbank, "Space-time codes for high data rate wireless communication: performance criterion and code construction," *IEEE Transactions on Information Theory*, 44(2), 744765. 1998.

[45] V. Tarokh, H. Jafarkhani, A. R. Calderbank, "Space-time bock coding for wireless communications: performance results," IEEE Journal on Selected Areas in Communications, 17(3), 451460. 1999.

[46] W. Firmanto, B. Vucetic, J. Yuan, "Space-time TCM with improved performance on fast fading channels," *IEEE Communications Letters*, 5(4), pp. 154156. 2001.

[47] C. Shen, Y. Zhu, S. Zhou, J. Jiang, "On the performance of V-BLAST with zero-forcing successive interference cancellation receiver," *IEEE Global Telecommunications Conference, 2004. GLOBECOM'04*, 2004.

[48] M. Chiani, "Introducing erasures in decision-feedback equalization to reduce error propagation," *IEEE Transactions on Communications*, vol. 45, no. 7, pp. 757-760, July 1997.

[49] M. Reuter, J. C. Allen, J. R. Zeidler, R. C. North, "Mitigating Error Propagation Effects in a Decision Feedback Equalizer", *IEEE Transactions on Communications*, vol. 49, no. 11, pp.2028-2041 Nov. 2001.

[50] S. Kim, K. Kim, K. "Log-likelihood ratio based detection ordering in V-BLAST," *IEEE Transactions on Communications,* 54(2), 302307. 2006.

[51] Y. Cho, J, Kim, W, Yang, C, Kang, MIMO-OFDM Wireless communications with MATLAB, John Wiley & Sons pte Ltd, 2010.

[52] E. Agrell, T. Eriksson, A. Vardy, K. Zeger, "Closest point search in lattices " *IEEE Transactions on Information Theory* vol. 48 no. 8 pp.2201-2214, Aug 2002.

[53] E. Viterbo, J. Boutros, "A universal lattice code decoder for fading channels," IEEE Transactions on Information Theory, 45(5), 16391642. 1999.

[54] F. Schreckenbach, "Iterative Decoding of Bit-Interleaved Coded Modulation," *P.h.D. thesis*, Munich University of Technology 2007.

[55] J. Hagenauer, "The turbo principle: Tutorial introduction and state of the art," *International Symposium on Turbo-Codes*, Brest, France, September 1997.

[56] X. Wang and H.V. Poor, "Iterative (Turbo) soft interference cancellation and decoding for coded CDMA," *IEEE Transactions on Communications*, vol. 47, no. 7, pp. 1046-1061, 1999.

[57] R. Koetter, A. C. Singer, and M. Tuchler, "Turbo equalization: an iterative equalization and decoding technique for coded data transmission," *IEEE Signal Processing Magazine,* pp. 67-80, Jan. 2004.

[58] X. Li, J. A. Ritcey, "Bit-interleaved coded modulation with iterative decoding," *IEEE Communications Letters*, vol. 1 no. 6 pp. 169-171. 1997.

[59] A. Chindapol, J. A. Ritcey, "Design, analysis, and performance evaluation for BICM-ID with square QAM constellations in Rayleigh fading channels," *IEEE Journal on Selected Areas in Communications,* vol. 19 no. 5 pp. 944-957, 2001.

[60] S. Khattak, W. Rave, G. Fettweis, "Multiuser turbo detection in a distributed antenna system," *15th IST Wireless and Mobile Communications summit*, June 2006.

[61] W. Choi, J. G. Andrews, and C. Yi, "The Capacity of Multicellular Distributed Antenna Networks," *IEEE Wireless com, Information theory symposium*, June 2005.

[62] W. Choi and J. G. Andrews, "Downlink Performance and Capacity of Distributed Antenna Systems in a Multicell Environment," *IEEE Transactions on Wireless Communications,* vol. 6, no. 1, pp. 6973, Jan. 2007.

[63] H. Mai, "Iterative Channel Estimation for Wireless Communications," P.h.D thesis, The University of York, March 2006.

[64] L. Liu and L. Ping, "Iterative detection of chip interleaved CDMA systems in multipath channels," *Electronics letters*, vol. 40, pp. 884-886, July 2004.

[65] L. Bahl, J. Cocke, F. Jelinek, and J. Raviv, "Optimal decoding of linear codes for minimizing symbol error rate," *IEEE Transactions on Information Theory,* 20:284287, March 1974.

[66] J. Hagenauer, P. Hoher, "A viterbi algorithm with soft-decision outputs and its applications," *IEEE Globecom Conference*, pages 16801686, Dallas, USA, January 1989.

[67] H. Vikalo, B. Hassibi, T. Kailath, "Iterative decoding for MIMO channels via modified sphere decoding," *IEEE Transactions on Wireless Communications,* vol. 3 no. 6 pp. 2299-2311, Nov. 2004.

[68] J Choi, A. C. Singer, J Lee, N Cho, "'Improved linear soft-input soft-output detection via soft feedback successive interference cancellation," *IEEE Transactions on Communications*, vol. 58, no. 3, March 2010.

[69] S. ten Brink, "Convergence behavior of iteratively decoded parallel concatenated codes," *IEEE Transactions on Communications*, vol. 49, no. 10, pp. 1727-1737, Oct 2001.

[70] J. Hagenauer, "The EXIT chart - Introduction to extrinsic information transfer in iterative processing," *European Signal Processing Conference, Vienna*, Austria, pp. 1541-1548, Sep. 2004.

[71] F. Schreckenbach, N. Gortz, J. Hagenauer, G. Bauch, "Optimization of symbol mappings for bit-interleaved coded Modulation with iterative decoding," *IEEE Communications Letters*, vol. 7, no. 12, pp. 593-595, Dec. 2003.

[72] H. Vikalo and B. Hassibi, "The Expected Complexity of Sphere Decoding, Part I: Theory, Part II: Applications," *IEEE Transactions on Signal Processing*, 2003.

[73] K. Wong, A. Paulraj, R. D. Murch, "Efficient High-Performance Decoding for Overloaded MIMO Antenna Systems," *IEEE Transactions on Communications*, vol. 6, no. 5, pp. 1833-1843, May 2007.

[74] J. Jalden, B. Ottersten, "On the Complexity of Sphere Decoding in Digital Communications" *IEEE Transactions on Signal Processing,* vol. 53, issue. 4 pp. 1474-1484, April 2005.

[75] G. Ginis, J. M. Cioffi, "On the relation between V-BLAST and the GDFE", *IEEE Communications Letters*, vol. 5, issue.9, pp. 364366, 2001.

[76] R. Fa, R. C. de Lamare, "Multi-Branch Successive Interference Cancellation for MIMO Spatial Multiplexing Systems", *IET Communications*, vol. 5, no. 4, pp. 484 - 494, March 2011.

[77] C. Windpassinger, L. Lampe, R. F. H. Fischer, T, Hehn, "A performance study of MIMO detectors," *IEEE Transactions on Wireless Communications*, vol. 5, no. 8, pp. 2004-2008, Aug. 2006.

[78] L. G. Barbero and J. S. Thompson, "Fixing the complexity of the sphere decoder for MIMO detection, *IEEE Transactions on Wireless Communications* , vol. 7, no. 6, pp. 2131-2142, June 2008.

[79] Y. H. Gan, C. Ling, W. H. Mow, "Complex Lattice Reduction Algorithm for Low-Complexity Full-Diversity MIMO Detection," *IEEE Transactions on Signal Processing*, vol. 57, no. 7, pp. 2701-2710, July 2009.

[80] E. Karami, "Tracking performance of least squares MIMO channel estimation algorithm", *IEEE Transactions on Communications*, vol.55, no.11, pp. 2201 2209, 2007.

[81] Q. Sun and D. C. Cox, "Training-based channel estimation for continuous flat fading BLAST," in *proc. IEEE ICC*, Helsinki, Finland, pp. 325-329, Jun. 2002.

[82] J. H. Choi, H. Y. Yu, Y. H. Lee, "Adaptive MIMO decision feedback equalization for receivers with time-varying channels", *IEEE Transactions on Signal Processing*, vol. 53, issue. 11, pp. 42954303, 2005.

[83] D. S. Chen and S. Roy, "An adaptive multiuser receiver for CDMA systems, *IEEE Journal on Selected Areas on Communications*, vol. 12, no. 6, pp. 808816, Jun. 1994.

[84] R. C. de Lamare, R. Sampaio-Neto, "Adaptive MBER decision feedback multiuser receivers in frequency selective fading channels", *IEEE Communications Letters*, vol. 7, no. 2, pp. 7375, 2003.

[85] P. B. Rapajic and B. S. Vucetic, "Adaptive receiver structures for asynchronous CDMA systems, *IEEE Journal on Selected Areas Communications*, vol. 12, no. 5, pp. 685697, May 1994.

[86] G. Ginis, Y. Bar-Ness, and J. M. Cioffi, "Blind adaptive MIMO decision feedback equalization using Givens rotations, in *IEEE ICC*, Helsinki, Finland, pp. 5963, Jun. 2002.

[87] M. T. Tuchler, R. Koetter, A. C. Singer, "Turbo equalization: principles and new results," *IEEE Transactions on Communications*, vol. 50, pp. 754-767, May 2002.

[88] M. L. Honig, G. K. Woodward, and Y. Sun, "Adaptive iterative multiuser decision feedback detection," *IEEE Transactions on Wireless Communications*, vol. 3, no. 2, pp. 477-485, Mar. 2004.

[89] C. Douillard, M. Jezequel, C. Berrou, A. Picart, P. Didier, and A. Glavieux, "Iterative correction of intersymbol interference: turbo equalization," *European Transactions Telecommunications*, vol. 6, pp. 507-511, Sept. 1995.

[90] H. Lee, B. Lee, and I. Lee, "Iterative detection and decoding with an improved V-BLAST for MIMO-OFDM Systems," *IEEE Journal on Selected Areas Communications*, vol. 24, pp. 504-513, Mar. 2006.

[91] J. W. Choi, A. C. Singer, J Lee, N. I. Cho, "Improved linear soft-input soft-output detection via soft feedback successive interference cancellation," *IEEE Transactions on Communications*, vol.58, no.3, pp.986-996, March 2010.

[92] R. C. de Lamare and R. Sampaio-Neto, "Minimum Mean Squared Error Iterative Successive Parallel Arbitrated Decision Feedback Detectors for DS-CDMA Systems,"*IEEE Transactions on Communications*, pp. 778 - 789, May, 2008.

[93] R. C. de Lamare, R. Sampaio-Neto, and A. Hjorungnes, "Joint Iterative Interference Cancellation and Parameter Estimation for CDMA Systems, *IEEE Communications Letters*, vol. 11 no. 12, pp. 916 - 918. December 2007.

[94] T. Minka, "The Lightspeed Matlab toolbox, Efficient operations for Matlab programming, Version 2.2", 17-Dec-2007, Microsoft Corporation.

[95] P. Robertson, E. Villebrun, and P. Hoeher, "A comparison of optimal and sub-optimal MAP decoding algorithms operating in the log domain," *IEEE International Conference on Communications 95*, pp. 1009-1013, June 1995.

[96] H. Yao, G. W. Wornell, "Lattice-reduction-aided detectors for MIMO communication systems," *IEEE GLOBECOM '02.* vol.1, pp. 424- 428 vol.1, 17-21 Nov. 2002.

[97] W. C. Jakes, *Microwave Mobile Communications*. New York: Wiley, 1974.

[98] S. Venkatesan, "Coordinating base stations for greater uplink spectral efficiency in a cellular network," *IEEE 18th International Symposium on Personal, Indoor and Mobile Radio Communications*, Athens, Sept. 2007.

[99] J. Hoydis, S. ten Brink, M. Debbah,"Massive MIMO: How many antennas do we need?", arXiv:1107.1709v2. 2011.

[100] R. C. de Lamare, R. Sampaio-Neto, "Adaptive reduced-rank MMSE filtering with interpolated FIR filters and adaptive interpolators," *IEEE Signal Processing Letters,* vol. 12, no. 3, pp. 177- 180, March 2005.

[101] M. L. Honig and J. S. Goldstein, "Adaptive reduced-rank interference suppression based on the multistage Wiener filter," *IEEE Transactions on Communications*, vol. 50, no. 6, June 2002.

[102] Y. Sun, V. Tripathi, and M. L. Honig, "Adaptive, Iterative, Reduced-Rank (Turbo) Equalization", *IEEE Transactions on Wirless Communications*, Vol. 4, No. 6, pp. 2789-2800, Nov. 2005.

[103] R. C. de Lamare, M. Haardt and R. Sampaio-Neto, "Blind Adaptive Constrained Reduced-Rank Parameter Estimation based on Constant Modulus Design for CDMA Interference Suppression," *IEEE Transactions on Signal Processing*, vol. 56., no. 6, June 2008.

[104] R. C. de Lamare and R. Sampaio-Neto, "Reduced-Rank Adaptive Filtering Based on Joint Iterative Optimization of Adaptive Filters," *IEEE Signal Processing Letters*, Vol. 14, no. 12, December 2007.

[105] R. C. de Lamare and R. Sampaio-Neto, "Adaptive Reduced-Rank Processing Based on Joint and Iterative Interpolation, Decimation, and Filtering," *IEEE Transactions on Signal Processing*, vol. 57, no. 7, pp. 2503 - 2514, July 2009.

[106] R. C. de Lamare and R. Sampaio-Neto, "Reduced-Rank Space-Time Adaptive Interference Suppression With Joint Iterative Least Squares Algorithms for Spread-Spectrum Systems," *IEEE Transactions on Vehicular Technology*, vol.59, no.3, pp.1217-1228, March 2010.

[107] R. C. de Lamare and R. Sampaio-Neto, "Adaptive Reduced-Rank Equalization Algorithms Based on Alternating Optimization Design Techniques for MIMO Systems," IEEE Transactions on Vehicular Technology, 2011.

[108] P. Li and R. C. de Lamare, "Adaptive Decision Feedback Detection with Constellation Constraints for MIMO Systems," *IEEE Transactions on Vehicular Technology,* vol. PP, no. 99, pp. 1, 0.

[109] P. Li, R. C. de Lamare and R. Fa, "Multiple Feedback Successive Interference Cancellation Detection for Multiuser MIMO Systems," *IEEE Transactions on Wireless Communications*, vol. 10, no. 8, pp. 2434 - 2439, August 2011.

[110] P. Li, R. C. de Lamare, "Adaptive Iterative Decision Multi-feedback Detection for Multi-user MIMO System", *IEEE International Conference on Acoustics, Speech and Signal Processing ICASSP*, accpted 2012.

[111] P. Li, R. C. de Lamare, "Parallel Multiple Candidate Interference Cancellation with Distributed Iterative Multi-cell Detection and Base Station Cooperation", *International ITG/IEEE Workshop on Smart Antennas WSA 2012*, accepted 2012.

[112] P. Li, R. C. de Lamare "Adaptive Iterative Decision Feedback with Constellation Constraints and Soft-Output Detection for MIMO Systems," *IEEE International Symposium on Wireless Communications Systems*, pp. 670-674, November. 2011.

[113] Y. Wang, P. Li, L. Li, A. G. Burr and R. C. de Lamare, "Irregular Code-Aided Low-Complexity Three-stage Turbo Space Time Processing", *IEEE International Symposium on Wireless Communications Systems*, pp. 604 - 608, Nov. 2011.

[114] J. Liu, P. Li, L. Li, R. C. de Lamare and A. G. Burr, "Iterative QR Decomposition-Based Detection Algorithms with Multiple Feedback and Dynamic Tree Search

for LDPC-Coded MIMO Systems", *Sensor Signal Processing for Defence (SSPD)*, accepted 2011.

[115] P. Li, R. C. de Lamare, "Adaptive Decision Feedback Detection with Constellation Constraints for Multi-Antenna Systems", *Sensor Signal Processing for Defence (SSPD)*, accepted 2011.

[116] P. Li, R. C. de Lamare and R. Fa, "Multi-Feedback Successive Interference Cancellation with Multi-Branch Processing for MIMO Systems", *Vehicular Technology Conference (VTC Spring), 2011 IEEE 73rd,* pp.1-5, May 2011.

[117] P. Li, R. C. de Lamare and R. Fa, "Iterative Successive Interference Cancellation Based on Multiple Feedback For Multiuser MIMO Systems," *European Wireless Conference*, Vienna, Austria, April 2011.

[118] P. Li, R. C. de Lamare and R. Fa, "Multiple Feedback Successive Interference Cancellation with Iterative Decoding for Point-to-Point MIMO Systems", *International ITG/IEEE Workshop on Smart Antennas WSA 2011*, Aachen, Germany, February 2011.

[119] P. Li, R. C. de Lamare and R. Fa, "Multiple Feedback Successive Interference Cancellation with Shadow Area Constraints for MIMO systems", *IEEE International Symposium on Wireless Communications Systems*, York, UK, September 2010.